EFFECT OF pH ON NON-PHOTOCHEMICAL QUENCHING IN SPINACH PHOTOSYSTEM 2 PARTICLES AS MEASURED BY PICOSECOND FLUORESCENCE DECAY KINETICS

by

Christene Carpenter, B.Sc. (Hons.)

A Thesis

submitted to the Department of Biological Sciences

in partial fulfilment of the requirements

for the degree of

Master of Science

August 1995

Brock University

St. Catharines, Ontario

ABSTRACT

Single photon timing was used to study picosecond chlorophyll a fluorescence decay kinetics of pH induced non-photochemical quenching in spinach photosystem 2 particles. The characteristics of this quenching are a decrease in chlorophyll a fluorescence yield as well as a decrease in photochemistry at low pH. Picosecond kinetics of room temperature fluorescence temporally resolve the individual components of the steady state fluorescence yield into components that are related to primary energy conversion processes in photosystem 2. Four components were resolved for dark adapted (Fo), light saturated (Fm), and chemically reduced (Na-dithionite) photosystem 2 reaction centres. The fastest and slowest components, indicative of energy transfer to and energy capture by the photosystem 2 reaction centre and uncoupled ("dead") chlorophyll, respectively, were not affected by changing pH from 6.5 to 4.0. The two intermediate components, indicative of electron transfer processes within the reaction centre of photosystem 2, were affected by the pH change. Results indicate that the decrease in the steady state fluorescence yield at low pH was primarily due to the decrease in lifetime and amplitude of the slower of the intermediate components. These results imply that the decrease in steady state fluorescence yield at low pH is not due to changes in energy transfer to and energy capture by the photosystem 2 reaction centre, but is related to changes in charge stabilization and charge recombination in the photosystem 2 reaction centre.

ACKNOWLEDGEMENTS

I would like to thank Dr. Doug Bruce for being my supervisor and for giving good constructive criticisms and boosting my confidence. We spent many an hour thinking about and discussing picosecond kinetics. Yet, he failed to teach me to juggle.

I would also like to thank Guy Samson for helping with the isolation of the photosystem 2 particles, which required two people. He also asked questions to get me thinking and shared experiences he had with other experiments.

I would like to thank the guys in Machine Shop for making the stand for the cuvette holder and the small metal tubing for the circulating system.

I would like to thank the guys in the Electrical Shop for fixing the really old power supply that had previously caught fire, to everyone's expectations but my own.

I would like to thank John, the glass guy, for fixing the very expensive cuvette when it was broken (not by me, I won't mention a name).

I would like to thank my mother for allowing me to use her computer with programs she is not fond of and which used up precious hard drive space. I would also like to thank my mom for the encouragement and love she gave to me during the course of my time at Brock.

Thank you for everything. Everyone was great.

TABLE OF CONTENTS

LIST OF FIGURES

LIST OF TABLES

INTRODUCTION

In the thylakoid membranes of chloroplasts there are two photosystems which trap light to drive photochemistry. This process powers electron and proton transport ultimately resulting in the production of NADPH and ATP. The proton pumping causes acidification of the lumen producing the build up of a difference in pH across the thylakoid membrane. Each photosystem consists of a reaction center and light harvesting complexes. The light harvesting complexes (LHC) collect light energy and transfer it to the reaction center. In excess light, the LHC may collect more photons than the reaction center can use, which would be harmful to the photosystem. When this occurs there are mechanisms which appear to be triggered by the acidification of the lumen causing excess energy to be lost as heat (Ruban and Horton, 1992). The mechanism has been named non-photochemical or energy dependent, or pH-induced quenching.

There are two characteristics that are most indicative of non-photochemical quenching. One characteristic is a decrease in variable fluorescence, which is the difference between the minimal level of fluorescence, Fo (dark adapted-reaction centers open; Q_A is oxidised) and the maximal level, Fm (light saturated-reaction centers closed; Q_A is reduced) (Krause, 1973; Krause, et. al., 1982). The other indicative characteristic is a decrease in photochemistry. Two basic mechanisms have been proposed for non-photochemical quenching. One mechanism is quenching within the antennae. Ruban et. al. proposed that non-photochemical quenching results from excitation energy dissipation in the LHC 2 (Ruban, et. al., 1993). "Quenching" in the antenna could occur by the direct action of a quencher or

by the self quenching of an aggregated state of the antenna chlorophyll. Another model states that quenching results from inactivation of photosystem 2 (PS2) via acidification of the lumen (Horton, et. al., 1991; Krieger, et. al., 1992; Ruban, et. al., 1993). It has been found that the acidification of the lumen hinders the water splitting process which eventually donates an electron to P_{680}^{+} (Schreiber and Neubauer, 1990). Both rapid charge recombination between P_{680}^{+} and Q_A^{-} and the direct action of P_{680}^{+} as a fluorescence quencher have been proposed as mechanisms for non-photochemical quenching. All of the above mechanisms predict decreased photochemical yield resulting from increased thermal deactivation.

It is difficult to distinguish between the proposed mechanisms for non-photochemical quenching by investigating steady state fluorescence yields alone. Picosecond spectroscopy allows the separation of processes which contribute to fluorescence emission and fluorescence quenching. Using picosecond fluorescence decay kinetics, the individual components associated with processes in the reaction centre can be resolved. Each component is described by a lifetime and an amplitude. Components with fast lifetimes are indicative of energy transfer and energy trapping by the photosystem 2 reaction centre. Components with slow lifetimes are representative of the electron transfer steps in the photosystem 2 reaction centre. The mechanism of non-photochemical quenching was investigated in isolated photosystem 2 particles by determining the picosecond fluorescence decay kinetics as a function of pH.

LITERATURE REVIEW

Photosynthesis and Pigments

A photosynthetic unit consists of the reaction centre chlorophyll, accessory pigments, such as carotenoids and phycobilins, and antennae chlorophyll (see Figure 1) (For a good review see Mauzerall and Greenbaum, 1989). By having many pigments, the efficiency of photosynthesis is increased, due to the increased number of pigments collecting light energy and transferring it to the reaction centre.

Carotenoids absorb light at wavelengths between 450 nm and 470 nm, therefore these pigments look orange. They consist of long strands of conjugated carbon atoms with trimethyl cyclohexene groups on both ends that contain a single double bond.

As chlorophyll contains many conjugated double bonds, there is a large delocalization of electrons into molecular orbitals differing very little in energy level. A relatively small amount of energy in the visible region can excite one electron in the molecule to an unoccupied orbital of higher energy within about a femtosecond. If the excited chlorophyll molecule is part of the chlorophyll dimer in a reaction centre, the electron that was excited into a higher energy orbital actually disassociates from the chlorophyll molecule and reduces pheophytin leaving the chlorophyll molecule oxidized. By this process light energy is converted into chemical potential energy.

Photochemistry occurs through redox reactions ultimately taking electrons from water molecules to reduce $NADP^+$ to NADPH, which is used as an energy source in the Calvin cycle of the dark reactions. Thus, the Z-scheme comprises all

Figure 1. The chemical structures of a chlorophyll and a carotenoid (from Smith, 1989). The structure of chlorophyll with many conjugated double bonds allows for excitation with visible light. For chlorophyll a the X is a CH_3 group and for chlorophyll b it is a CHO group. β-Carotene is made up of a long chain of conjugated carbon atoms which also allows it to absorb light in the visible region.

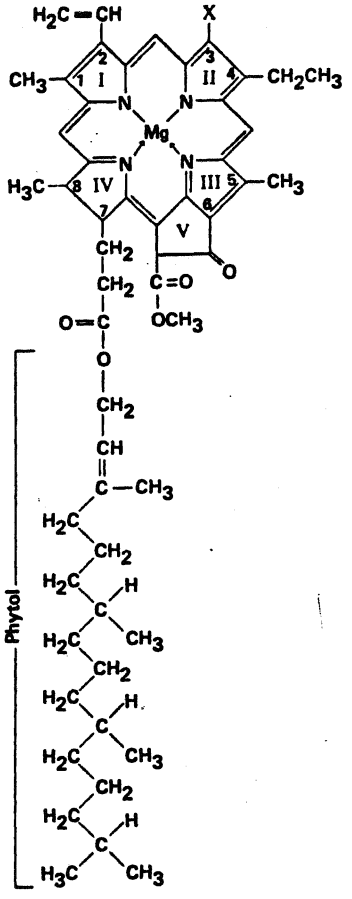

Chlorophyll

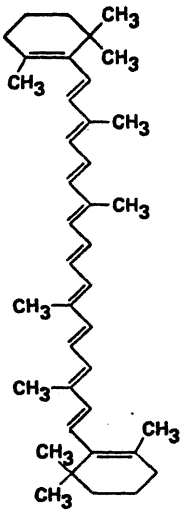

β – Carotene

electron donating and accepting molecules pictured horizontally with their redox potentials on the vertical axis. Figure 3 is a representation of the Z-scheme.

Chloroplast Structure

In higher plants, chloroplasts are oval shaped at ~0.5 μm thick and ~1 μm in diameter (see Figure 2). Inside the chloroplast are membranes containing the photosynthetic apparati that form enlarged flattened vacuoles called thylakoids. The space inside the thylakoid membranes is called the lumen and the space surrounding the thylakoid membrane is called the stroma. Inside the chloroplast, many thylakoid membranes are stacked forming grana stacks. The single membrane connections between the granal stacks are called stroma lamellae. The stroma contains all of the enzymes required for the dark reaction (such as the Calvin cycle) and pigment production.

The Z-scheme

The Z-scheme describes the movement of electrons from one molecule to another in photosysnthesis (Figure 3). When the chlorophyll dimer of photosystem 2 (P_{680}) becomes excited by the absorption of a photon of light, it gives up an electron to pheophytin (Pheo). From pheophytin the electron is transferred to a primary quinone (Q_A), which then transfers the electron to a secondary quinone (Q_B). Once Q_B has been reduced twice, it dissociates from the pigment-protein complex of photosystem 2, pulling two protons from the stroma. The electroneutral quinone joins the plastoquinone (PQ) pool. Back at the photosystem 2 reaction centre, the

Figure 2. A figure showing the structure of a chloroplast (from Wallace, et. al.,1991). Inside the chloroplast are thylakoid membranes arranged in grana stacks or stromal regions. Inside the thylakoid membrane is the lumen and the outside is the stroma.

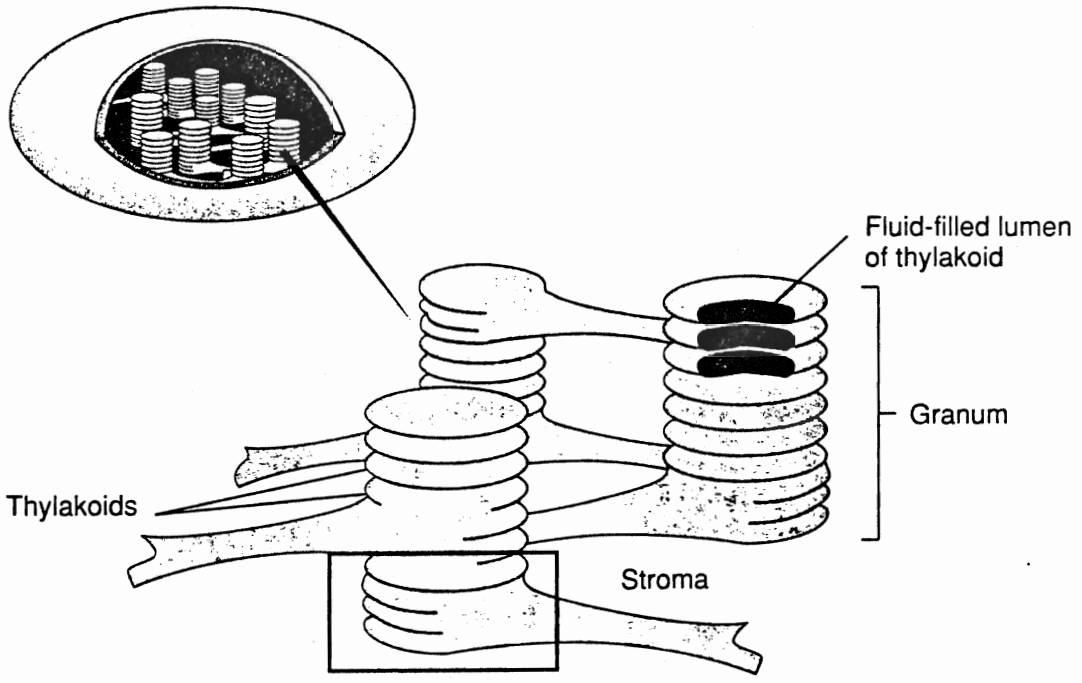
Fluid-filled lumen
of thylakoid
Granum
Thylakoids
Stroma

Figure 3. The Z-scheme (from Nicholls and Ferguson, 1992). Electron transfer from water to NADPH is driven by photochemistry through two photosystems. This figure depicts the electron acceptors and their redox potentials on the vertical axis. Inside of the dashed lines are the electron donors and acceptors bound in or to the photosystem specified in the figure.

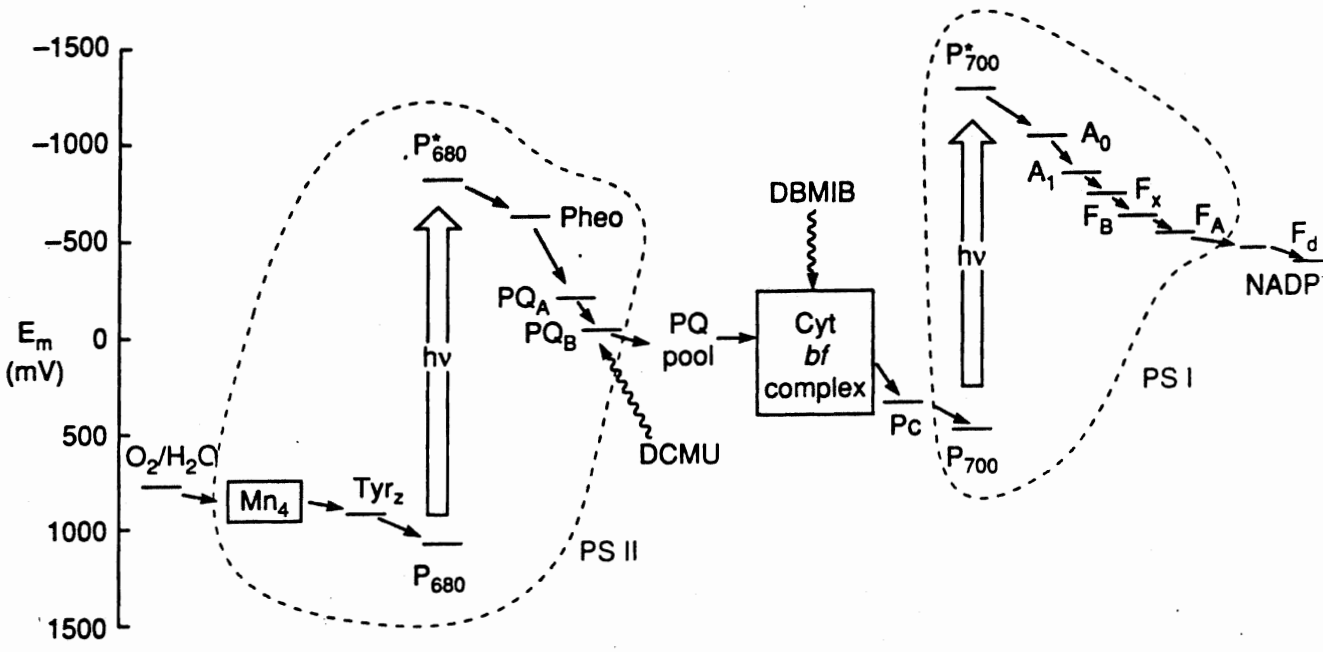
−1500
−1000
−500
0
500
1000
1500
E_m (mV)
O_2/H_2O
Mn_4
Tyr_z
P_{680}
P^*_{680}
hν
Pheo
PQ_A
PQ_B
PS II
DCMU
PQ pool
DBMIB
Cyt *bf* complex
Pc
P_{700}
P^*_{700}
hν
A_0
A_1
F_x
F_B
F_A
F_d
NADP
PS I

manganese-protein water splitting complex gives an electron to P_{680}+ and releases a proton into the lumen, reducing the pigment such that the dimer can absorb another photon. A plastoquinone from the PQ pool gives two electrons to the Cytochrome b_6/f complex (Cyt bf), releasing two protons to the lumen.

When the reaction centre chlorophyll of photosystem 1 (P_{700}) absorbs a photon and becomes excited, the pigment gives up an electron which eventually reduces ferredoxin (FD). An electron is transfered from the Cyt b_6/f complex by plastocyanin (PC) to the P_{700}+ reducing it. The reduced ferredoxin transfers the electron to NADP+ to produce NADPH.

Fates of The Excited State

When a photon of light is absorbed by a pigment molecule, the pigment will be promoted to an excited state. There are four (4) ways that the energy of this excited state can be lost. The energy can be (i) transferred to another pigment, (ii) lost as heat (internal conversion), (iii) used in photochemistry, or (iv) given off as fluorescence (For a good description of these processes see Smith, 1989). There are three criteria for the transfer of energy from one molecule to another. The rate of energy transfer depends on (a) the distance between the two molecules, (b) the orientation of the transition dipoles, and (c) the amount of spectral overlap between the fluorescence of the donor and the absorbance of the acceptor (For a review of this topic see van Grondelle, 1985). The distance between the two molecules is very important due to the fact that the rate of energy transfer is proportional to $1 / R^6$, where R is the distance between the molecules (Forster, 1965). The rate of energy transfer between two molecules is also

dependent on the amount of spectral overlap there is between the fluorescence of the donor and the absorbance of the acceptor. In simple terms, the more overlap between the spectra the better the chance that the energy will be transferred. When a molecule becomes excited the electron density distribution is moved into a higher energy state. The movement of the electron (or change in electron distribution) can be described by a dipole (vector) motion. The rate of energy transfer is also dependent on the orientation of the dipoles of the two molecules. Depending on the different energy levels that a molecule will possess, a pigment molecule will accept photons from a spectrum of energies. The energy of a photon equates with a particular wavelength and, therefore, a spectrum of wavelengths, also known as the molecules absorption spectrum, describes the energy difference between the ground and excited states. A molecule also has a fluorescence spectrum, which is the spectrum of wavelengths (or energies) at which the energy of an excited state can be released as fluorescence. Heat loss, also known as internal conversion, is another way that excitation energy can be lost. With internal conversion the excitation energy takes many small energy steps (heat) before reaching the ground state. Photochemistry includes the process of electron transfer and for photosynthesis, through a series of carriers, ultimately resulting in the transfer of an electron from a chlorophyll pigment to NADPH (an electron donor to many metabolic reactions throughout the plant). Fluorescence is the release of a photon of light with a specific energy equal to the difference in energy between the ground and excited states.

The Kinetics of Excited State Fates

The lifetime of a population of molecules in an excited state will depend on the

rates of these four energy loss pathways. The population of excited states "n" will decrease exponentially with time as described by

$n = n_o e^{-kt}$ (equation 1)

$k = k_f + k_h + k_p + k_{et}$

where n_o is the number of excited molecules at time 0, k is the overall rate constant for loss of energy, k_f is the rate of energy loss via fluorescence, k_h is the rate of energy loss via heat, k_p is the rate of energy loss via photochemistry, and k_{et} is the rate of energy loss via energy transfer. In photosynthetic systems the rate constant for k_f and k_h are usually regarded as constant for particular types of pigment molecules. In contrast, k_p and k_{et} depend on the ability of the reaction centre to accept energy from the antenna pigments (trapping efficiency) the efficiency of excitation energy transfer between groups of antenna pigments and between antenna pigments and the reaction centre. If we assume that k_f is constant then the population of excited states is directly proportional to the fluorescence yield. Therefore, fluorescence decay kinetics are a direct measure of excited state decay kinetics. Excitation energy transfer and energy trapping efficiencies which affect excited states decay kinetics will affect picosecond fluorescence decay kinetics. In the photosynthetic system there are heterogeneous populations of antenna pigments. There can be the transfer of energy between these populations, or between a population of antenna pigments and a reaction centre. There are also two different reaction centres (PS2 and PS1) which the excitation energy can be transferred to. Then there is the trapping of the energy by the reaction centres. All of these energy transfer and energy trapping possibilities lead to many fluorescence decay constituents. Within the literature there is usually the requirement for four decay components (Holzwarth,

1986; Holzwarth, 1988). The observed fluorescence decay kinetics are actually the sum of many single exponential decays. The exponential decay kinetics are measured by modelling with a sum of single exponential decays each with its own amplitude (A) and its own lifetime ($\tau = 1/k$) (refer to equation 1).

The fates of an excited state that have a direct role in this thesis are transfer of energy, fluorescence, and photochemistry. Picosecond fluorescence decay kinetics can, therefore, be used to directly measure the time of energy transfer, the time of energy "trapping", and electron transport in photochemistry.

Time-Resolved Single Photon Counting

When a sample of pigments is hit with a laser pulse, there is a probability that the fluorescence will be emitted at a specific time afterward. The probability for a photon to be emitted at certain times after the pigments are excited with a laser pulse reflects the actual fluorescence curve (Schneckenburger, et. al., 1988). The fluorescence decay curves are generated by repetitions of excitation, single fluorescent photon detection and the measurement of the time between excitation and photon detection. This technique has become one of the best tools for measuring the excited state decay kinetics of many systems, molecules and processes. Aside from looking at excited state decays of photosynthetic systems many chemists and biologists alike have directly measured fluorescence decay properties of dyes and pigment molecules. Zimmerman, et. al. (1982) used single photon counting to measure the fluorescent lifetimes of dyes such as Coumarin 450, Sodium fluorescein, and Rose bengal. Time-resolved single photon counting can be used to measure fluorescence decays from higher plants and

algae alike. Many researchers have used the technique for measuring chlorophyll fluorescence to resolve the kinetics of photosynthetic energy transfer (For a review see Holzwarth, 1986). The observed fluorescence decay is an average of many energy and electron transfer processes and of the different states of many reaction centres. The situation is simplified by the study of stable defined states of the reaction centre. These states include the Fo state, in which all reaction centres are open and Q_A is oxidised, the Fm state, in which all reaction centres are closed with actinic light and Q_A is reduced, and the state in which a chemical reductant is applied to virtually guarantee the reduction of Q_A and the closure of all reaction centres.

Models for Photosystem 2 Kinetics

In 1994, Dau published a review article on variable photosystem 2 fluorescence. In the review article he discussed a number of models for photosystem 2 kinetics in the order of the when they were proposed, from the earliest to the most recently proposed. The same approach will be taken here.

Homogeneous Lattice Model

In this model, it was assumed that the reaction centre P_{680} chlorophyll and N antenna chlorophyll formed a regular lattice (Pearlstein, 1982) (see Figure 4). The absorption and emission spectra are assumed to be the same for all pigments and excitation energy transfer is between neighbouring pigments only, with identical rate constants, k_T, for all pigment pairs. The formation of P_{680+} $Pheo^-$ is assumed to be irreversible. The decay of the excitation energy is predicted to be exponential with a

Figure 4. Models for photosystem 2 kinetics. A) The Homogeneous Lattice Model (from Dau, 1994). The rate constant for primary charge separation is k_1; the rate constant for excitation energy transfer between all neighbouring pigments is k_T. B) The Bipartite Model (from Holzwarth, 1991). The rate constant for excitation energy transfer to the reaction centre from the antenna is k_T and the back transfer from the reaction centre to the antenna is k_t. The rate constant for primary charge separation is k_P and it is assumed irreversible. The rate constant for fluorescence from the antenna is k_F. The rate constants for deactivation from the antenna and the reaction centre are k_D and k_d, respectively. When the reaction centre is open k_P is much greater than k_t, such that the kinetics are diffusion limited. When the reaction centre is closed k_P is equal to zero, such that charge separation cannot occur when the reaction centre is already charge separated. C) The Exciton/Radical Pair Equilibrium Model (from Holzwarth, 1991). The rate constant of energy transfer from the antenna to the reaction centre is k_t, while the rate constant for the back transfer from the reaction centre to the antenna is k_{-t}. The rate constant for primary charge separation is k_1 and the rate constant for primary charge recombination is k_{-1}. The rate constant for secondary charge separation (charge stabilization) is k_2 and this reaction is irreversible. The rate constant for deactivation from the antenna is k_A. The rate constant for the relaxation of the primary radical pair is k_r. The rate constant for the reduction of P_{680}^+ by Z is k_3. The kinetics are trap limited.

A) HOMOGENEOUS LATTICE MODEL

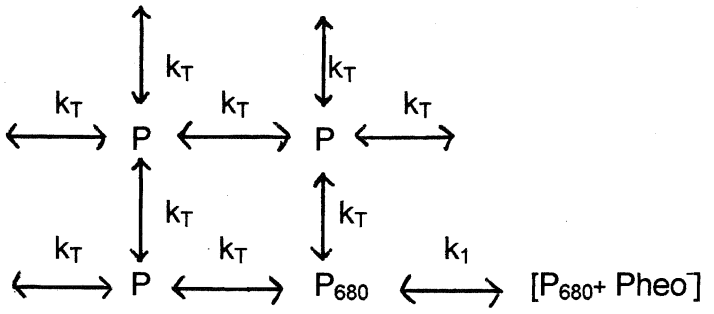

B) BIPARTITE MODEL

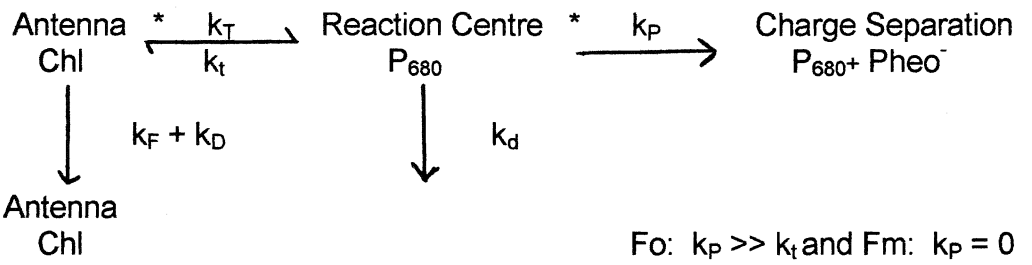

C) EXCITON/RADICAL PAIR EQUILIBRIUM MODEL

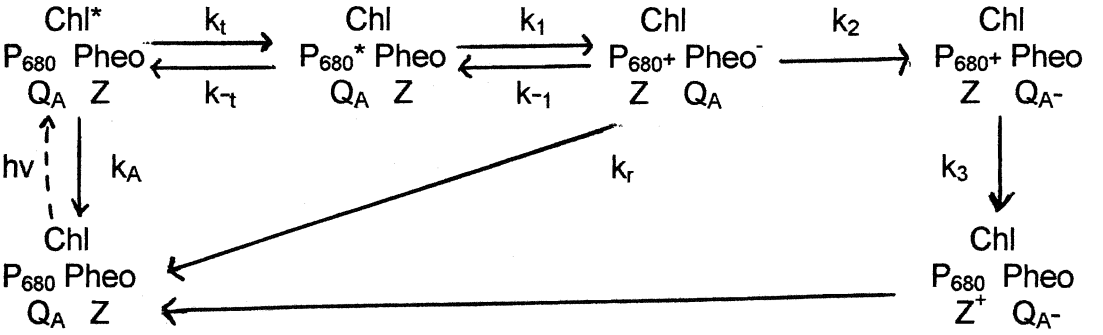

lifetime that is equal to the sum of the "diffusion time", τ_{diff}, and the "trapping time", τ_{trap}. The quantum yield (Φ_F) would then be equal to the product of the rate of fluorescence decay (k_F) and the lifetime (τ_{life}). If $\tau_{diff} << \tau_{trap}$, then the rate of charge separation, k_1, is inversely proportional to τ_{life} and the decay of the exciton is trap limited. If $\tau_{diff} >> \tau_{trap}$, then the decay is diffusion limited. Studies on spectral properties have found photosystem 2 to be inhomogeneous due to absorption spectra and emission spectra with many peaks not just one (Pearlstein, 1982). An extension of this model which includes the evidence of an inhomogeneous lattice is the Funnel Model.

Funnel Model

This model proposed that excitation energy is transferred from higher excited-state energy antenna pigments to pigments of lower excited-state energy and finally to the reaction centre chlorophyll (Seely, 1973). This would suggest that higher excited-state energy chlorophylls would be found on the outside of the photosystem and from there decreasingly lower excited-state energy chlorophylls to the reaction centre. The finding of lower excited-state energy chlorophyll in the outer regions of the antenna complex, of higher plant photosystem 2 (Zucchelli, et. al., 1990; Jennings, et. al., 1993), is evidence against this model. Also, calculations show the funnel model is not necessary to explain the speed or efficiency of energy transfer from the antenna to the reaction centre (Laible, et. al., 1994). The funnel model is, therefore, not necessary to describe energy transfer to the reaction centre since the excitation energy can "bounce" back to the antenna a number of times before trapping occurs.

Bipartite Model

In this model it is assumed that fluorescence originates from the antenna, one pigment pool, and the kinetics are biexponential due to the reversible energy transfer between the antenna and P_{680}, the second pigment pool (Holzwarth, 1991; Butler, 1978; Berens, et. al., 1985) (see Figure 4). Energy transfer between the pigments in the antenna is not considered in this model. Primary charge separation is assumed to be irreversible as in the homogeneous lattice model (Butler, 1978; Roelofs, et. al., 1992). The model predicts that when the reaction centres are closed, the rate of primary charge separation, k_P, is equal to zero and the antenna would not "feel" the redox state of the primary quinone (Q_A). For open reaction centres, it is assumed that the k_P is much larger than the rate of excitation energy transfer from the reaction centre to the antenna (k_t). This describes diffusion limited kinetics with the probability of detrapping being close to zero.

Rapid Exciton Equilibrium Model

In this model it is assumed that there is a rapid exciton equilibrium between all pigments including the reaction centre chlorophyll (Dau, 1994). It is based on the assumption that each pigment has an excited-state energy and that the kinetics of the excited-state decay does not depend on the excitation or emission wavelength. Some criteria for rapid exciton equilibration are that (1) the excitation wavelength does not determine the emission spectrum, (2) the excitation spectra should be the same no matter what wavelength is used to detect the fluorescence, (3) the emission and excitation spectra should not be affected by quenching of the excited antenna state

through primary charge separation or extrinsic quenchers, (4) there are no changes in the emission spectrum for times greater than the equilibrium lifetime for picosecond fluorescence-relaxation measurements, and (5) the mean lifetime is greater than the equilibrium time (Dau, 1994). From this model the Reversible radical pair (RRP) Model was proposed.

Reversible Radical Pair Model

It is assumed in the model that rapid exciton equilibrium occurs between all photosystem 2 pigments including P_{680} and that the reversibility of primary charge separation greatly influences the fluorescence decay kinetics (Dau, 1994). This model results in an excited antenna state and a radical pair state, which leads to biexponential decay for picosecond fluorescence. Assuming that energy transfer from P_{680} to the antenna is fast compared to primary charge separation, the rate of exciton trapping by P_{680} is then the product of the probability that P_{680} is excited and the rate constant for primary charge separation (Dau, 1994). Therefore, the picosecond fluorescence decay kinetics are trap limited. One group of researchers has combined the rapid exciton equilibrium model and the reversible radical pair model to propose the Exciton/Radical Pair Equilibrium Model (Holzwarth, 1991; Roelofs, et. al., 1992).

Exciton/Radical Pair Equilibrium Model

In this model, there is an assumed equilibrium of excitation energy between antenna, reaction centre and the primary charge separation state (see Figure 4) (Holzwarth, 1991; Roelofs, et. al., 1992). The excitation equilibrium is described as a

"compound state" when energy transfer is much faster than primary charge separation leading to photochemistry. Biexponential picosecond kinetics are predicted for photosystem 2. The rate of primary charge separation is dependent on the redox state of Q_A. With oxidised Q_A (open reaction centre) the two kinetic components would be representative of (1) all kinetic events in the equilibrium (excitation energy transfer and trapping, and primary charge separation) which would contribute to the faster kinetic component and (2) slower secondary charge separation (charge stabilisation). With reduced Q_A (closed reaction centre) the two kinetic components would be representative of (1) the kinetic events in equilibrium would contribute to the faster component and; (2) the slow relaxation of the primary radical pair (P_{680}+ $Pheo^-$). Again the picosecond kinetics of the fluorescence decay would be trap limited since the rate of energy transfer between the reaction centre and the antenna is much larger than the rate of primary charge separation (Roelofs, et. al., 1992). This model was adequate for the results of picosecond fluorescence decay kinetics which resolved two lifetime components for photosystem 2, but Roelofs, et. al. (1992) resolved four lifetime components on their photosystem 2 particles. They proposed that two photosystem 2 (PS2α and PS2β) exist and therefore would each have their own specific biexponential kinetics, such that the model was there after called the Heterogeneous Exciton/Radical Pair Equilibrium Model, with the same assumptions as the homogeneous model, that takes into account both types of photosystem 2.

Non-photochemical Quenching

Proton pumping coupled to photosynthetic electron transport causes acidification of the lumen and produces the build up of a difference in pH across the thylakoid membrane (see Figure 5). When this occurs there are mechanisms which appear to be triggered by the acidification of the lumen and/or the difference in pH across the thylakoid membrane causing excess excitation energy to be lost as heat (Ruban and Horton, 1992). The mechanism has been named non-photochemical, or energy dependent, or pH-induced quenching.

There are a number of characteristics associated with non-photochemical quenching. The one characteristic most easily seen is a decrease in variable fluorescence, which is the difference between dark adapted (Fo: minimum fluorescence-reaction centers open) and light saturated (Fm: maximum fluorescence-reaction centers closed) (Krause, 1973; Krause, et. al., 1982). Some report quenching of the Fo level as well (Noctor, et. al., 1991; Ruban, et. al., 1992). Limitation at the donor side of PS2 has also been correlated to the quenching of Fv (Krieger, et. al., 1992). It has been found that the acidification of the lumen hinders the water splitting process which eventually donates an electron to P_{680}^+ (Schreiber and Neubauer, 1990). The inhibition of the water splitting process causing the build up of P_{680}^+ could be a possible mechanism as P_{680}^+ is a known quencher (Dau, 1994). All these characteristics lead to a decrease in the fluorescence and a resulting decrease in photochemical yield which would result from increased thermal deactivation (Dau, 1994).

Figure 5. A representation of the thylakoid membrane (from Wallace, et. al.,1991). Depicted is noncyclic electron transfer as in the Z-scheme as well as the build up of protons in the lumen creating a difference in pH across the thylakoid membrane.

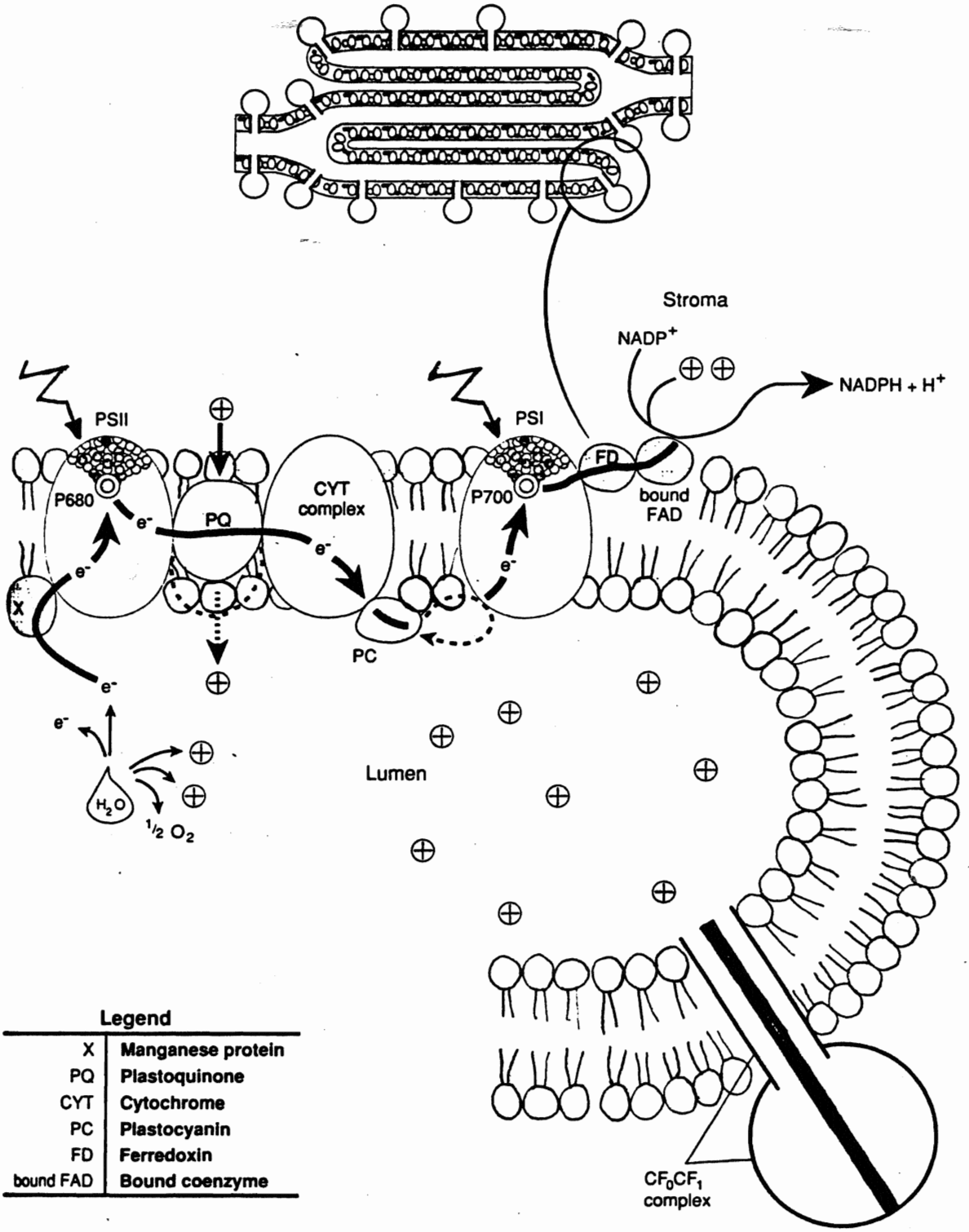

Legend	
X	Manganese protein
PQ	Plastoquinone
CYT	Cytochrome
PC	Plastocyanin
FD	Ferredoxin
bound FAD	Bound coenzyme

There are a few models that have been proposed to explain non-photochemical quenching. One model states that quenching results from an acidification of the lumen inactivating the photosystem 2 (PS2) reaction centre. This acidification induces a donor side limitation leading to the accumulation of P_{680}^+ which may be reduced by a rapid charge recombination between P_{680}^+ and Q_A^- (Krieger, et. al., 1992). Ruban, et. al. (1993) believed that this model does not adequately explain non-photochemical quenching because rapid charge recombination in the reaction center should not quench the minimum fluorescence state (Fo) and Ruban, et. al. (1992) have observed significant Fo quenching. Krieger, et. al. (1992) did not see Fo quenching at low pH and concluded that their thylakoid and photosystem 2 preparations must have differed from the preparations of the groups that observed quenching at Fo. Most of the evidence for both mechanisms comes from studies of quenching at the Fo level with disagreement on the amount of Fo quenching and steady state fluorescence levels.

Previous experiments had found a correlation between energy dependent quenching and zeaxanthin concentration (Demmig-Adams, 1990). From this, it was proposed that energy dissipation occurs by zeaxanthin quenching excitation energy in the antenna. Although, Noctor, et. al. (1991) were able to see quenching without zeaxanthin, zeaxanthin still seems to act as an aid in energy dependent quenching. Since zeaxanthin is known to be associated with the light harvesting complexes (LHC), Ruban, et. al. (1993) proposed that non-photochemical quenching results from excitation energy dissipation in the LHC2. This model was proposed due to evidence of 77K chlorophyll fluorescence spectra which had shown preferential

quenching bands at 680 nm and 700 nm, after induction of non-photochemical quenching (Ruban, et. al, 1992; Ruban, et. al, 1993; Horton, et. al., 1991). These bands originate from the LHC 2. Horton, et. al. (1991) added antimycin A, which is known to inhibit energy dependent quenching and found that it also inhibits the aggregation of the LHC 2. The model was then expanded to say that quenching results from organizational changes in the thylakoid membranes which involved the aggregation of the LHC2. Later it was proposed that the protonation of lumen-exposed amino acid residues of the LHC protein complex could modify the pigment environment resulting in quenching centers of LHC2 (Ruban, et. al., 1992).

MATERIALS

Plant Material

Spinach was bought at local grocery stores the day before or the day of the preparation of photosystem 2 particles (refer to methods).

Solutions

Photosystem 2 Isolation Media

Grinding Medium: 0.3 M NaCl, 30 mM Tricine, 3 mM $MgCl_2$, 0.5 mM Na_2EDTA

Suspension Medium: 0.2 M Sorbitol, 5 mM HEPES, 2 mM $MgCl_2$, 0.5 mg/ml BSA

Basic BBY Medium: 50 mM MES (pH 6.0/NaOH), 5 mM $MgCl_2$, 15 mM NaCl

Triton Stock Solution: 37.5 ml Basic BBY Medium, 12.5 ml Triton X-100

BBY Medium 1: 100 ml Basic BBY Medium, 1 mM ascorbate

BBY Medium 2: 0.4 M sucrose, < 100 ml Basic BBY Medium (total = 100 ml)

pH Solutions: 0.3 M Sorbitol, 50 mM KCl, 5 mM $MgCl_2$ and

(a) 30 mM MES for pH 6.5 - 5.5

(b) 30 mM succinic acid for pH 5.5 - 4.0

Picosecond Time-Resolved Single Photon Timing Apparatus

Picosecond fluorescence decay curves were determined with the apparatus described by Bruce and Miners (1993) (see Figure 6). Excitation pulses are given by a picosecond light pulser (Hammamatsu PLP-01 with an LDH067 laser head) operated at 10 MHz. Excitation wavelength was 665 nm. The pulse width of the laser was approximately 60 ps as specified by Hammamatsu. Laser output was polarised

Figure 6. A representation of the picosecond apparatus used in this thesis. See Materials for a description of the apparatus. The PMT is the photomultiplier tube. The CFD is the constant fraction discriminator. The TAC is the time to amplitude converter.

The Picosecond Apparatus

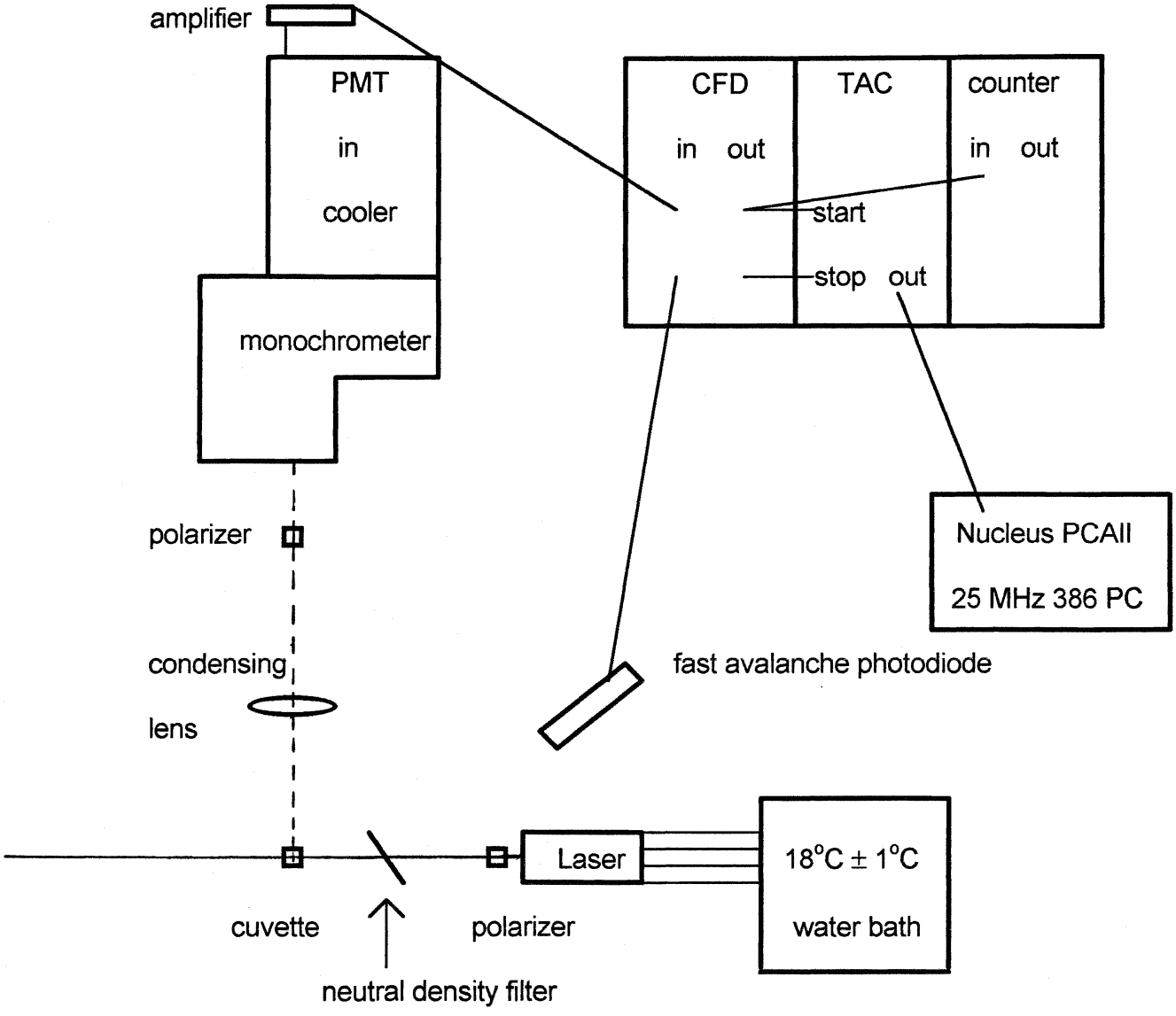

horizontally with the laser head in normal operating position. To produce a collimated beam the laser was factory modified by the addition of a small focusing lens. The laser head was mounted in a water jacketed holder (Brock University Machine Shop) which was kept at 18 $\pm$ 0.1°C with a temperature controlled circulation water bath. Ten percent (10%) of the excitation pulse was used as the timing reference by placing a neutral density filter at the appropriate place in front of the laser beam, thereby, reflecting and focusing 10% of the pulse into a fast avalanche photodiode (Hammamatsu S2381). The photon flux incident on the sample was 3.5×10^8 photons / cm^{-2} / pulse. Fluorescence from the sample, held in a standard 1 cm^2 glass cuvette for the sodium dithionite experiments or a 1 cm x 3 mm for the dark adapted and light saturated experiments, was detected at 90° to the incoming excitation pulse.

On fluorescence detection, all but 2 mm near the centre of the cuvette was masked. The 2 mm area was focused onto the entrance slit (1 mm) of an American Instruments AS Inc. Jobin Yvon DH10 double monochrometer with a 50 mm condensing lens. A calcite polarising crystal set at magic angle to the polarisation axis of the laser was placed in front of the monochrometer to eliminate polarisation anisotropy effects. The exit slit of the monochrometer was positioned 10 cm from the photocathode of a Hammamatsu R2809U-11 proximity focused (6 m) MCP photomultiplier. The 10 cm allowed for uniform illumination of the entire photocathode surface. The MCP was mounted inside a Hammamatsu MCP cooler (#C2773) operated at -40°C. All optical mounts, holders and light shields were constructed by the Brock University Machine Shop. The MCP was operated at 3000V supplied by a regulated high voltage DC power supply (Hammamatsu #C3360). The output of the MCP was first attenuated by a 3dB

attenuator (Minicircuits SMA3) and was then amplified by a high speed (50 KHz to 1.2 GHz bandwidth) pulse shaping amplifier (Hammamatsu #C4267). Pulses from the MCP and the fast reference photodiode were input to two channels of a factory modified (internal delay) constant fraction discriminator (CFD) (Tennelec TC454). MCP pulses output from the CFD were counted (Tennelec TC533) before acting as the start pulses for the time to amplitude converter (TAC) (Tennelec TC 864 TAC/biased amplifier). Reference photodiode pulses output from the CFD were delayed (Tennelec TC412A) and used as the stop pulses for the TAC which was used in reverse timing mode. Output pulses from the TAC/biased amplifier were analysed by a multichannel pulse height analyser (The Nucleus PCAII board) mounted in a 25MHz 386 personal computer. Software supplied with the PCAII board controlled data collection.

Data Collection

Setting the monochrometer to the peak wavelength of the laser (665 nm) and collection of the excitation pulses from a suspension of 0.49 μm latex beads in double distilled water gave the instrument response function. The instrument response function was obtained after every fluorescence decay. In accumulating fluorescence decay data the peak channel level was allowed to reach 10^4 counts and contained 512 channels. An optical delay line was used to determine the time per channel. Fluorescence decay data was collected at room temperature (25^0C).

METHODS

Isolation of the photosystem 2 enriched particles

The isolation of the photosystem 2 particles was performed as in Ganotakis, et. al. (1984) with a few modifications. The midribs of spinach leaves were removed and the leaves were then washed, resulting in a total of 300 g to 400 g of leaf pieces collected in a large beaker. The leaves were ground in an ice-cold blender by three pulses for two seconds each. The debris was separated by filtering the blended suspension through ten layers of ice-cold cheesecloth. The suspension was divided into six large centrifuge tubes and placed into a precooled JA-872 rotor. The tubes were then centrifuged at 4000 rpm (2000 g) for two minutes. The supernatant was then discarded and the pellet was carefully resuspended by paint brush in a total of about 400 ml of suspension medium. The suspension was then centrifuged in two tubes for two minutes at 4000 rpm. The pellets were again resuspended by paint brush to a total volume of about 100 ml of suspension buffer and then filtered through a single layer of KimWipe to remove the fine debris. The filtered suspension was centrifuged in two tubes (total volume about 400 ml) for seven minutes at 4000 rpm. The pellet was resuspended by paint brush in about 20 ml of the BBY medium 1. The chlorophyll concentration of the final suspension was measured and the concentration was adjusted to 2.5 mg Chl a + b/ ml. The suspension was placed in a small beaker with a stir bar on ice. The Triton stock solution (equal to 1/4 of the volume of the thylakoid suspension) was slowly added (drop by drop) to the beaker containing the thylakoid suspension. The suspension was then gently stirred for 30 minutes in the dark. The suspension was divided into a pair of centrifuge tubes and the tubes were placed in a precooled JA-870

rotor and then centrifuged at 19000 rpm (40000 g) for 30 minutes. The supernatant was discarded (PS1) and the pellet was resuspended by paint brush in BBY medium 2, leaving the starch on the walls of the tubes. The suspension was centrifuged in two tubes at 19000 rpm for 30 minutes and the pellet was resuspended in BBY medium 2 to a total volume of about 15 ml. The photosystem 2 suspension was then homogenised in a glass homogeniser. The chlorophyll concentration was then measured and was about 2 mg Chl a + b/ ml. The photosystem 2 particles were then frozen in Eppendorf tubes by liquid nitrogen and stored in a -80°C freezer. For the pH experiments the photosystem 2 particles were suspended in media of various pH (6.5, 6.0, 5.5 [MES], 5.5 [succinic acid], 5.0, 4.5, 4.0) to a concentration of 2 μg Chl/ ml. Before each experiment, the variable fluorescence of the photosystem 2 particles (at 5 μg Chl/ ml) was measured using a fluorimeter, under similar conditions as the methods used to collect the picosecond fluorescence decay curves.

Determination of Chl concentration

From thawed stock photosystem 2 particles, 20 μl of photosystem 2 particles was added to methanol for a total volume of 10 ml (dilution of 500 times). Using the DU50 spectrophotometer, absorbance values for the chlorophyll methanol solution were measured at 652 nm and 665.2 nm. The method of Arnon (1942) was used to calculate the concentration of chlorophyll in the samples used.

Data Collection of Picosecond Fluorescence Decay Curves

A clean optical cuvette was placed in the holder in front of the detector. The front surface of the optical cuvette was blacked out except for a slit of 2 mm for fluorescence to escape. For the dark adapted and light saturated experiments the circulating system was turned on and the 50 ml suspension was moving in and out of the 200 µl optical cuvette at 53 ml/min. For the dark adapted experiments the samples were kept in the dark except for the short exposure to the laser (~240 ms). For the light saturated experiments the sample flowed through a white light illuminated (2000 $\mu Em^{-2}s^{-1}$) glass bulb (2 ml) just previous (~200 ms) to the exposure to the laser. This allowed for a 1 minute dark incubation and a 2 second saturating light treatment (closed reaction centres), with 200 ms of dark before measurement. For the dithionite experiments, the sample was stagnant in a 1 cm^2 cuvette. The sample was hit with the laser at a frequency of 10 MHz and a fluorescence decay curve was collected over approximately five minutes. This procedure was repeated such that fluorescence decay curves were collected at 680 nm, 685 nm, 690 nm, 695 nm, 700 nm, using the monochrometer, for the production of "amplitude spectra" (Decay associated spectra; see Figure 8) of photosystem 2 fluorescence emission. Collection times were as long as ten minutes at long wavelengths.

Data Fitting

Decay curves were modelled with a sum of single exponential decays. Data fitting was done with a kinetic modelling program developed by Warren Zipfel (ICS, Ithaca, NY) which utilises the Levenburg-Marquardt algorithm for least squares

estimation of non-linear parameters. Two programs were developed, one to fit single fluorescence decays and another to fit many fluorescence decays simultaneously. Given an initial estimate of amplitudes and lifetimes for the individual decay components, with a single fluorescence decay, the fitting program varied both amplitude and lifetime until a minimal difference between model and data was found as determined by least squares. With the global lifetime program, which simultaneously fits many fluorescence decays collected at different wavelengths, the lifetime of each kinetic component is held constant, assuming the lifetimes of the components should not vary with wavelength, while the amplitudes of the components vary. The global lifetime program allows for the resolution of the different kinetic components in the form of spectra and also utilises the same algorithm for least squares as the program for single fluorescence decays. The χ^2 value that would indicate a perfect fit is one (1), therefore, χ^2 values of 1.0 to 1.2 were considered statistically valuable. As well as the χ^2 value, another way to interpret the wellness of the fit is by the residuals, which shows the variation of the fluorescence decay about the model decay. The more evenly distributed the residuals are, the better the fit of the fluorescence decay to the model decay.

RESULTS

To study the effects of pH on non-photochemical quenching in the picosecond fluorescence decay kinetics of photosystem 2, isolated photosystem 2 particles were suspended in buffers with pH between 6.5 and 4.0 and fluorescence was measured at wavelengths between 680 nm and 700 nm in dark adapted, light saturated or sodium dithionite treated conditions. The fluorescence decay curves that were collected, from the five wavelengths (680 nm to 700 nm) at one pH and in one of the three conditions, were then fit using the global lifetime analysis. All fluorescence decays resolved into four components, each component described by a lifetime (τ) and an amplitude (A) (see Figure 7). The global spectra resolved from the global lifetime analysis consist of relative amplitudes as a function of wavelength, while each spectrum describes a single component (for example, see Figure 8 and Appendix II) (All of the following figures include standard error of the mean). From these global spectra, average lifetime, average amplitude, relative yield, and steady state fluorescence yield were calculated (see Appendix I). The average amplitude (A) of each component at one pH and in one of the conditions (Fo, Fm, Dithionite treated) was calculated by averaging the amplitudes over all of the wavelengths. The average amplitude (A) was then multiplied by the lifetime (τ) of the component to calculate the relative yield of that component at one pH and in one of the conditions. The sum of all relative yields at one pH gives the total steady state fluorescence yield. Figure 9 shows the steady state fluorescence yield as a function of pH in the dark adapted (Fo), light saturated (Fm), and sodium dithionite treated (Dithionite) photosystem 2 particles. The steady state fluorescence yield of dark adapted photosystem 2 particles (Fo) increases slightly as pH decreases, while the

Figure 7. A single fluorescence decay fit. The fluorescence decay is the red "noisy" curve, the instrument response function (IRF) is the shape of the laser (purple curve), the model decay fit is the dark line on the fluorescence decay, and the residuals are at the top in blue. The fluorescence decay was collected from PS2 reduced chemically with sodium dithionite at pH 6.5. The single decay fit resulted in a χ^2 of 1.033 and the following four kinetic components were resolved. (τ_1 = 68ps, A_1 = 329 ; τ_2 = 320ps, A_2 = 778 ; τ_3 = 992ps, A_3 = 554 ; τ_4 = 3.9ns, A_4 = 81)

A three component fit to the same decay yielded a $\chi 2$ of 1.16 with the following kinetics. (τ_1 = 64 ps, A_1 = 367; τ_2 = 660 ps, A_2 = 385; τ_3 = 1.37 ns, A_3 = 1000).

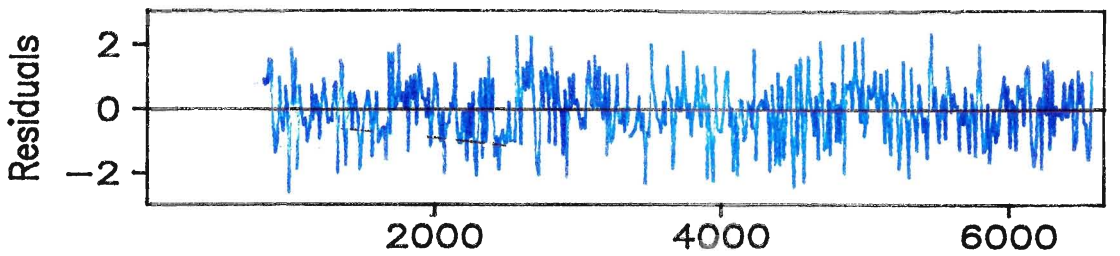
Residuals
2
0
−2
2000
4000
6000

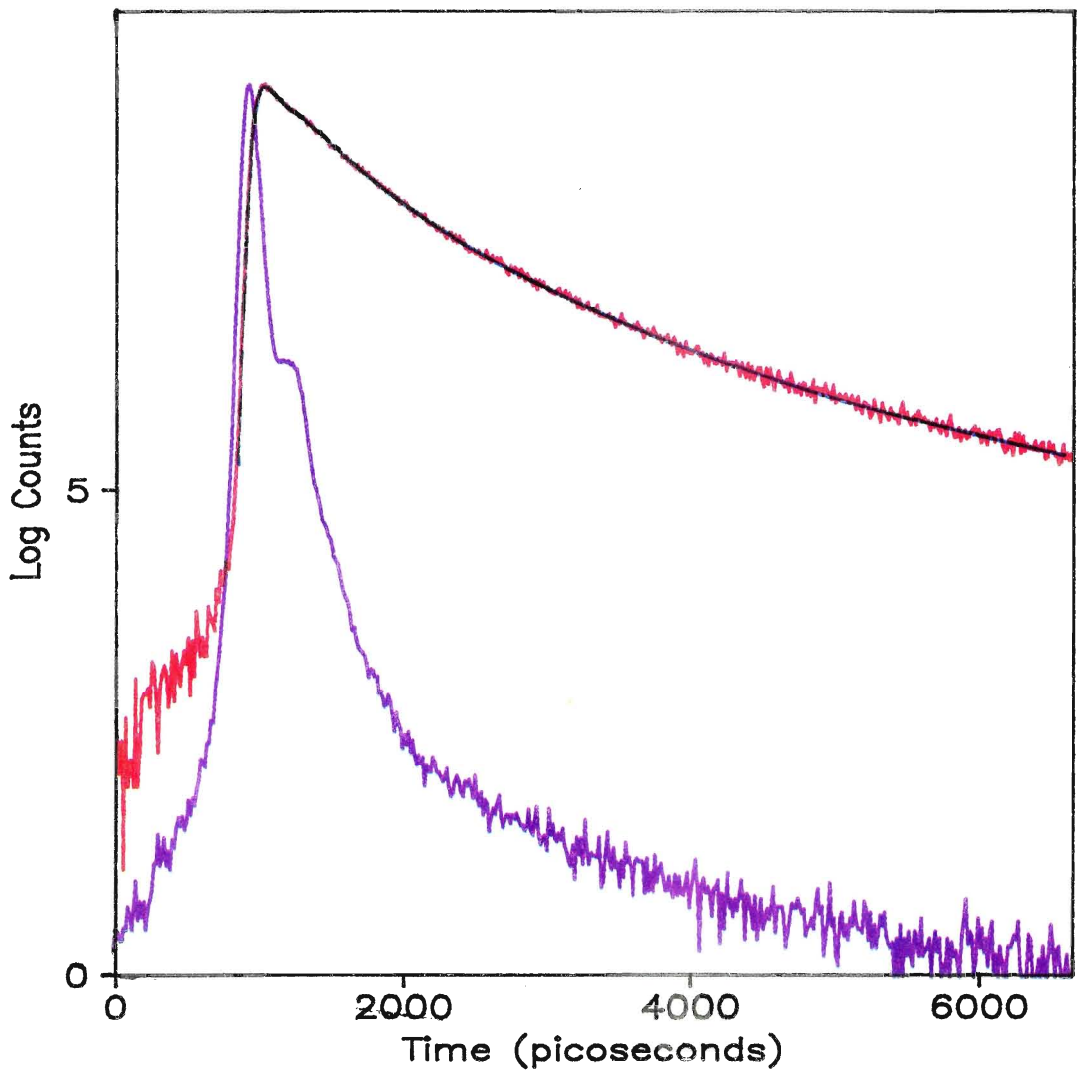
Log Counts
5
0
0
2000
4000
6000
Time (picoseconds)

Figure 8. Decay associated spectra of the relative amplitude of the four kinetic components of light saturated photosystem 2 particles at pH 6.5. The fast component is denoted as C1 (96 ps), the faster of the two intermediate components is C2 (499 ps), the slower of the intermediate components is C3 (1302 ps), and the slowest component is C4 (2371 ps). The spectra were averaged from three individual experiments.

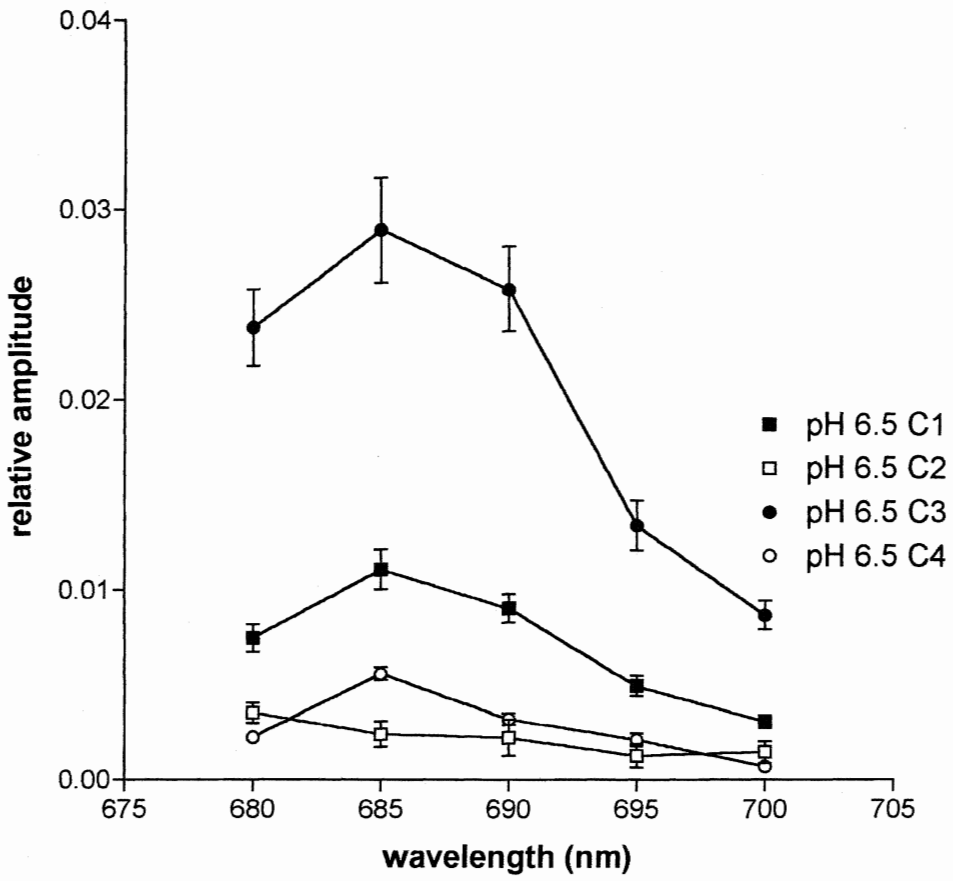
0.04
0.03
0.02
0.01
0.00
relative amplitude
675
680
685
690
695
700
705
wavelength (nm)
pH 6.5 C1
pH 6.5 C2
pH 6.5 C3
pH 6.5 C4

Figure 9. Steady State Fluorescence Yield of dark adapted (Fo), light saturated (Fm) and sodium dithionite (Dithionite) treated photosystem 2 particles as a function of pH (pH 5.5 succinic acid). All values are an average of three (except for Fo [pH 4.5 and 5.5(S)] and Fm [pH 4.0 and 6.0] which are an average of two) individual experiments.

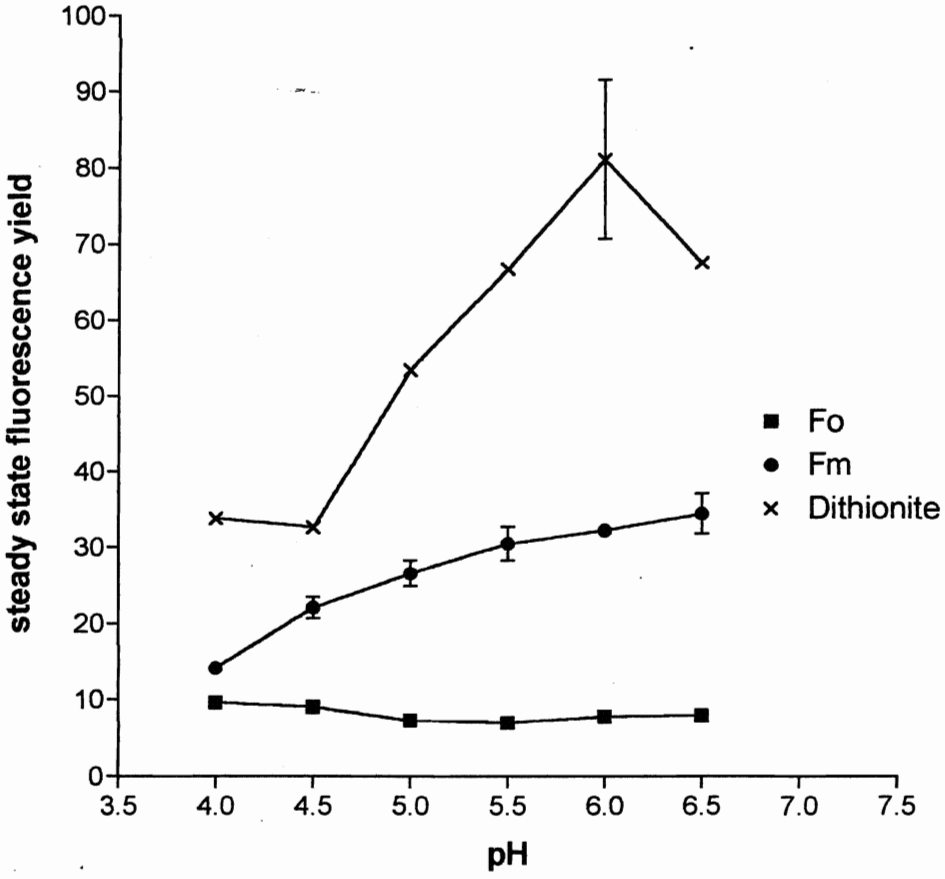
steady state fluorescence yield
100
90
80
70
60
50
40
30
20
10
0
3.5
4.0
4.5
5.0
5.5
6.0
6.5
7.0
7.5
pH
Fo
Fm
Dithionite

steady state fluorescence yield of both light saturated (Fm) and sodium dithionite treated (Dithionite) photosystem 2 particles decreased with decreasing pH. With dark adapted photosystem 2 particles (Fo) having the minimum steady state fluorescence yield, the steady state fluorescence yield of the light saturated photosystem 2 particles (Fm) was about four times larger and the steady state fluorescence yield of the sodium dithionite treated photosystem 2 particles (Dithionite) was about eight times larger at pH 6.5. At pH 4.0 the steady state fluorescence yield of the light saturated photosystem 2 particles (Fm) was only about fifty percent larger than that of the dark adapted photosystem 2 particles (Fo) while the steady state fluorescence yield of the sodium dithionite treated photosystem 2 particles (Dithionite) was about three times larger than that of the dark adapted photosystem 2 particles.

For the dark adapted photosystem 2 particles (Fo), the relative yield of each component was plotted against pH (Figure 10). The relative yield of the fastest component (C1; ~80 ps) did not significantly change with pH, while the relative yield of the fastest intermediate component (C2; ~250 ps) decreased with decreasing pH. The relative yield of the two slowest components (C3; ~500 ps, C4; ~1500 ps) increased as pH decreased. When the lifetime of each component was plotted against pH (Figure 11), it was shown that the lifetimes of the three slowest components all decreased as pH decreased and the lifetime of the fastest component did not change. The amplitudes of the four components all increased when comparing the amplitudes from pH 6.5 to pH 4.0 (Figure 12).

The relative yields of the slowest three components of the light saturated photosystem 2 particles (Fm), behaved in an opposite manner to that of the dark

Figure 10. Relative yield of the four kinetic decay components of dark adapted photosystem 2 particles as a function of pH (pH 5.5 MES). The fast component is denoted as C1, the faster of the two intermediate components is C2, the slower of the intermediate components is C3, and the slowest component is C4. All values are an average of three (except for pH 4.5 which is an average of two) individual experiments.

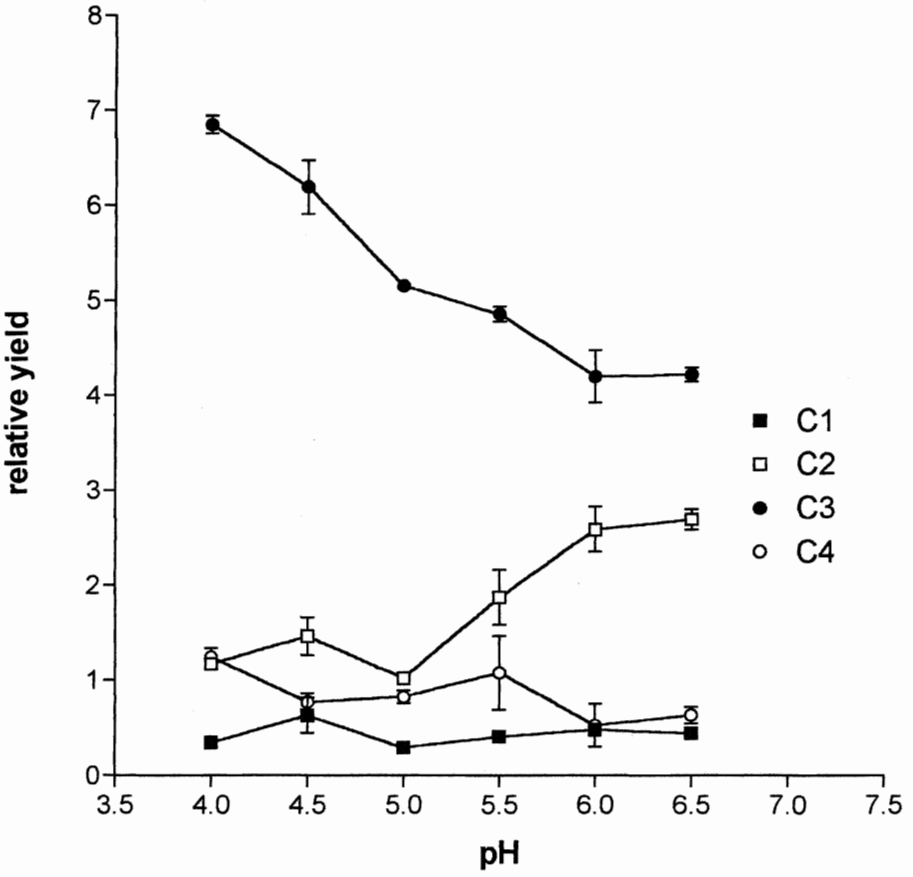
relative yield
pH
C1
C2
C3
C4
0
1
2
3
4
5
6
7
8
3.5
4.0
4.5
5.0
5.5
6.0
6.5
7.0
7.5

Figure 11. Lifetimes (in picoseconds) of the four components of dark adapted photosystem 2 particles as a function of pH (pH 5.5 MES). The fast component is denoted as C1, the faster of the two intermediate components is C2, the slower of the intermediate components is C3, and the slowest component is C4. All values are an average of three (except for pH 4.5 which is an average of two) individual experiments.

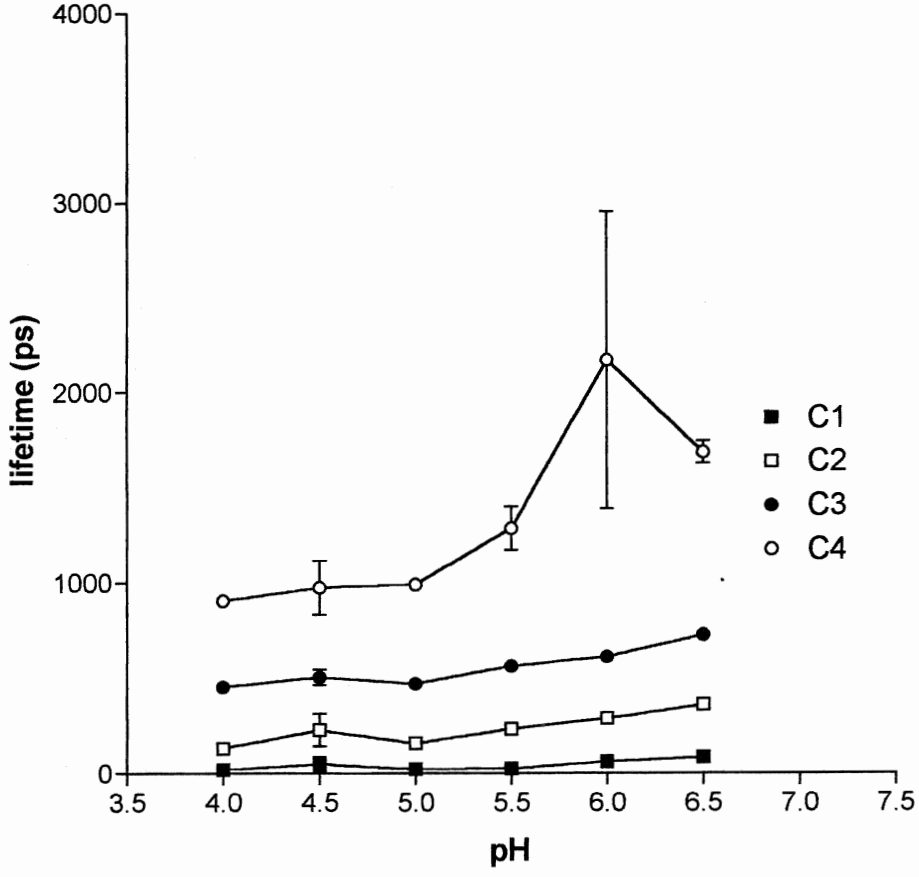
4000
3000
2000
1000
0
lifetime (ps)
3.5
4.0
4.5
5.0
5.5
6.0
6.5
7.0
7.5
pH
C1
C2
C3
C4

Figure 12. Average amplitude of the four components of dark adapted photosystem 2 particles as a function of pH (pH 5.5 MES). The fast component is denoted as C1, the faster of the two intermediate components is C2, the slower of the intermediate components is C3, and the slowest component is C4. All values are an average of three (except for pH 4.5 which is an average of two) individual experiments.

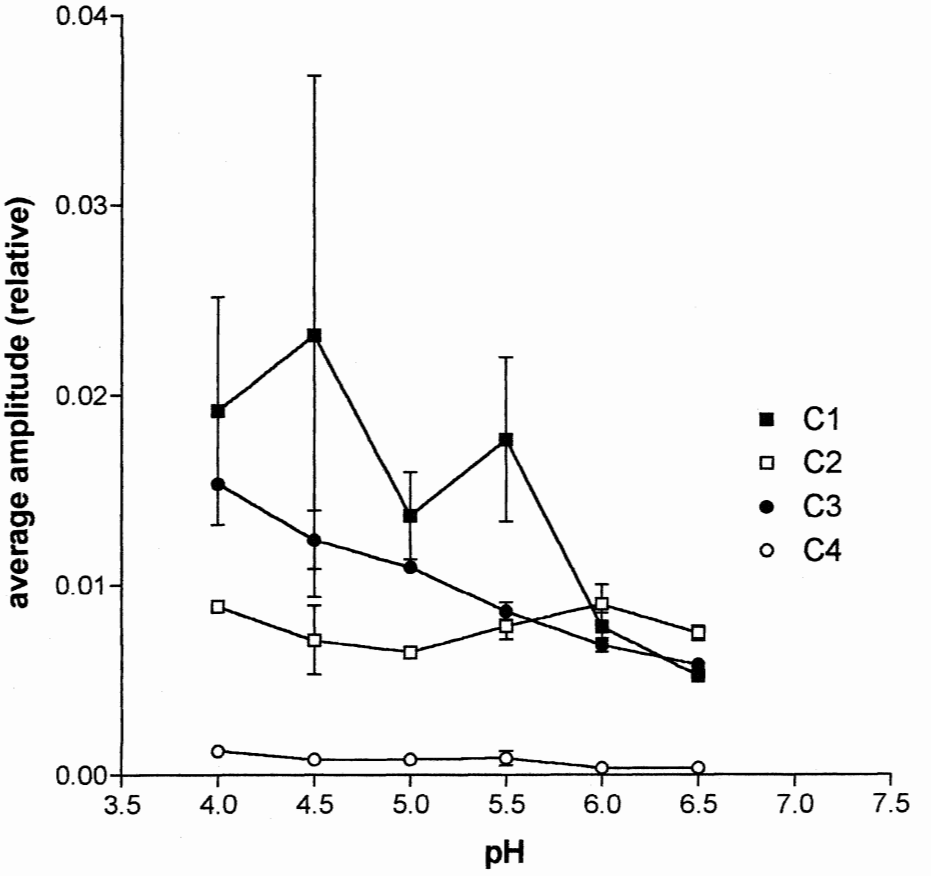
0.04
0.03
0.02
0.01
0.00
average amplitude (relative)
3.5
4.0
4.5
5.0
5.5
6.0
6.5
7.0
7.5
pH
C1
C2
C3
C4

adapted photosystem 2 particles (Figure 13). The relative yield of the fastest component (C1; ~80 ps) again did not significantly change as pH was decreased, while the relative yield of C2 (~400 ps) increased and the relative yields of C3 (~1100 ps) and C4 (~2000 ps) decreased. The lifetimes of the two slowest components decreased as pH decreased while the lifetimes of the two fastest components did not significantly change (Figure 14). The relative amplitudes of the two slowest components decreased and the relative amplitudes of the two fastest components increased as the pH was decreased (Figure 15).

The relative yields of the components of the sodium dithionite treated photosystem 2 particles (Dithionite) were also plotted against pH (Figure 16). The relative yields of the two fastest components (C1; ~90 ps, C2; ~350 ps) did not significantly change as pH decreased, while the relative yields of the two slowest components (C3; ~1100 ps, C4; ~4500 ps) decreased with decreasing pH. The lifetimes of C1 and C2 did not change and the lifetimes of C3 and C4 decreased as pH decreased (Figure 17). The amplitudes of all components, except the amplitude of C2 which does not change, (C1, C3 and C4) decreased with decreasing pH (Figure 18).

The mean lifetime, denoted as τ_{AVG} , was calculated (see Appendix I) for each pH value. For the dark adapted (Fo), light saturated (Fm), and sodium dithionite treated (Dithionite) photosystem 2 particles, τ_{AVG} decreased as pH decreased (Figure 19). As with the steady state fluorescence yield, τ_{AVG} was highest for the sodium dithionite treated (Dithionite) photosystem 2 particles and lowest for the dark adapted (Fo) photosystem 2 particles, with light saturated (Fm) photosystem 2 particles falling in-

Figure 13. Relative yield of the four components of light saturated photosystem 2 particles as a function of pH (pH 5.5 succinic acid). The fast component is denoted as C1, the faster of the two intermediate components is C2, the slower of the intermediate components is C3, and the slowest component is C4. All values are an average of three (except for pH 4.0 and 6.0 which are an average of two) individual experiments.

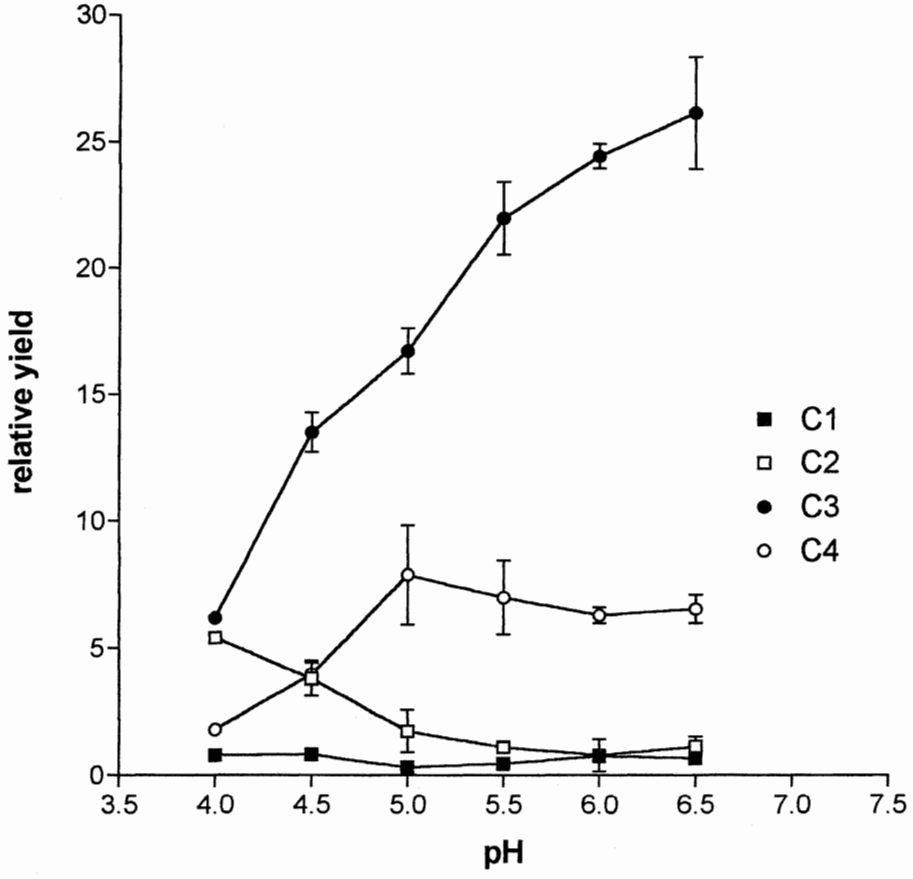
relative yield
30
25
20
15
10
5
0
3.5
4.0
4.5
5.0
5.5
6.0
6.5
7.0
7.5
pH
C1
C2
C3
C4

Figure 14. Lifetimes (in picoseconds) of the four components of light saturated photosystem 2 particles as a function of pH (pH 5.5 succinic acid). The fast component is denoted as C1, the faster of the two intermediate components is C2, the slower of the intermediate components is C3, and the slowest component is C4. All values are an average of three (except for pH 4.0 and 6.0 which are an average of two) individual experiments.

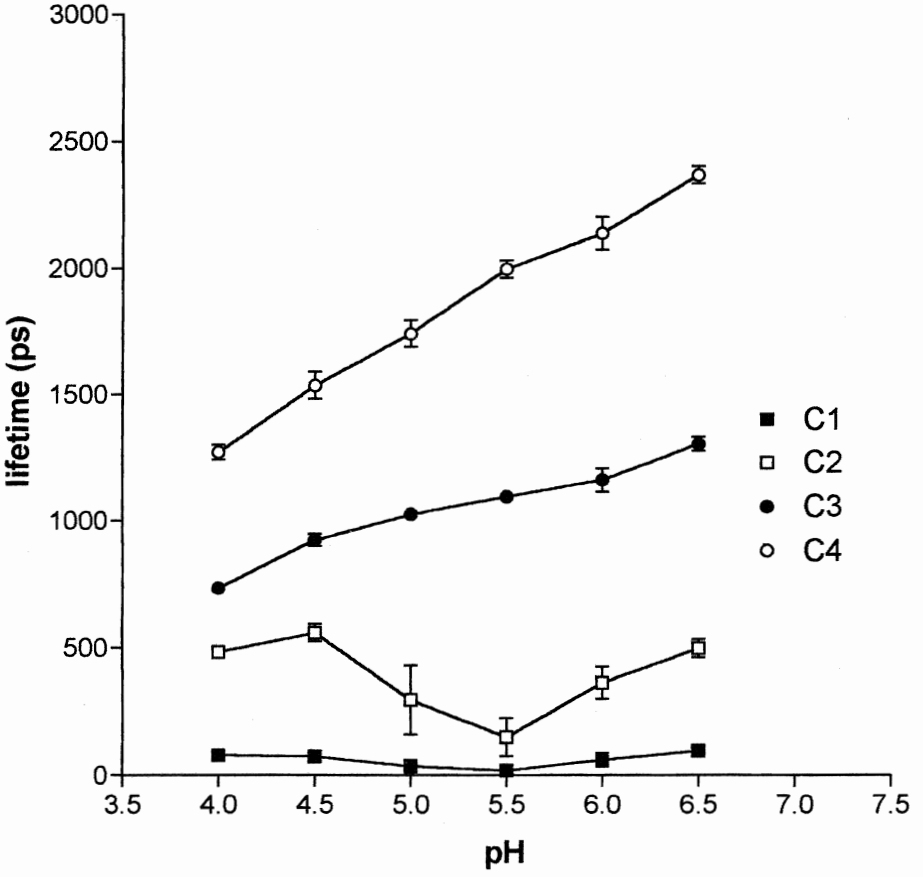
3000
2500
2000
1500
1000
500
0
lifetime (ps)
3.5
4.0
4.5
5.0
5.5
6.0
6.5
7.0
7.5
pH
C1
C2
C3
C4

Figure 15. Average amplitude of the four components of light saturated photosystem 2 particles as a function of pH (pH 5.5 succinic acid). The fast component is denoted as C1, the faster of the two intermediate components is C2, the slower of the intermediate components is C3, and the slowest component is C4. All values are an average of three (except for pH 4.0 and 6.0 which are an average of two) individual experiments.

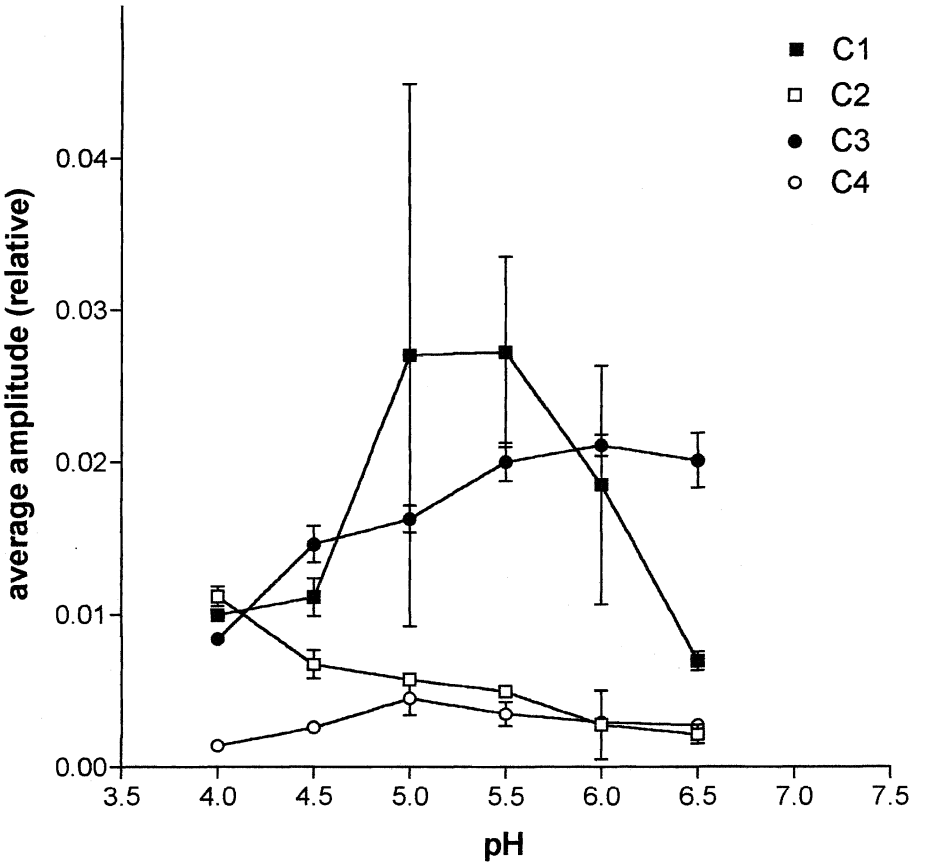
C1
C2
C3
C4
average amplitude (relative)
0.00
0.01
0.02
0.03
0.04
3.5
4.0
4.5
5.0
5.5
6.0
6.5
7.0
7.5
pH

Figure 16. Relative yield of the four components of sodium dithionite treated photosystem 2 particles as a function of pH (pH 5.5 succinic acid). The fast component is denoted as C1, the faster of the two intermediate components is C2, the slower of the intermediate components is C3, and the slowest component is C4. All values are an average of three individual experiments.

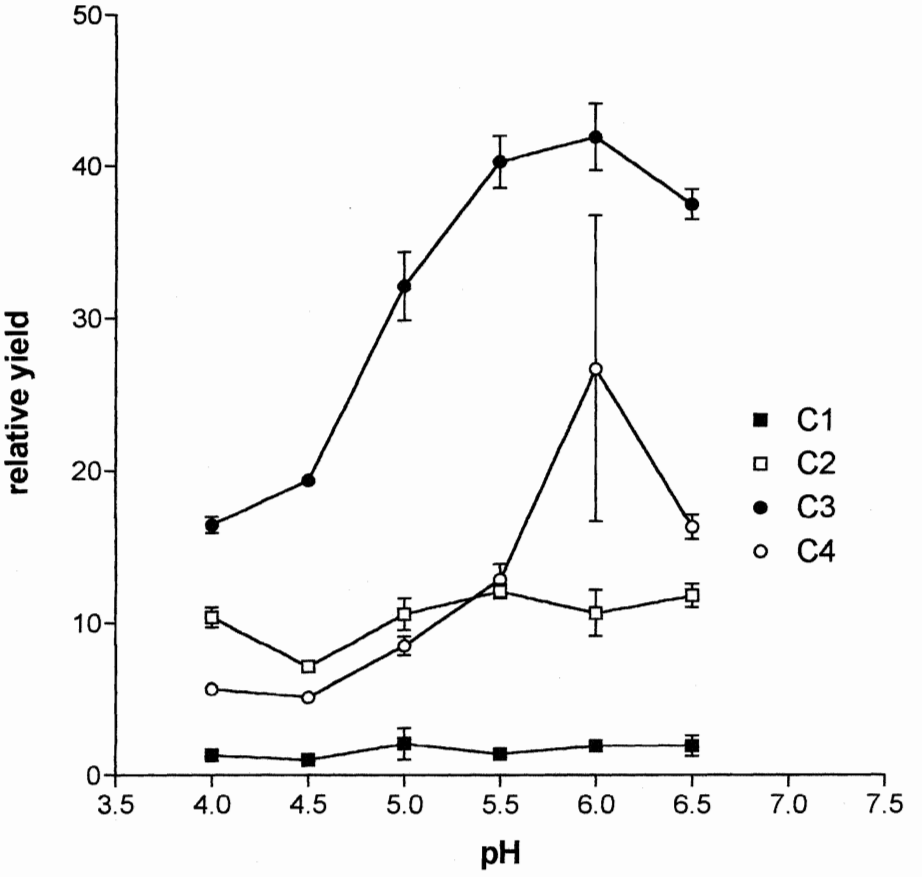
50
40
30
20
10
0
relative yield
3.5
4.0
4.5
5.0
5.5
6.0
6.5
7.0
7.5
pH
C1
C2
C3
C4

Figure 17. Lifetimes (in picoseconds) of the four components of sodium dithionite treated photosystem 2 particles as a function of pH (pH 5.5 succinic acid). The fast component is denoted as C1, the faster of the two intermediate components is C2, the slower of the intermediate components is C3, and the slowest component is C4. All values are an average of three individual experiments.

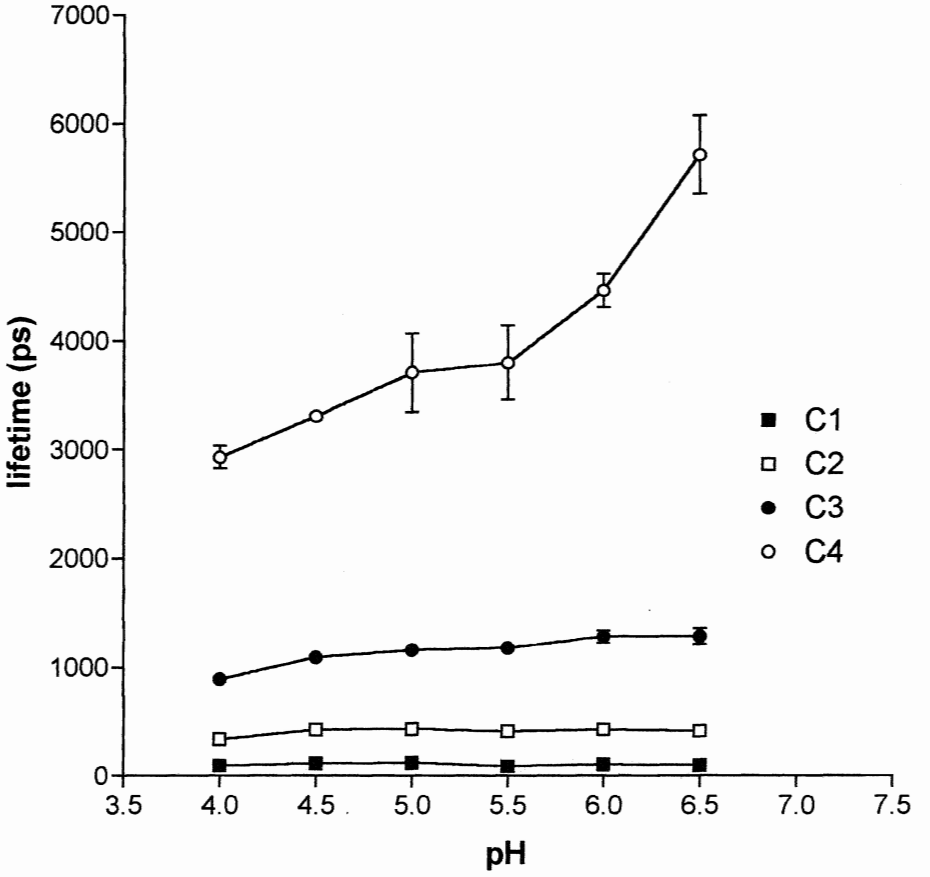
7000
6000
5000
4000
3000
2000
1000
0
lifetime (ps)
3.5
4.0
4.5
5.0
5.5
6.0
6.5
7.0
7.5
pH
C1
C2
C3
C4

Figure 18. Average amplitude of the four components of sodium dithionite treated photosystem 2 particles as a function of pH (pH 5.5 succinic acid). The fast component is denoted as C1, the faster of the two intermediate components is C2, the slower of the intermediate components is C3, and the slowest component is C4. All values are an average of three individual experiments.

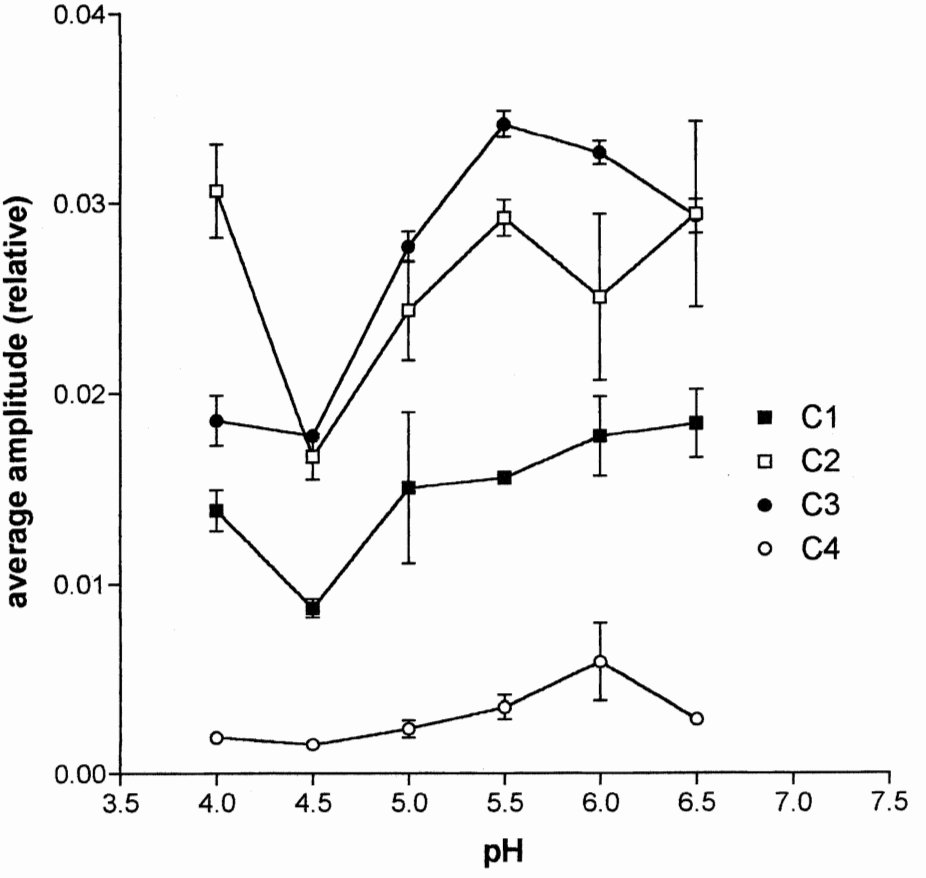
0.04
0.03
0.02
0.01
0.00
average amplitude (relative)
3.5
4.0
4.5
5.0
5.5
6.0
6.5
7.0
7.5
pH
C1
C2
C3
C4

Figure 19. Average lifetime (τ_{AVG}) of dark adapted (Fo), light saturated (Fm), and sodium dithionite treated (Dithionite) photosystem 2 particles as a function of pH (pH 5.5 succinic acid). All values are an average of three (except for Fo [pH 4.5 and 5.5] and Fm [pH 4.0 and 6.0] which are an average of two) indidvidual experiments.

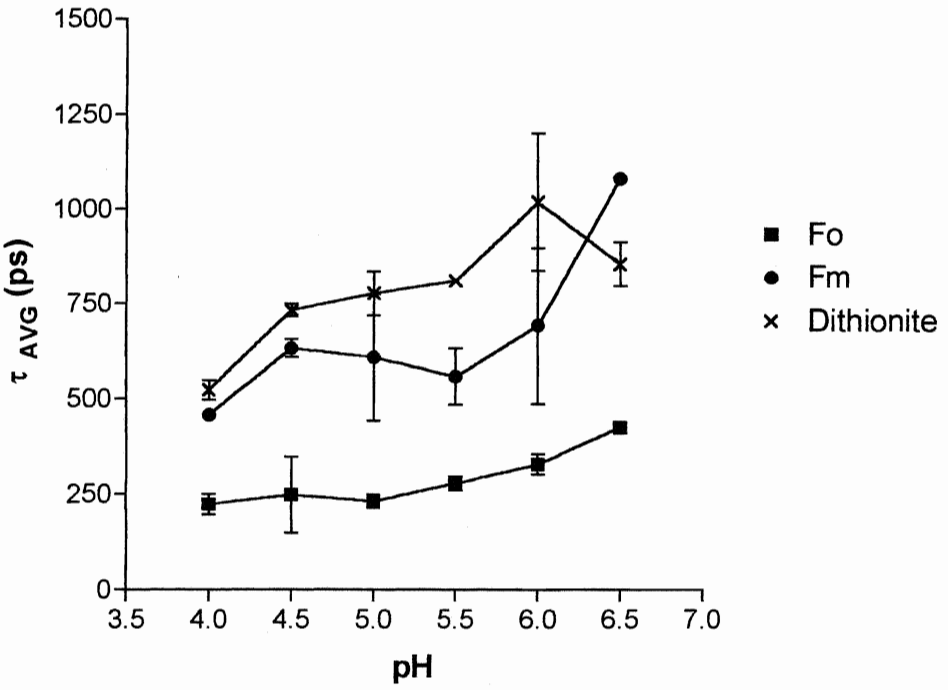
1500
1250
1000
750
500
250
0
τ AVG (ps)
3.5
4.0
4.5
5.0
5.5
6.0
6.5
7.0
pH
Fo
Fm
Dithionite

between (except at pH 6.5). The τ_{AVG} values for both the dark adapted (Fo) and light saturated (Fm) photosystem 2 particles significantly decreased at pH values <6.5, while the τ_{AVG} values for the sodium dithionite treated (Dithionite) photosystem 2 particles did not significantly decrease until the pH was <4.5.

Krieger, et. al. (1992) collected fluorescence decays at only one wavelength and describe their components as the lifetimes and amplitudes at the one wavelength (usually ~685 nm). To ease comparisons, the data in this study has also been expressed in this manner and is shown in Table 1. The kinetic results found by Krieger, et. al. (1992) at pH 6.5 include 0.03ns (11%), 0.18ns (45%), .40ns (40%), and 1.3ns (4%) with open reaction centres, and with closed reaction centres 0.02ns (13%), 0.57ns (35%), 1.5ns (49%), and 4.2ns (3%). The results of Vass, et. al. (1993) at pH 6.3 were 0.08ns (26%), 0.20ns (58%), 0.39ns (15%), and 2.2ns (0.07%) with open reaction centres, and 0.26ns (23%), 0.87ns (31%), 1.75ns (41%), and 3.9ns (4.9%) with closed reaction centres. At pH 4.0, Krieger, et. al. (1992) resolved 0.03ns (12%), 0.20ns (45%), 0.45ns (40%), and 1.4ns (3%) for open reaction centres, and 0.01ns (11%), 0.36ns (45%), 0.80ns (42%), and 2.3ns (2%) with closed reaction centres. Although the specific numbers are very different, there are many trends in common which are dealt with in the discussion.

Table 1. A table of the lifetimes and amplitude resolved in this study. The values are from data at 685 nm at pH 6.5 and 4.0, with open (Fo), closed (Fm), and chemically reduced (Dithionite) reaction centres. The units of the lifetimes are in picoseconds or nanoseconds as indicated. The amplitude is shown as the percentage of the total amplitude of all the kinetic components combined.

pH	State of the reaction centre	C1	C2	C3	C4
6.5	Fo	85 ps 26 %	362 ps 40 %	729 ps 32 %	1.694 ns 2 %
6.5	Fm	96 ps 22 %	499 ps 6 %	1.3 ns 63 %	2.37 ns 9 %
6.5	**Dithionite**	102 ps 23 %	418 ps 37 %	1.28 ns 37 %	5.71 ns 4 %
4.0	Fo	20 ps 43 %	133 ps 20 %	456 ps 34 %	907 ps 3 %
4.0	Fm	80 ps 32 %	484 ps 36 %	735 ps 27 %	1.27 ns 5 %
4.0	**Dithionite**	96 ps 21 %	342 ps 47 %	892 ps 29 %	2.93 ns 3 %

To assist in the description of the results presented above, I will conclude with a few comparisons and observations.

i) The decrease in the steady state fluorescence yield with decreasing pH is mainly due to the decrease in the relative yield of C3. This was seen in the difference in the amplitude and lifetime of C3 in the light saturated (Fm) and sodium dithionite treated (Dithionite) photosystem 2 particles at pH 6.5 and pH 4.0 and in the graphs of relative yield as a function of pH.

ii) Interestingly the yield of the fastest component (C1) of light saturated (Fm) photosystem 2 particles at pH 4.0 was very similar to the yield of the fastest component (C1) of dark adapted (Fo) photosystem 2 particles at pH 6.5 which suggests a similar state in the reaction centre.

iii) The relative yield of C4 also decreased with pH, as C3 did, but the relative yield of C4 is much smaller than C3.

iv) The amplitude of C2 increased as pH decreased in the light saturated (Fm) and chemically reduced (Dithionite) photosystem 2 particles.

DISCUSSION

The Assignment Of Kinetic Decay Components

The picosecond fluorescence decay kinetics of photosystem 2 particles resolved into four exponential decay components at Fo, Fm, and with chemically reduced reaction centres. Recently other groups have also resolved four components for their photosystem 2 particles (Krieger, et. al., 1992; Vass, et. al., 1993; Roelofs, et. al., 1992).

The most widely used model to interpret picosecond fluorescence decay kinetics is the exciton/radical pair equilibrium model. As described in the literature review, this model explains a complex equilibrium state between the antenna chlorophyll, the reaction centre chlorophyll and primary charge separation. It predicts biexponential kinetics for photosystem 2. Each of these kinetics are contributed to by a number of different energy or electron transfer processes in the photosystem. The group that originally proposed the exciton/radical pair equilibrium model (Vass, et. al., 1993) recently resolved four kinetic components for both open and closed reaction centres in photosystem 2 (PS2) enriched membranes and have, therefore, expanded the model by invoking heterogeneity of photosystem 2 into photosystem 2 α (PS2α) and photosystem 2 β (PS2β) which have slightly different kinetics. Therefore, C1 and C3 were assigned to PS2α and were attributed to be the fast energy transfer, primary charge separation/recombination processes and the slow secondary charge separation (in open reaction centres) or primary radical pair relaxation (in closed reaction centres), respectively. While, C2 and C4 were assigned to PS2β and were attributed to be the same respective processes as in PS2α. Previous research on the heterogeneity of PS2

was conducted by Anderson and Melis (1983). They found two types of PS2 that have different antenna sizes and different Q_A midpoint redox potentials. Substantial work has shown that PS2α is located in the grana stacks of thylakoid membranes, whereas, PS2β is located in the stromal regions of thylakoid membranes (Melis and Thielen, 1980; Thielen and van Gorkom, 1981; Anderson and Melis, 1983). This last result implies, however, that the PS2 enriched particles used by Vass, et. al. (1993), Krieger, et. al. (1992), and in this thesis should contain mostly PS2α, as they originate in the grana stacks.

Although the kinetic lifetimes and amplitudes vary between the studies of Krieger, et. al. (1992), Vass, et. al. (1993) and this work many trends do remain the same. We all see an increase in the amplitude of C3 in closed reaction centres as compared to open reaction centres. Also a commonality between us is that in the PS2 particles with open reaction centres, the faster components dominate the fluorescence decay and with closed reaction centres, the slower components dominate the fluorescence decay. These trends support the exciton/radical pair equilibrium model which predicts that with open reaction centres, excitation energy transfer, trapping and primary charge separation (fast processes) dominate the kinetic events, and, with closed reaction centres, relaxation of the primary radical pair (slow processes) dominates the kinetic events occurring in the photosystems. I observed that with the closure of the reaction centre either by light or by a chemical reductant, the relative yield of C3 and C4 both increase while the relative yield of C1 and C2 stay the same, as their amplitudes decreased and the lifetimes slightly increased. The heterogeneous assignment of the kinetic components is well represented by the similar increase in the relative yield of C3

and C4 when the reaction centre is closing, in the respect that C3 is representative of primary radical pair relaxation in PS2α centres and C4 is the same in PS2β centres. Therefore I will use the same assignments for decay components as Vass, et. al. (1993) and will discuss my data in terms of the heterogeneous exciton/radical pair equilibrium model.

The Effect Of pH

At low pH, when non-photochemical quenching is induced, there is a decrease in the steady state fluorescence yield. With the use of picosecond fluorescence decay kinetics the changes in the lifetime and amplitude of the kinetic components in PS2, with pH, indicate the possible mechanism of quenching and the possible quencher. The majority of the components did not change drastically at low pH. The decrease in fluorescence due to low pH was not seen as a reduction in fluorescence from dark adapted (open reaction centre) photosystem 2 particles or in the yield of the fastest components (C1). This indicates that, in the photosystem 2 particles studied, the quenching did not originate in the antenna. If either zeaxanthin or chlorophyll aggregation was quenching fluorescence, the excitation energy would not be transferred to P_{680} and the lifetime and amplitude of C1 would decrease. As no changes in C1 were observed, quenching by antenna chlorophyll or zeaxanthin in the antenna was not occurring. In contrast to the expected decrease in the relative yield of C1 proposed to be associated with antenna quenching, I saw a small increase in the fluorescence yield of the dark adapted PS2 particles at low pH that was associated with an increase in the

relative yield of C3. This increase in the relative yield of C3 indicates a partial closure of some reaction centres, seen as an increase in primary radical pair relaxation.

The significant changes observed in this study were in the components C2, C3, and C4. The increase in the amplitude of C2 with decreased pH was an unexpected result that indicated an independent pH effect on PS2β, seen as an increase in the amount of excitation energy transfer, trapping, and primary charge separation/recombination, that is not seen in PS2α. The large decrease in steady state fluorescence yield was due mostly to the decrease in the relative yield of C3 at low pH. Krieger, et. al. (1992) observed similar results with their C3 component, but were able to reverse the quenching with chemical reductant. I did not see a reversal of quenching with a chemical reductant at low pH. Irreversible quenching at low pH was also observed by Rees, et. al. (1992) and Ruban, et. al. (1993) who reported that below pH 5.0 non-photochemical quenching became irreversible.

Krieger, et. al. proposed a kinetic model for the pH induced non-photochemical quenching they observed. They describe the decrease in the yield of C3 at low pH in a recombination model (see Figure 20). Their model proposed a recombination between P_{680}^+ and Q_A^- within a few microseconds, with the energy being dissipated as heat, rather than fluorescence. This is proposed to be due to a shift to a more positive value of the redox potential of Q_A^- at low pH, which would decrease the amount of energy available from Q_A^- to below that required to generate P_{680}^*. Recombination would, therefore, not yield enough energy to release a photon. Assumed in the recombination model is that the electron on Q_A^- would directly reduce P_{680}^+, such that the kinetics of P_{680}^+ reduction and Q_A^- oxidation should be identical. Research in our laboratory has

Figure 20. A) The Non-photochemically Quenched State (modified after Holzwarth, 1991). The rate constant for energy transfer from the antenna to P_{680+} is k_v and the rate constant for energy transfer from P_{680+} to the antenna is k_{-v}. The rate constant for deactivation by the antenna is k_W. The rate constant for the loss of excitation energy as heat by P_{680+}^* is k_H and is assumed to be irreversible. B) Recombination Model proposed by Krieger, et. al. (1992) (from Krieger, et. al., 1992). In this model, the tyr_Z that usually donates an electron to P_{680+} is inhibited. When there is charge separation, the electron does not go to Q_B, but stays with Q_A until it recombines with P_{680+}. The recombination yields heat due to increased redox potential of Q_A at low pH, such that an excited state cannot be achieved. The recombination takes a few microseconds (Krieger, et. al., 1992).

A) NON-PHOTOCHEMICALLY QUENCHED STATE

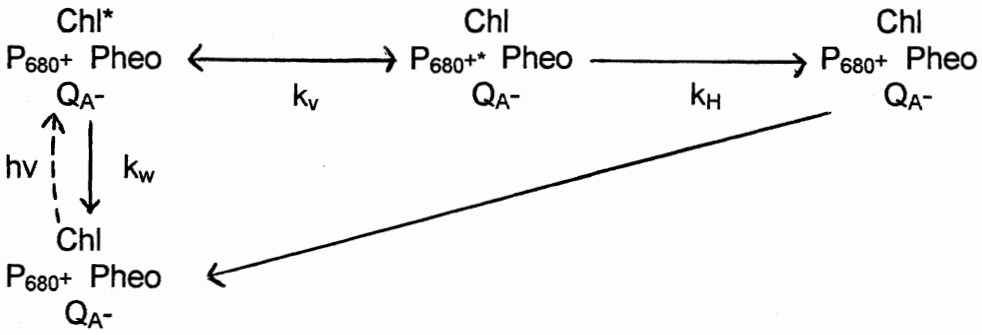

B) RECOMBINATION MODEL

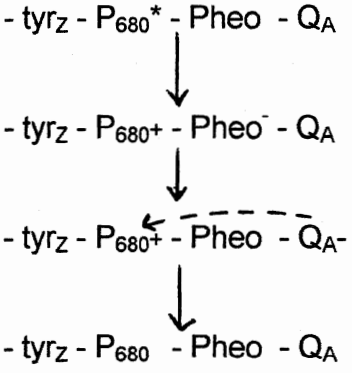

shown that P_{680}^+ is reduced much more quickly than Q_A^- is oxidised (Guy Samson, personal communication) indicating that the electron in Q_A^- is not directly reducing P_{680}^+. This evidence does not support the recombination model proposed by Krieger, et. al. (1992).

It is known, from the heterogeneous exciton/radical pair equilibrium model, that C3 and C4 are representative of primary radical pair relaxation for PS2α and PS2β, respectively. With pH, the relative yield of both these components decreased, therefore, the amount of radical pair relaxation has decreased. The relative yields of C1 and C2 have not decreased at low pH, so there is just as much excitation energy reaching P_{680} as at normal pH. One route for energy loss would be by secondary charge recombination as proposed by Krieger, et. al. (1992), but it has been shown that Q_A^- is not reducing P_{680}^+ directly. With P_{680}^+ present in the reaction centre, what is the only other way that the excitation energy may be quenched?

Proposal For P_{680}^+ As A Quencher

I propose that in illuminated photosystems, at low pH a significant number of reaction centres contain P_{680}^+ and that the excitation energy from the antenna can be transferred to P_{680}^+ (k_t) which acts as a quencher releasing the energy as heat (Figure 20). In photosystems with P_{680} reduced and Q_A oxidised, the excitation energy in the antenna transfers to P_{680} (k_t) which then can either be transferred back to the antenna (k_{-t}) or drive primary charge separation (k_1). With charge separation leading to photochemistry (k_2), the antenna does not "see" the exciton again because energy is taken away from the equilibrium. If P_{680}^+ quenches the exciton through internal

conversion, the antenna would also not be able to "see" the exciton again. If C3 is the relaxation of the primary radical pair as in the exciton/radical pair equilibrium model, then when the exciton is quenched by P_{680}^+ in non-photochemical quenching, the yield of this slower component should be and was found to be small. Relaxation of the primary radical pair cannot occur in these reaction centres as charge separation does not occur in the presence of P_{680}^+. The decrease in the lifetime of C3, with decreasing pH, suggests that there is an independent effect of pH on the reaction centres with P_{680}, which can undergo charge separation. This effect is seen as an increase in the rate of primary radical pair relaxation to the ground state, such that the relaxation of the radical pair occurs faster at low pH as compared to pH 6.5.

The similarity between the fastest decay components of dark adapted, pH 6.5, and light saturated, pH 4.0, photosystem 2 particles indicate similar energy transfer and trapping characteristics under these two conditions. This is consistent with the P_{680}^+ quenching model if P_{680}^+ and P_{680} have similar trapping kinetics. At pH 6.5, in dark adapted reaction centres P_{680} is able to trap excitation energy which will eventually lead to photochemistry. In the P_{680}^+ quenching model, at pH 4.0, light saturated reaction centres containing P_{680}^+ cannot perform charge separation leading to photochemistry, yet trap excitation energy just as quickly. This indicates efficient energy transfer to the reaction centre from the antenna that is independent of the redox state of P_{680} (and maybe even the redox state of Q_A), supporting the P_{680}^+ quenching model I proposed.

My results clearly display the kinetic changes that accompany non-photochemical quenching induced by low pH. The indifference of open reaction centres and the kinetic events associated with energy transfer in the antenna to pH rule out antenna quenching

by zeaxanthin or chlorophyll aggregation in the photosystem 2 particles used in this study. The decrease in the steady state fluorescence yield at low pH was mostly due to the large decrease in the amplitude of C3, which is attributed to primary radical pair relaxation. If P_{680} is oxidised, then primary charge separation could not occur and, therefore, primary radical pair relaxation cannot occur. In conclusion, the results presented compel me to propose that P_{680}^{+} is quenching fluorescence at low pH and is, therefore, the non-photochemical quencher in the reaction centre. ☺

REFERENCES

Anderson, J.M. and Melis, A. (1983). Proc. Natl. Acad. Sci. USA. 80: 745 - 749.

Arnon, D.I. (1949). Plant Physiol. 24: 1 - 15.

Berens, S.J., Scheele, J., Butler, W.L., and Madge, D. (1985). Photochem Photobiol. 42 (1): 59 - 68.

Bruce, D. and Miners, J. (1993). Photochem. Photobiol. 58 (3): 464 - 468.

Butler, W.L. (1978). Annu. Rev. Plant Physiol. 29: 345 - 378.

Crofts, J. and Horton, P. (1991). Biochim. Biophys. Acta. 1058: 187 - 193.

Dau, H. (1994). Photochem. Photobiol. 60 (1): 1 - 23.

Demmig-Adams, B. (1990). Biochim. Biophys. Acta. 1020: 1 - 24.

Forster, T. (1965). *In*: Modern Quantum Chemistry, Part III, Action of Light and Organic Molecules, O. Sinanoglu, Ed. Academic Press (New York, NY). pp. 93 - 173.

Ghanotakis, D.F., Babcock, G.T. and Yocum, C.F. (1984). Biochim. Biophys. Acta. 765: 388 - 398.

Holzwarth, A.R. (1986). Photochem. Photobiol. 43 (6): 707 - 725.

Holzwarth, A.R. (1987). In Topics in Photosynthesis, Volume 8, The Light Reactions, Barber, J., Ed. Elsevier (Amsterdam, Britain). pp. 95 - 157.

Holzwarth, A.R. (1988). In Applications of Chlorophyll Fluorescence. Lichtenthaler, H.K., Ed., Kluwer Academic Publishers (Dordrecht, Germany), pp. 21 - 31.

Holzwarth, A.R. (1991). In Chlorophylls. CRC Handbook, H. Scheer, editor. CRC Press (Boca Raton, FL). pp. 1125 - 1151.

Horton, P., Ruban, A.V., Rees, D., Pascal, A.A., Noctor, G., and Young, A.J. (1991). FEBS Lett. 292 (1,2): 1 - 4.

Jennings, R.C., Bassi, R., Garlaschi, F.M., Dainese, P., and Zucchelli, G. (1993). Biochemistry. 32: 3203 - 3210.

Krause, G.H. (1973). Biochim. Biophys. Acta. 292: 715 - 728.

Krause, G.H., Vernotte, C., and Briantais, J.-M. (1982). Biochim. Biophys. Acta. 679: 116 - 124.

Krieger, A., Moya, I., and Weis, E. (1992). Biochim. Biophys. Acta. 1102: 167 - 176.

Laible, P.D., Zipfel,W., and Owens, T.G. (1994). Biophys. J. 66: 884 - 860.

Mauzerall, D. and Greenbaum, N.L. (1989). Biochim. Biophys. Acta. 974: 119 - 140.

Melis, A. and Thielen, A.P.G.M. (1980). Biochim. Biophys. Acta. 589: 275 - 286.

Nicholls, D.G., and Ferguson, S.J. (1992). Bioenergetics 2. Academic Press Limited. (San Diego, CA).

Noctor, G., Rees, D., Young, A., and Horton, P. (1991). Biochim. Biophys. Acta. 1057: 320 - 330.

Noctor,G., Ruban, A., and Horton, P. (1993). Biochim. Biophys. Acta. 1183: 339 - 334.

Pearlstein, R.M. (1982). In Photosysthesis: Energy Conversion by Plants and Bacteria, Volume I (Edited by Govindjee). Academic Press (New York, NY). pp. 293 - 330.

Rees, D., Noctor, G., Ruban, A.V., Crofts, J., Young, A., and Horton, P. (1992). Photosyn. Res. 31: 11 - 19.

Rees, D., Young, A., Noctor, G., Britton, G., and Horton, P. (1989). FEBS Lett. 256 (1,2): 85 - 90.

Roelofs, T.A., Lee, C.-H., and Holzwarth, A.R. (1992). Biophys. J. 61: 1147 - 1163.

Ruban, A.V. and Horton, P. (1992). Biochim. Biophys. Acta. 1102: 30 - 38.

Ruban, A.V., Rees, D., Pascal, A.A., and Horton, P. (1992). Biochim. Biophys. Acta. 1102: 39 - 44.

Ruban, A.V., Walters, R.G., and Horton, P. (1992). FEBS Let. 309: 175 - 179.

Ruban, A.V., Young, A.J., and Horton, P. (1993). Plant Physiol. 102: 741 - 750.

Schneckenburger, H., Seidlitz, H.K., and Eberz, J. (1988). Photochem. Photobiol. 2: 1 - 19.

Schreiber, U. and Neubauer, C. (1990). Photosynth. Res. 25: 279 - 293.

Seely, G.R. (1973). J. Theor. Biol. 40: 173 - 187.

Smith, K.C. (1989). The Science of Photobiology: Second Edition. Plenum Press (New York, NY).

Thielen, A.P.G.M. and van Gorkon, H.J. (1981). Biochim. Biophys. Acta. 635: 111 - 120.

van Grondelle, R. (1985). Biochim. Biophys. Acta. 811: 147 - 195.

Vass, I., Gatzen, G., and Holzwarth, A.R. (1993). Biochim. Biophys. Acta. 1183:388 - 396.

Wallace, R.A., Sanders, G.P. and Ferl, R.J. (1991). Biology: The Science of Life, Third Edition. Harper Collins Publishers Inc. (New York, New York).

Weis, E. and Berry, J.A. (1987). Biochim. Biophys. Acta. 894: 198 - 208.

Wendler, J. and Holzwarth, A.R. (1987). Biophys. J. 52: 717 - 728.

Zimmerman, H.E., Penn, J.H., and Carpenter, C.W. (1982). Proc. Natl. Acad. Sci. USA. 79: 2128 - 2132.

Zucchelli, G., Jennings, R.C., and Garlashi, F.M. (1990). J. Photochem. Photobiol. B. Biol. 6: 381 - 394.

APPENDIX I

Calculations

Average Amplitude (A)

$A_i = (A_{680nm} + A_{685nm} + A_{690nm} + A_{695nm} + A_{700nm}) / 5$

Relative Yield (Φ)

$\Phi_i = A_i * \tau_i$ i = C1, C2, C3, C4

Steady State Fluorescence Yield (Φ_{total})

$\Phi_{total} = \Sigma \Phi_i$ i = C1, C2, C3, C4

Average Lifetime (τ_{AVG})

$\tau_{AVG} = \Sigma^n A_i * \tau_i / \Sigma^n A_i$ i = C1, C2, C3, C4

APPENDIX II

Graphs

Figure 21. Decay associated spectra of the relative amplitude of the four kinetic components of dark adapted photosystem 2 particles at pH 4.0. The fast component is denoted as C1 (20 ps), the faster of the two intermediate components is C2 (133 ps), the slower of the intermediate components is C3 (456 ps), and the slowest component is C4 (907 ps). The spectra were averaged from three individual experiments.

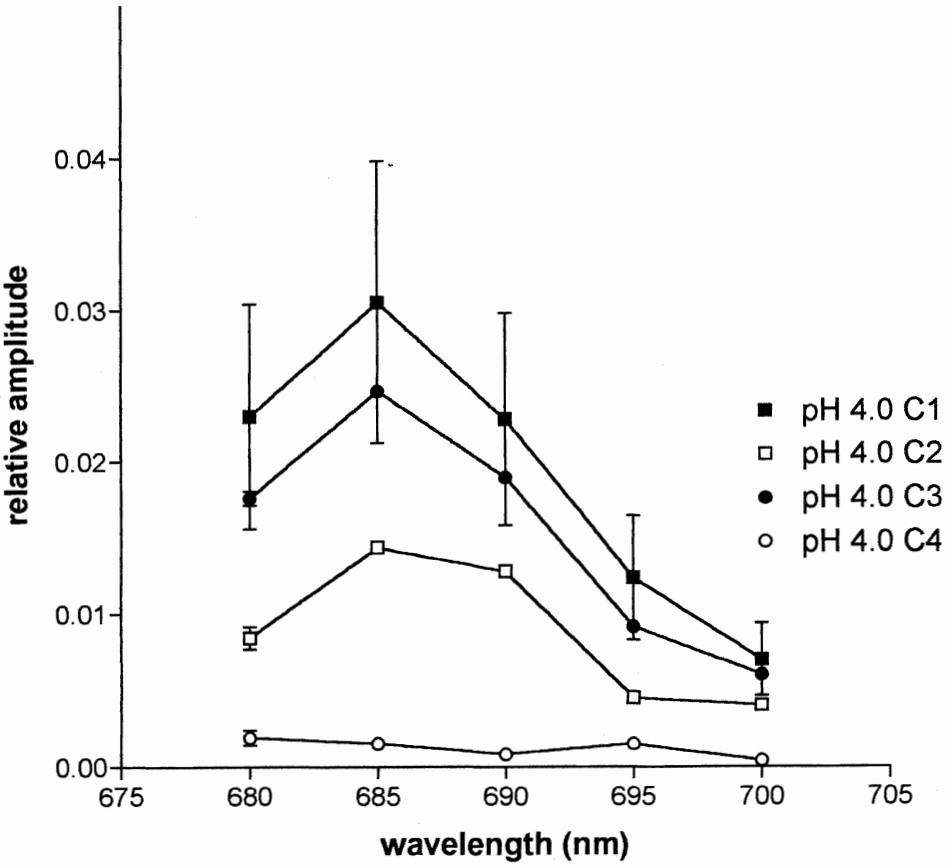
relative amplitude
0.04
0.03
0.02
0.01
0.00
675
680
685
690
695
700
705
wavelength (nm)
pH 4.0 C1
pH 4.0 C2
pH 4.0 C3
pH 4.0 C4

Figure 22. Decay associated spectra of the relative amplitude of the four kinetic components of dark adapted photosystem 2 particles at pH 4.5. The fast component is denoted as C1 (49 ps), the faster of the two intermediate components is C2 (229 ps), the slower of the intermediate components is C3 (506 ps), and the slowest component is C4 (977 ps). The spectra were averaged from two individual experiments.

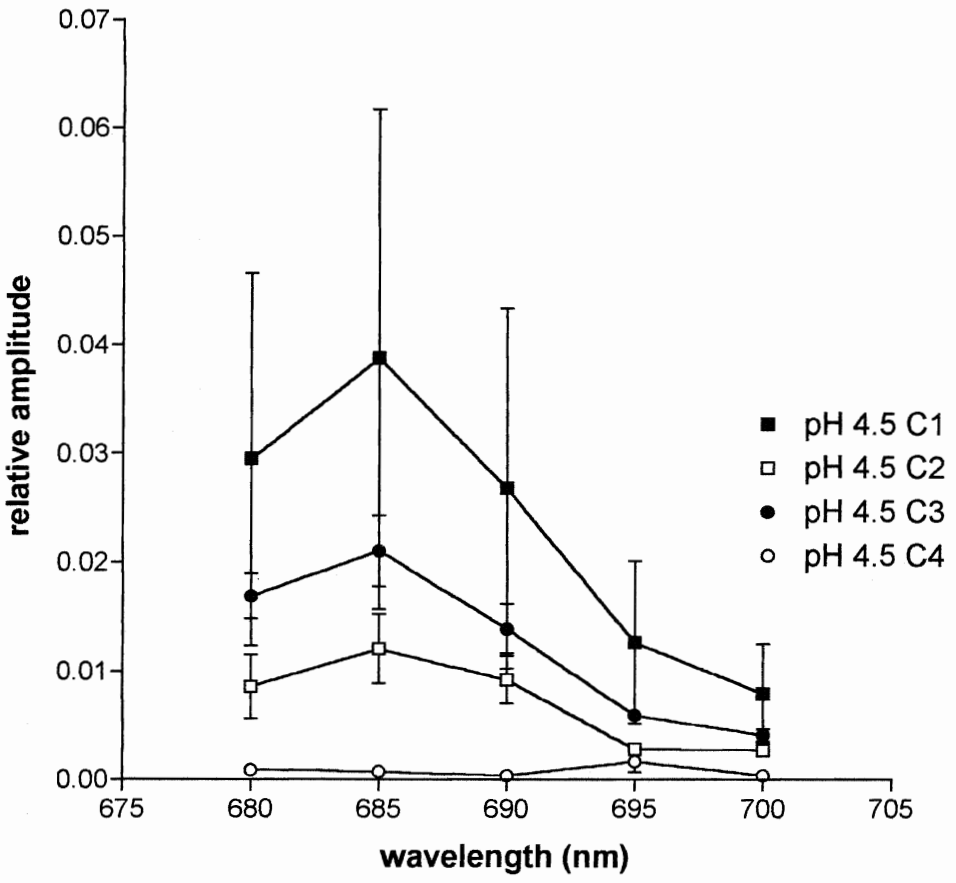
0.07
0.06
0.05
0.04
0.03
0.02
0.01
0.00
relative amplitude
675
680
685
690
695
700
705
wavelength (nm)
pH 4.5 C1
pH 4.5 C2
pH 4.5 C3
pH 4.5 C4

Figure 23. Decay associated spectra of the relative amplitude of the four kinetic components of dark adapted photosystem 2 particles at pH 5.0. The fast component is denoted as C1 (24 ps), the faster of the two intermediate components is C2 (161 ps), the slower of the intermediate components is C3 (474 ps), and the slowest component is C4 (999 ps). The spectra were averaged from three individual experiments.

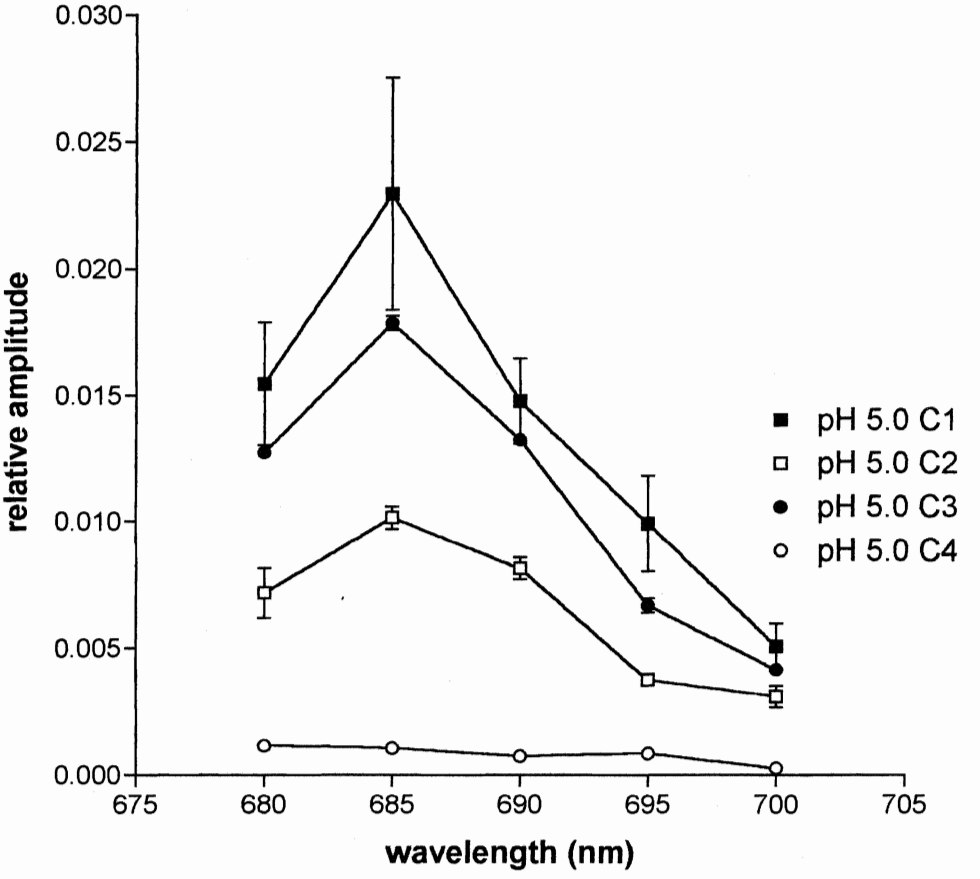
0.030
0.025
0.020
0.015
0.010
0.005
0.000
relative amplitude
675
680
685
690
695
700
705
wavelength (nm)
pH 5.0 C1
pH 5.0 C2
pH 5.0 C3
pH 5.0 C4

Figure 24. Decay associated spectra of the relative amplitude of the four kinetic components of dark adapted photosystem 2 particles at pH 5.5 (succinic acid). The fast component is denoted as C1 (42 ps), the faster of the two intermediate components is C2 (285 ps), the slower of the intermediate components is C3 (604 ps), and the slowest component is C4 (2429 ps). The spectra were averaged from two individual experiments.

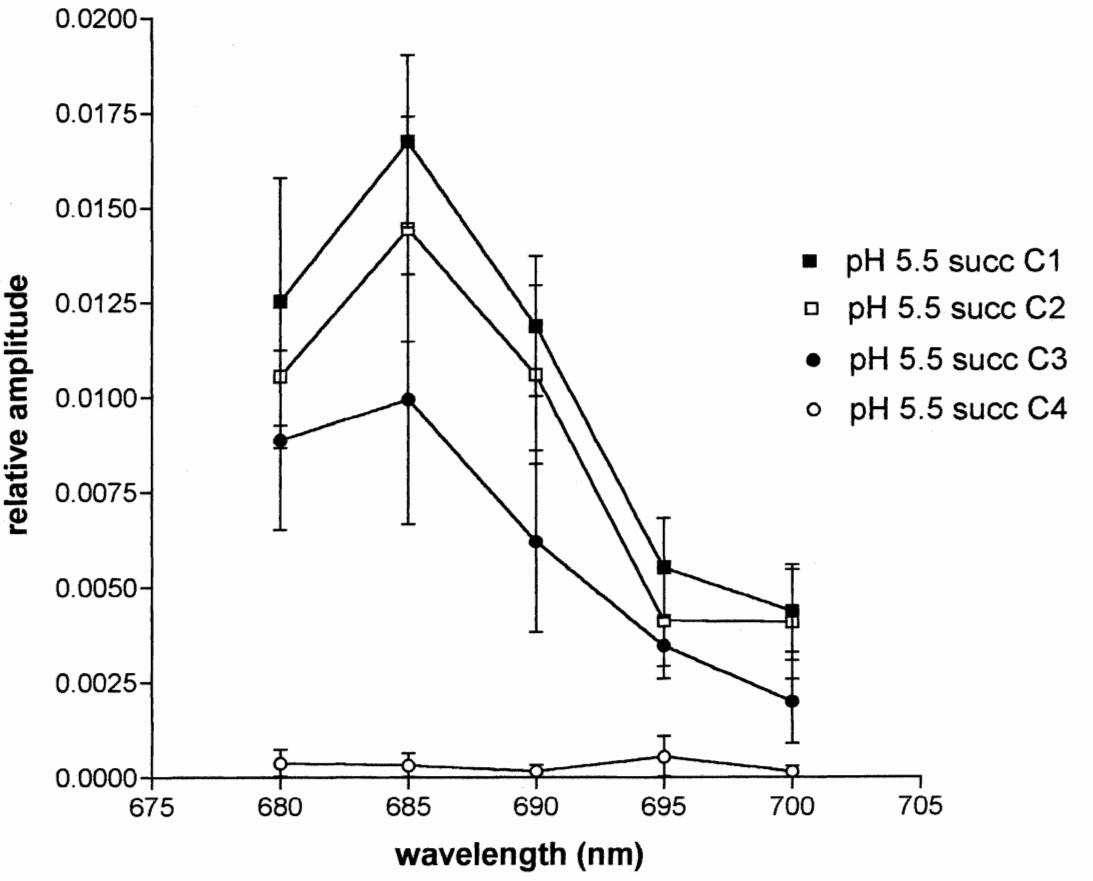
0.0200
0.0175
0.0150
0.0125
0.0100
0.0075
0.0050
0.0025
0.0000
relative amplitude
675
680
685
690
695
700
705
wavelength (nm)
pH 5.5 succ C1
pH 5.5 succ C2
pH 5.5 succ C3
pH 5.5 succ C4

Figure 25. Decay associated spectra of the relative amplitude of the four kinetic components of dark adapted photosystem 2 particles at pH 5.5 (MES). The fast component is denoted as C1 (26 ps), the faster of the two intermediate components is C2 (235 ps), the slower of the intermediate components is C3 (567 ps), and the slowest component is C4 (1282 ps). The spectra were averaged from three individual experiments.

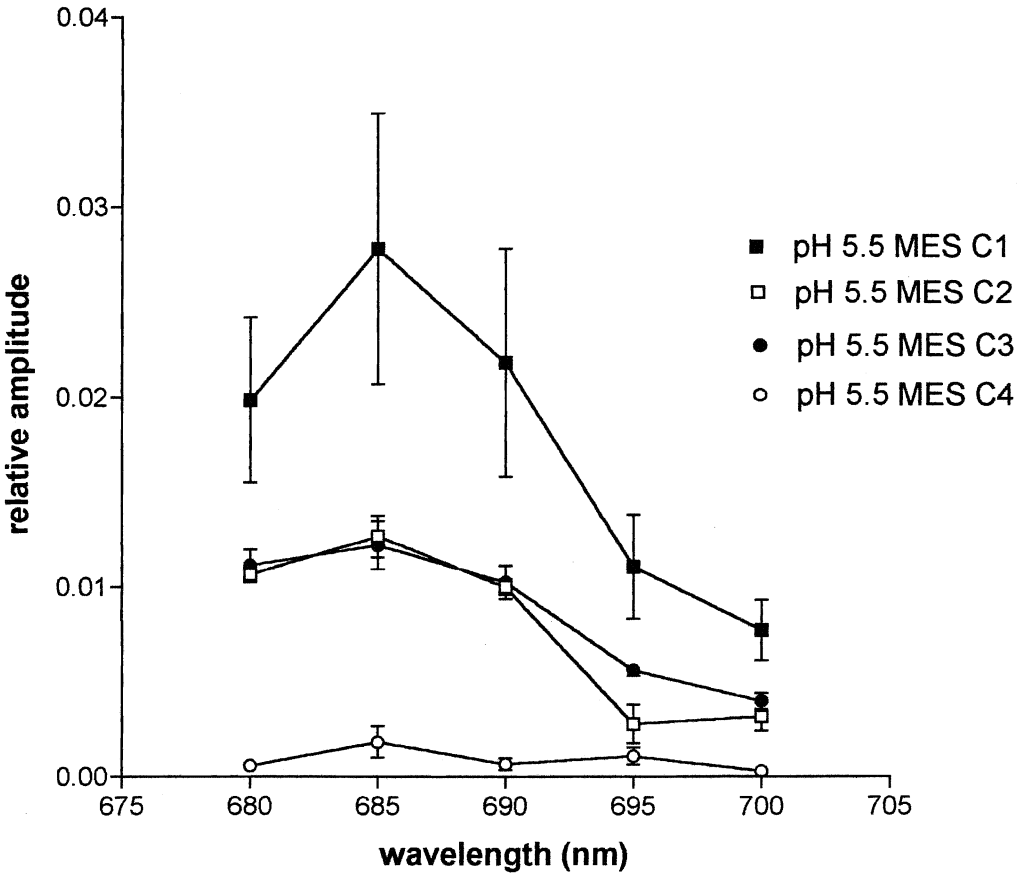
0.04
0.03
0.02
0.01
0.00
relative amplitude
675
680
685
690
695
700
705
wavelength (nm)
pH 5.5 MES C1
pH 5.5 MES C2
pH 5.5 MES C3
pH 5.5 MES C4

Figure 26. Decay associated spectra of the relative amplitude of the four kinetic components of dark adapted photosystem 2 particles at pH 6.0. The fast component is denoted as C1 (62 ps), the faster of the two intermediate components is C2 (290 ps), the slower of the intermediate components is C3 (614 ps), and the slowest component is C4 (2160 ps). The spectra were averaged from three individual experiments.

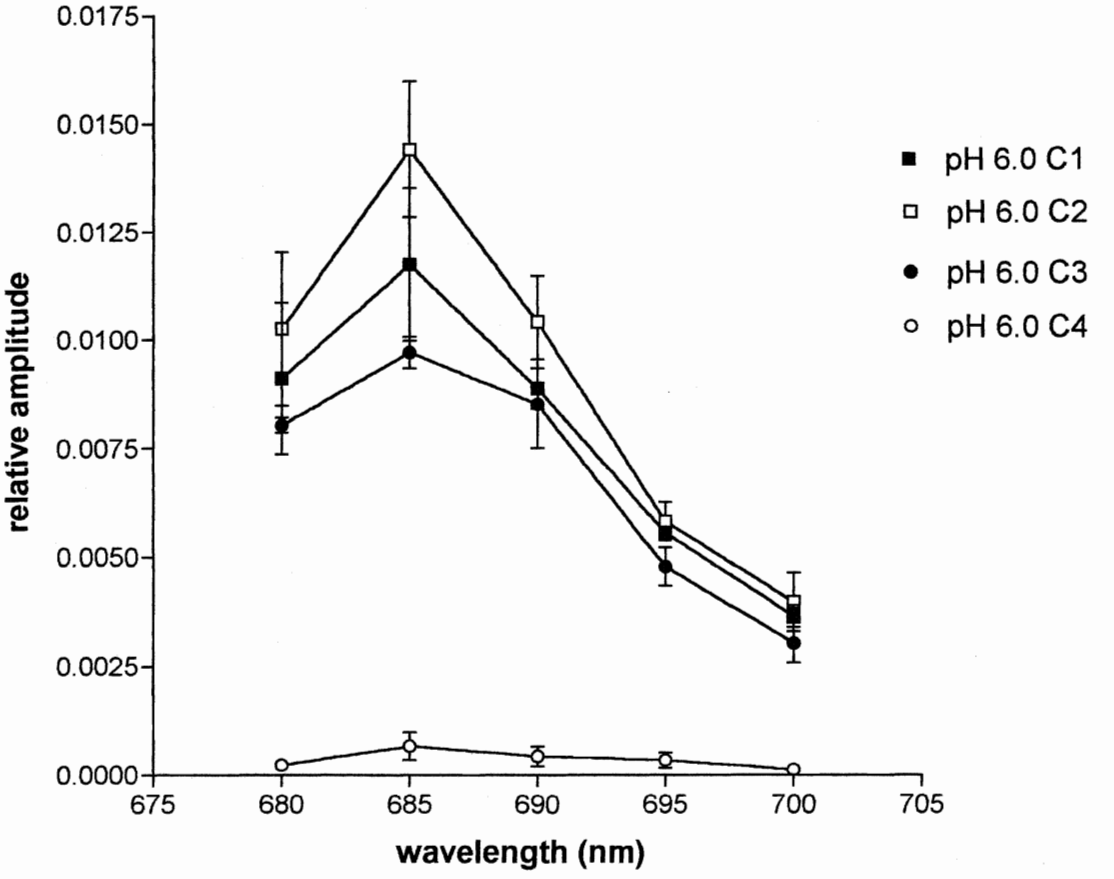
0.0175
0.0150
0.0125
0.0100
0.0075
0.0050
0.0025
0.0000
relative amplitude
675
680
685
690
695
700
705
wavelength (nm)
pH 6.0 C1
pH 6.0 C2
pH 6.0 C3
pH 6.0 C4

Figure 27. Decay associated spectra of the relative amplitude of the four kinetic components of dark adapted photosystem 2 particles at pH 6.5. The fast component is denoted as C1 (86 ps), the faster of the two intermediate components is C2 (362 ps), the slower of the intermediate components is C3 (729 ps), and the slowest component is C4 (1684 ps). The spectra were averaged from three individual experiments.

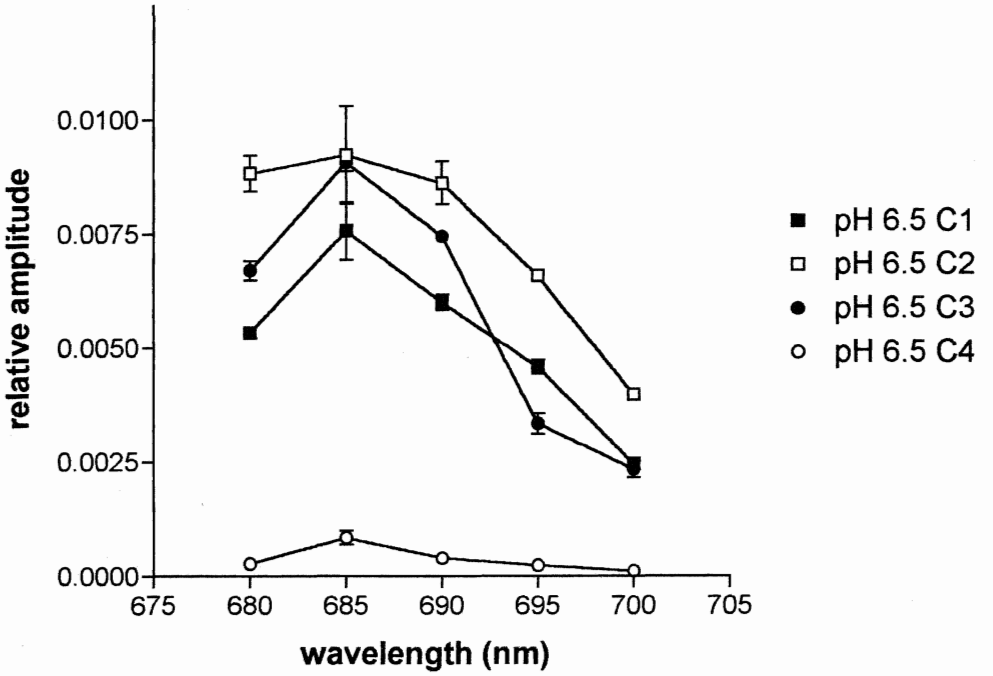
relative amplitude
0.0100
0.0075
0.0050
0.0025
0.0000
675
680
685
690
695
700
705
wavelength (nm)
pH 6.5 C1
pH 6.5 C2
pH 6.5 C3
pH 6.5 C4

Figure 28. Decay associated spectra of the relative amplitude of the four kinetic components of light saturated photosystem 2 particles at pH 4.0. The fast component is denoted as C1 (80 ps), the faster of the two intermediate components is C2 (484 ps), the slower of the intermediate components is C3 (735 ps), and the slowest component is C4 (1270 ps). The spectra were averaged from two individual experiments.

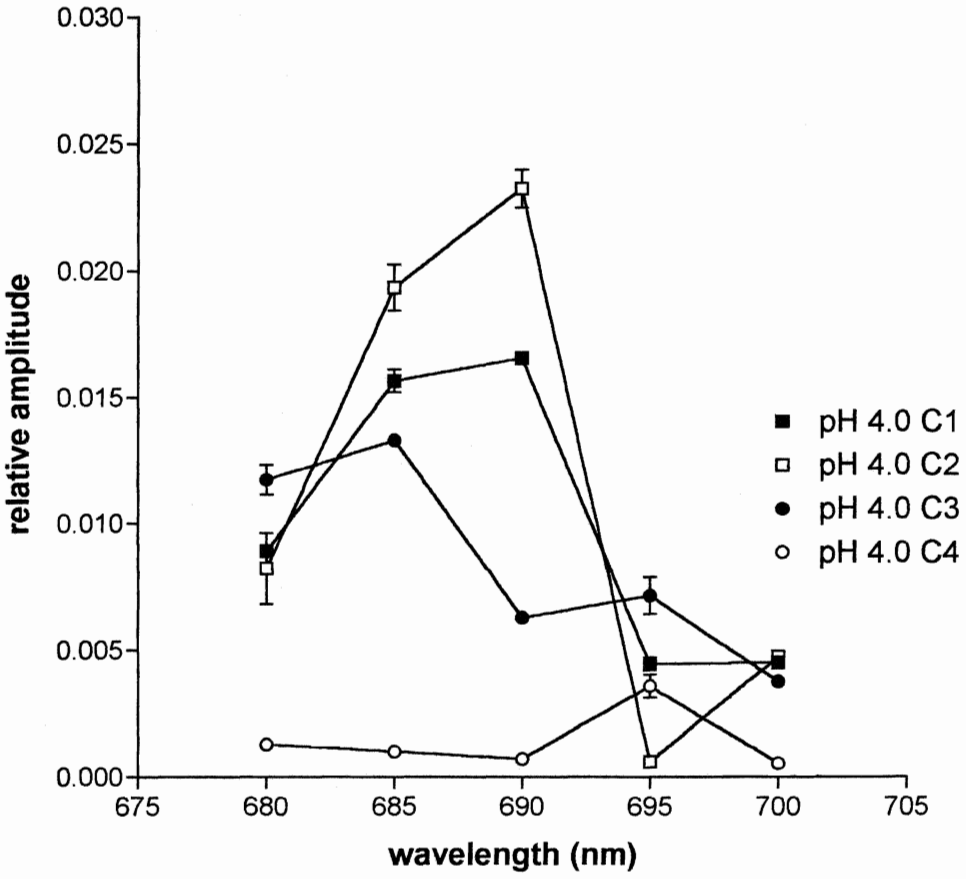
0.030
0.025
0.020
0.015
0.010
0.005
0.000
relative amplitude
675
680
685
690
695
700
705
wavelength (nm)
pH 4.0 C1
pH 4.0 C2
pH 4.0 C3
pH 4.0 C4

Figure 29. Decay associated spectra of the relative amplitude of the four kinetic components of light saturated photosystem 2 particles at pH 4.5. The fast component is denoted as C1 (75 ps), the faster of the two intermediate components is C2 (588 ps), the slower of the intermediate components is C3 (926 ps), and the slowest component is C4 (1536 ps). The spectra were averaged from three individual experiments.

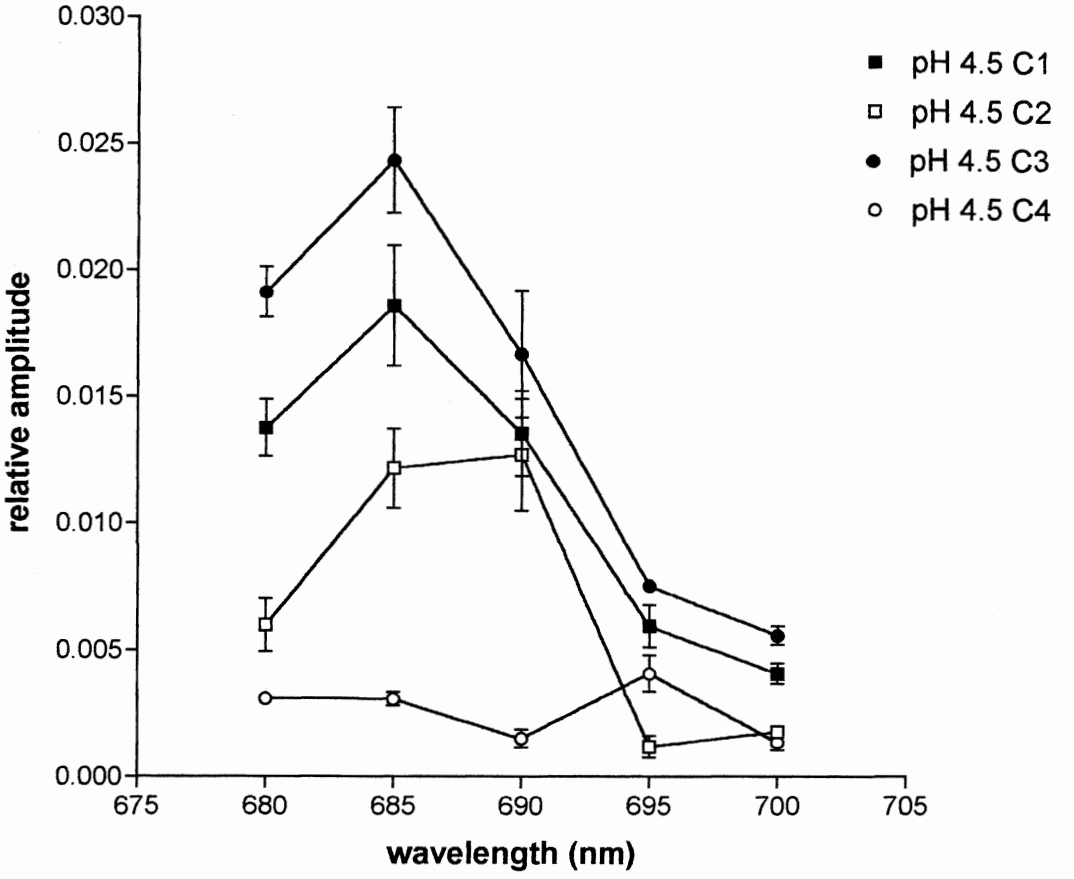
0.030
0.025
0.020
0.015
0.010
0.005
0.000
relative amplitude
675
680
685
690
695
700
705
wavelength (nm)
pH 4.5 C1
pH 4.5 C2
pH 4.5 C3
pH 4.5 C4

Figure 30. Decay associated spectra of the relative amplitude of the four kinetic components of light saturated photosystem 2 particles at pH 5.0. The fast component is denoted as C1 (36 ps), the faster of the two intermediate components is C2 (296 ps), the slower of the intermediate components is C3 (1026 ps), and the slowest component is C4 (1742 ps). The spectra were averaged from three individual experiments.

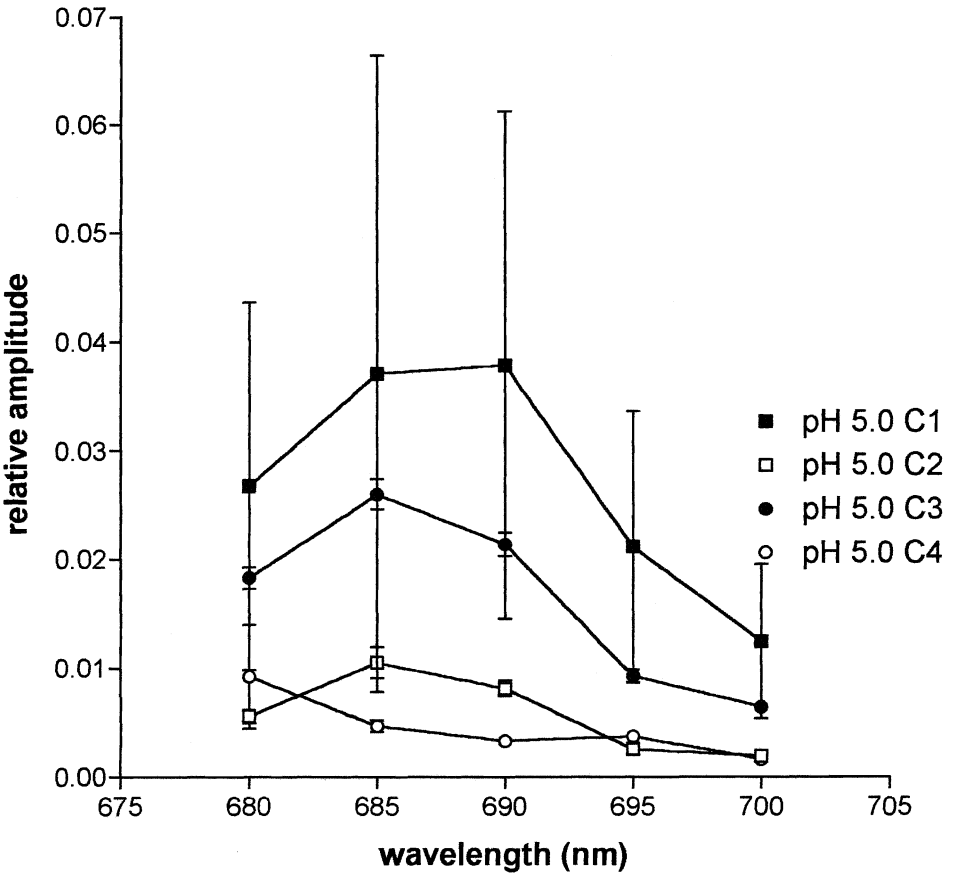
0.07
0.06
0.05
0.04
0.03
0.02
0.01
0.00
relative amplitude
675
680
685
690
695
700
705
wavelength (nm)
pH 5.0 C1
pH 5.0 C2
pH 5.0 C3
pH 5.0 C4

Figure 31. Decay associated spectra of the relative amplitude of the four kinetic components of light saturated photosystem 2 particles at pH 5.5 (succinic acid). The fast component is denoted as C1 (20 ps), the faster of the two intermediate components is C2 (154 ps), the slower of the intermediate components is C3 (1096 ps), and the slowest component is C4 (2000 ps). The spectra were averaged from three individual experiments.

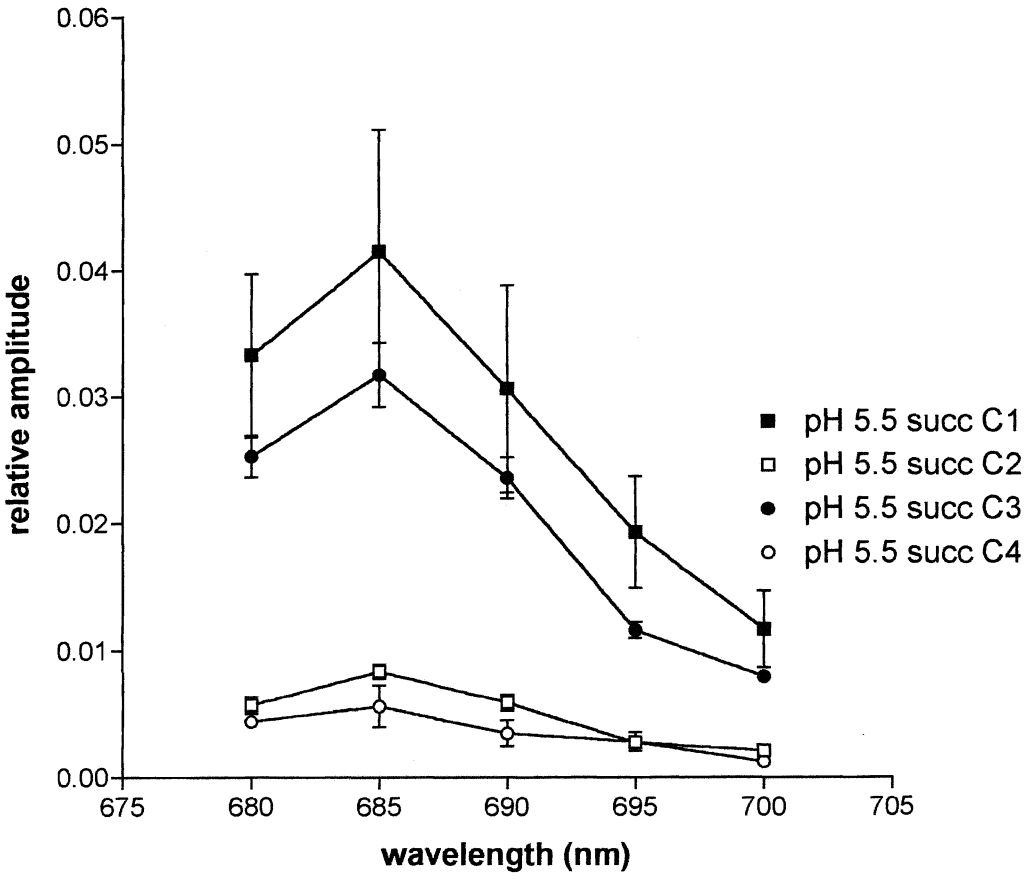
0.06
0.05
0.04
0.03
0.02
0.01
0.00
relative amplitude
675
680
685
690
695
700
705
wavelength (nm)
pH 5.5 succ C1
pH 5.5 succ C2
pH 5.5 succ C3
pH 5.5 succ C4

Figure 32. Decay associated spectra of the relative amplitude of the four kinetic components of light saturated photosystem 2 particles at pH 5.5 (MES). The fast component is denoted as C1 (16 ps), the faster of the two intermediate components is C2 (209 ps), the slower of the intermediate components is C3 (1112 ps), and the slowest component is C4 (1998 ps). The spectra were averaged from two individual experiments.

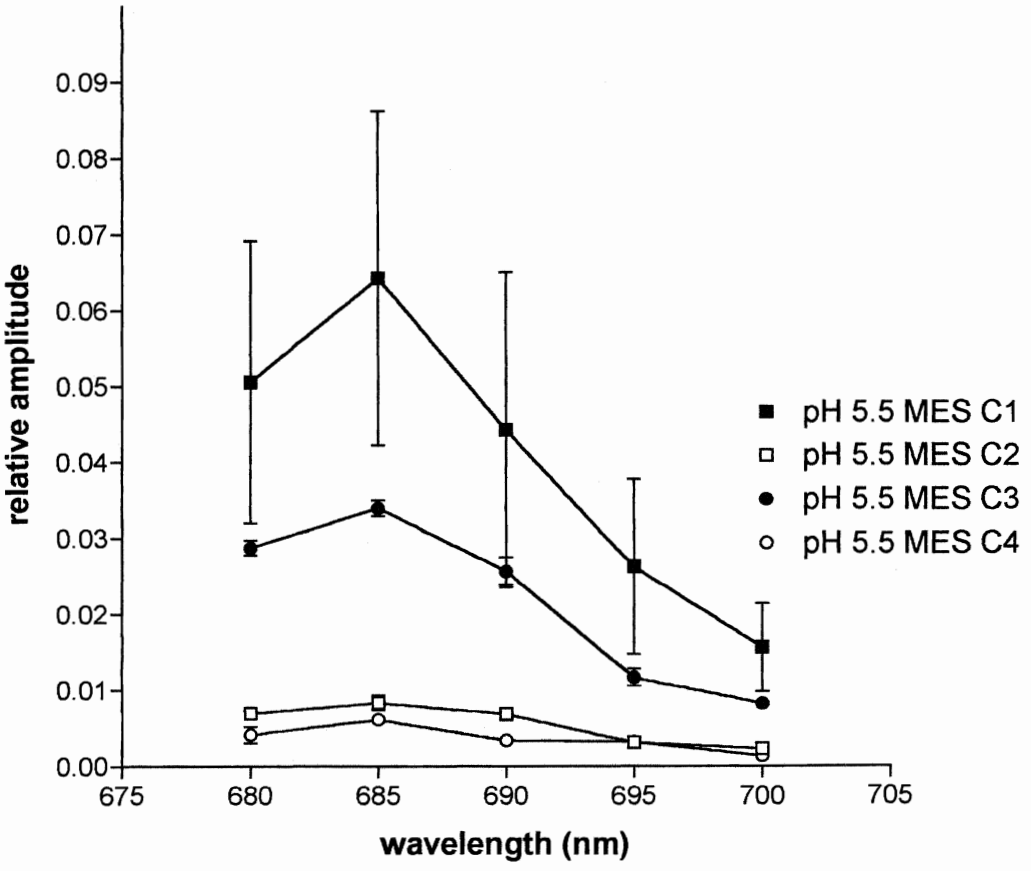
relative amplitude
0.09
0.08
0.07
0.06
0.05
0.04
0.03
0.02
0.01
0.00
675
680
685
690
695
700
705
wavelength (nm)
pH 5.5 MES C1
pH 5.5 MES C2
pH 5.5 MES C3
pH 5.5 MES C4

Figure 33. Decay associated spectra of the relative amplitude of the four kinetic components of light saturated photosystem 2 at pH 6.0. The fast component is denoted as C1 (61 ps), the faster of the two intermediate components is C2 (364 ps), the slower of the intermediate components is C3 (1160 ps), and the slowest component is C4 (2137 ps). The spectra were averaged from two individual experiments.

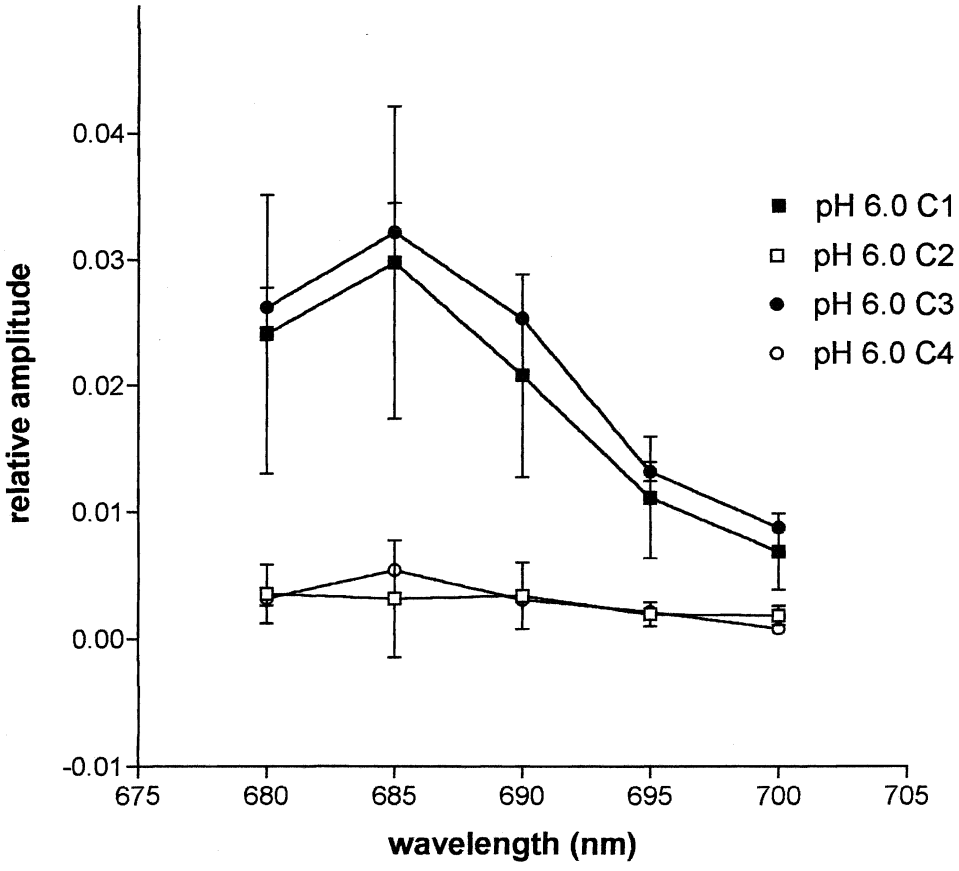
relative amplitude
0.04
0.03
0.02
0.01
0.00
-0.01
675
680
685
690
695
700
705
wavelength (nm)
pH 6.0 C1
pH 6.0 C2
pH 6.0 C3
pH 6.0 C4

Figure 34. Decay associated spectra of the relative amplitude of the four kinetic components of sodium dithionite treated photosystem 2 particles pH 4.0. The fast component is denoted as C1 (96 ps), the faster of the two intermediate components is C2 (342 ps), the slower of the intermediate components is C3 (892 ps), and the slowest component is C4 (2931 ps). The spectra were averaged from three individual experiments.

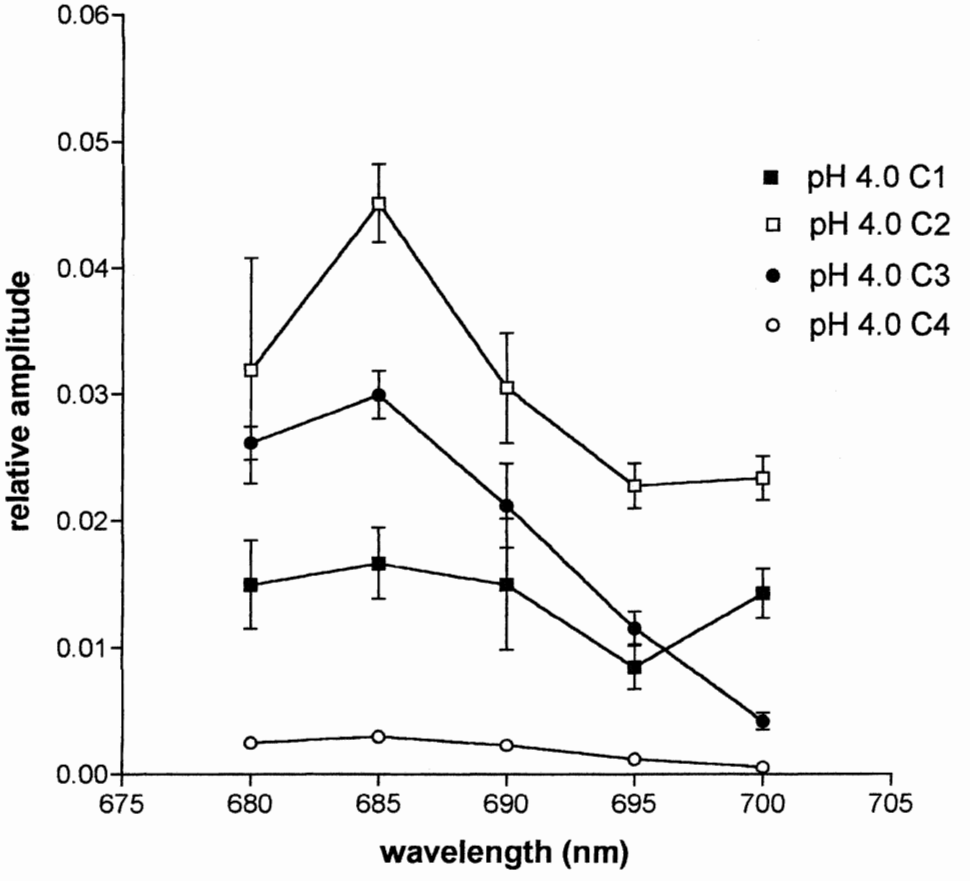
0.06
0.05
0.04
0.03
0.02
0.01
0.00
relative amplitude
675
680
685
690
695
700
705
wavelength (nm)
pH 4.0 C1
pH 4.0 C2
pH 4.0 C3
pH 4.0 C4

Figure 35. Decay associated spectra of the relative amplitude of the four kinetic components of sodium dithionite treated photosystem 2 particles at pH 4.5. The fast component is denoted as C1 (117 ps), the faster of the two intermediate components is C2 (429 ps), the slower of the intermediate components is C3 (1094 ps), and the slowest component is C4 (3310 ps). The spectra were averaged from three individual experiments.

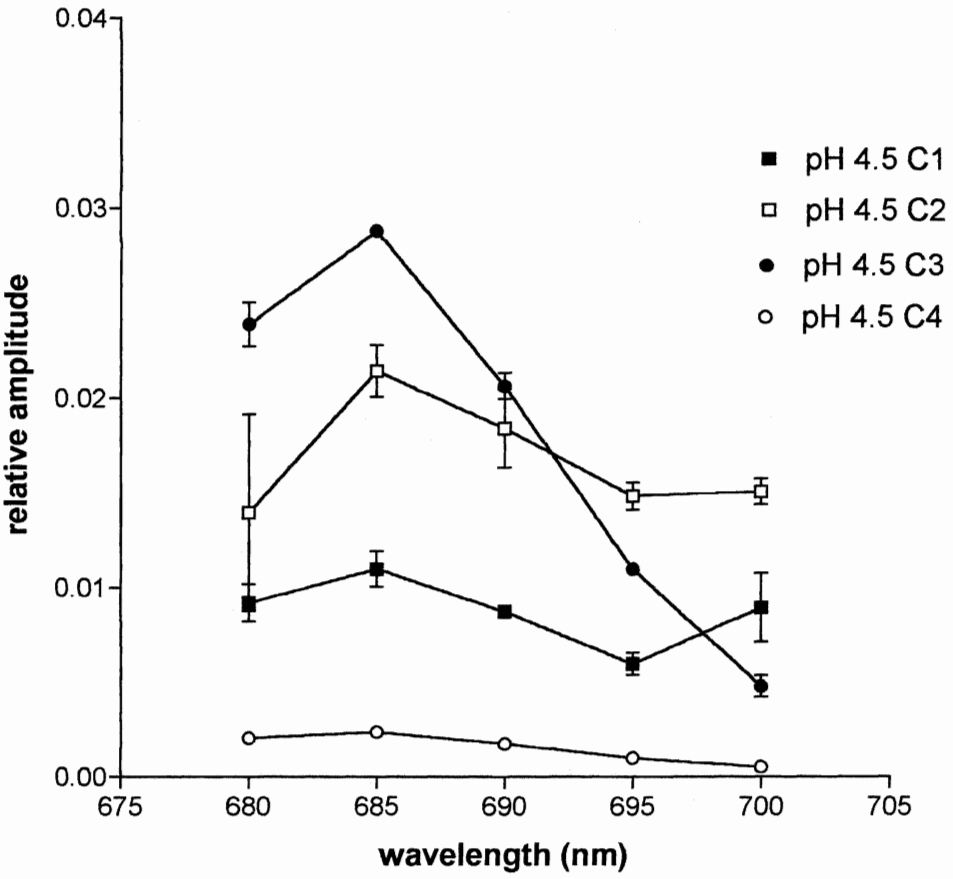
0.04
0.03
0.02
0.01
0.00
relative amplitude
675
680
685
690
695
700
705
wavelength (nm)
pH 4.5 C1
pH 4.5 C2
pH 4.5 C3
pH 4.5 C4

Figure 36. Decay associated spectra of the relative amplitude of the four kinetic components of sodium dithionite treated photosystem 2 particles at pH 5.0. The fast component is denoted as C1 (125 ps), the faster of the two intermediate components is C2 (437 ps), the slower of the intermediate components is C3 (1161 ps), and the slowest component is C4 (3717 ps). The spectra were averaged from three individual experiments.

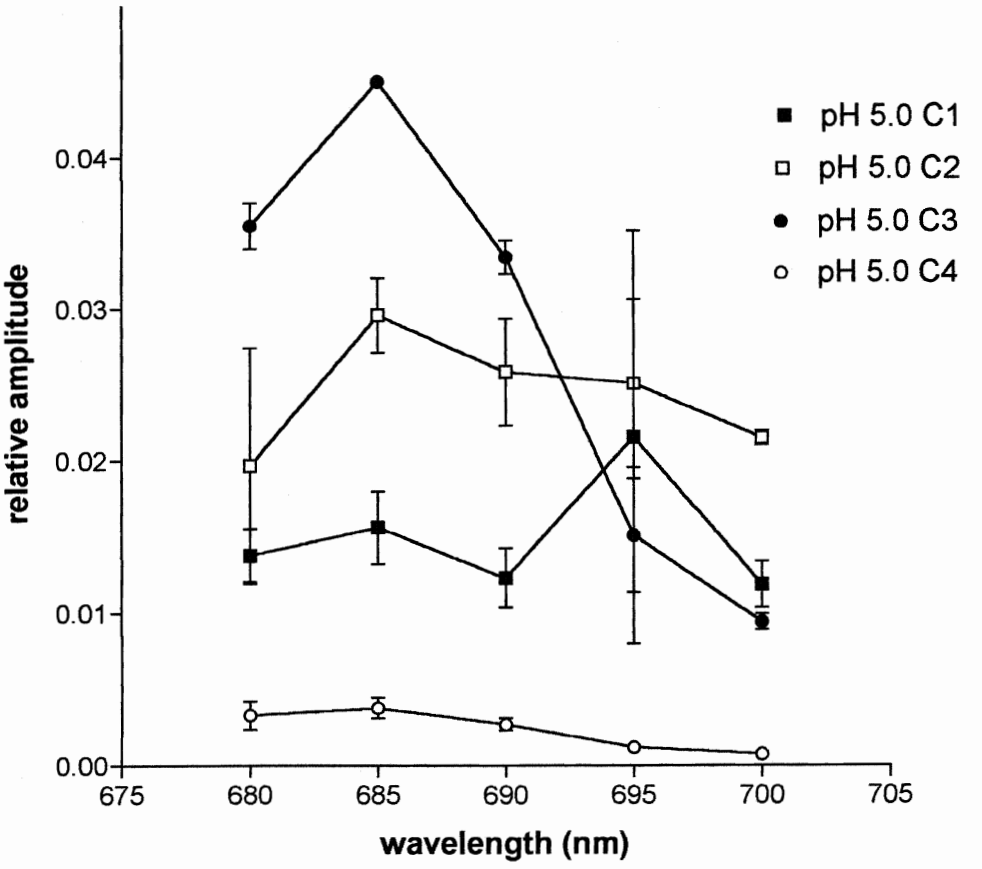
relative amplitude
0.04
0.03
0.02
0.01
0.00
675
680
685
690
695
700
705
wavelength (nm)
pH 5.0 C1
pH 5.0 C2
pH 5.0 C3
pH 5.0 C4

Figure 37. Decay associated spectra of the relative amplitude of the four kinetic components of sodium dithionite treated photosystem 2 particles at pH 5.5 (succinic acid). The fast component is denoted as C1 (92 ps), the faster of the two intermediate components is C2 (415 ps), the slower of the intermediate components is C3 (1181 ps), and the slowest component is C4 (3804 ps). The spectra were averaged from three individual experiments.

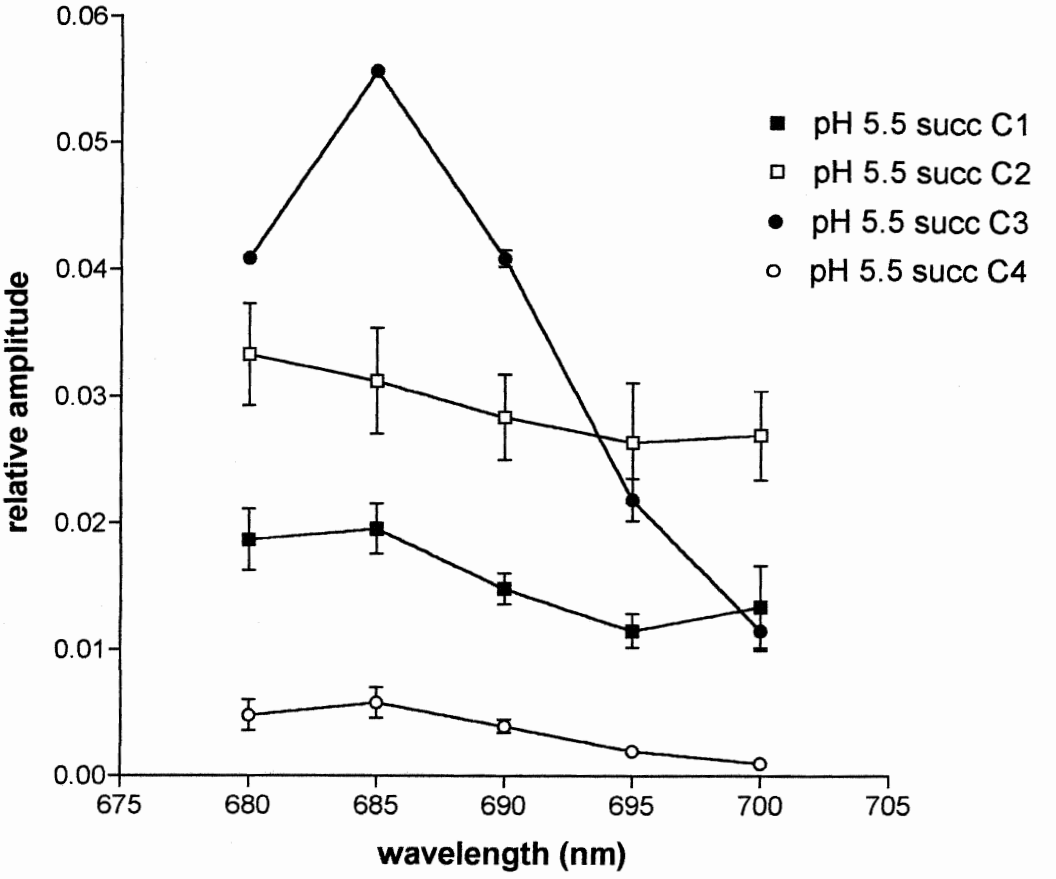
0.06
0.05
0.04
0.03
0.02
0.01
0.00
relative amplitude
675
680
685
690
695
700
705
wavelength (nm)
pH 5.5 succ C1
pH 5.5 succ C2
pH 5.5 succ C3
pH 5.5 succ C4

Figure 38. Decay associated spectra of the relative amplitude of the four kinetic components of sodium dithionite treated photosystem 2 particles at pH 5.5 (MES). The fast component is denoted as C1 (93 ps), the faster of the two intermediate components is C2 (450 ps), the slower of the intermediate components is C3 (1293 ps), and the slowest component is C4 (4458 ps). The spectra were averaged from three individual experiments.

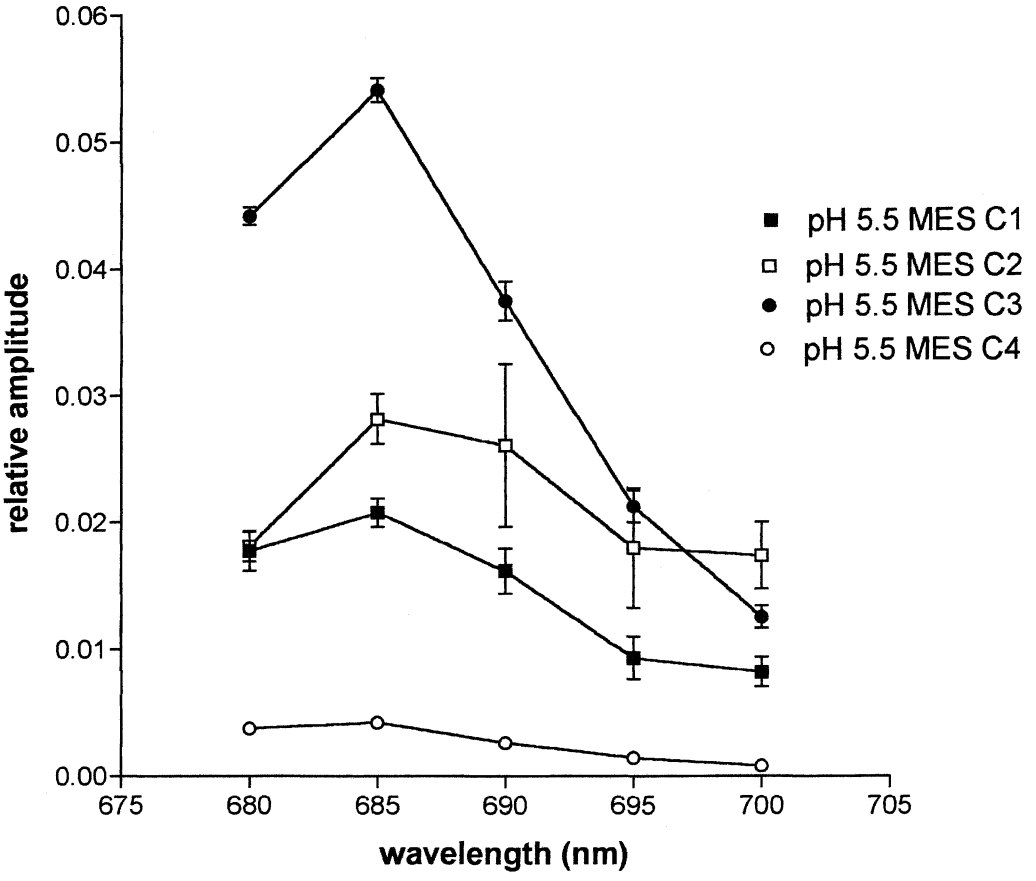
0.06
0.05
0.04
0.03
0.02
0.01
0.00
relative amplitude
675
680
685
690
695
700
705
wavelength (nm)
pH 5.5 MES C1
pH 5.5 MES C2
pH 5.5 MES C3
pH 5.5 MES C4

Figure 39. Decay associated spectra of the relative amplitude of the four kinetic components of sodium dithionite treated photosystem 2 particles at pH 6.0. The fast component is denoted as C1 (109 ps), the faster of the two intermediate components is C2 (433 ps), the slower of the intermediate components is C3 (1285 ps), and the slowest component is C4 (4458 ps). The spectra were averaged from three individual experiments.

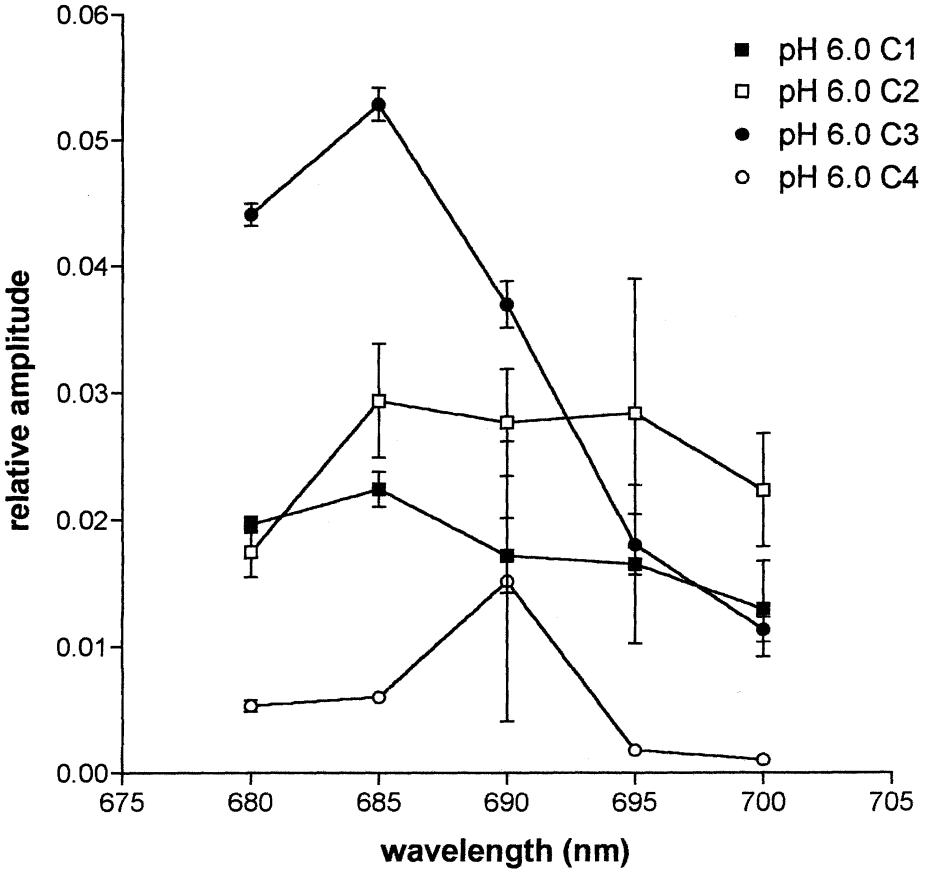
0.06
0.05
0.04
0.03
0.02
0.01
0.00
relative amplitude
675
680
685
690
695
700
705
wavelength (nm)
pH 6.0 C1
pH 6.0 C2
pH 6.0 C3
pH 6.0 C4

Figure 40. Decay associated spectra of the relative amplitude of the four kinetic components of sodium dithionite treated photosystem 2 particles at pH 6.5. The fast component is denoted as C1 (102 ps), the faster of the two intermediate components is C2 (418 ps), the slower of the intermediate components is C3 (1284 ps), and the slowest component is C4 (5713 ps). The spectra were averaged from three individual experiments.

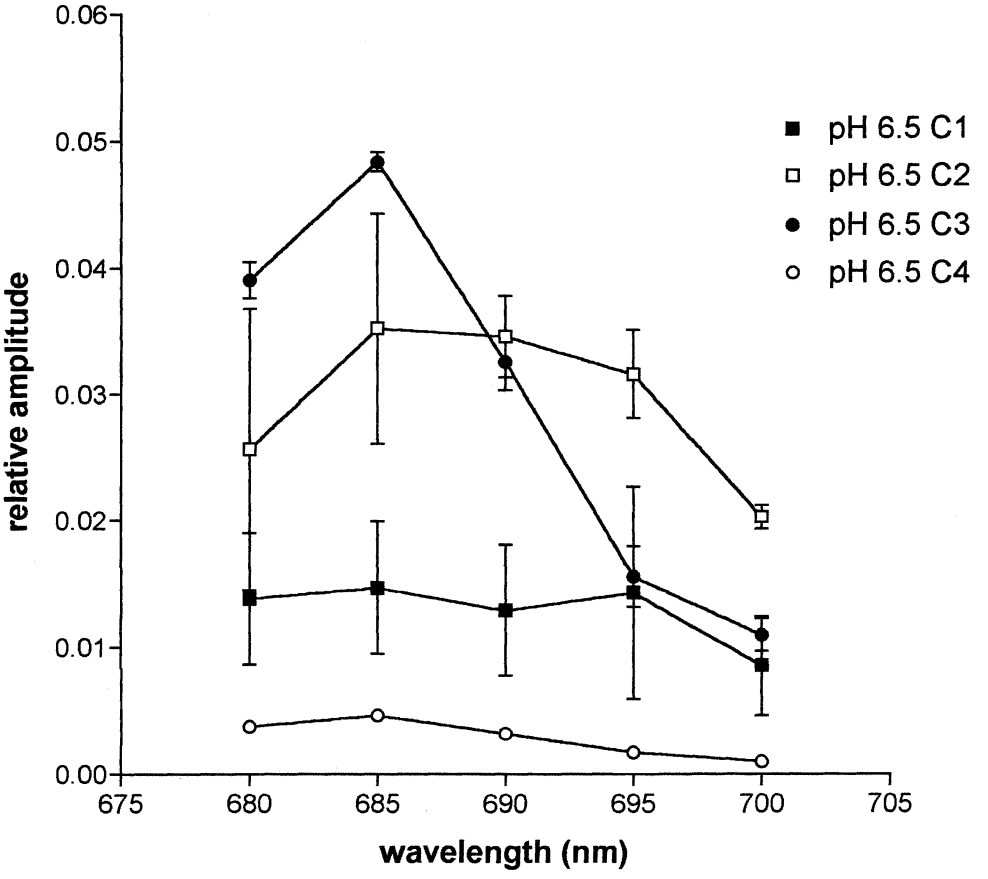
0.06
0.05
0.04
0.03
0.02
0.01
0.00
relative amplitude
675
680
685
690
695
700
705
wavelength (nm)
pH 6.5 C1
pH 6.5 C2
pH 6.5 C3
pH 6.5 C4

Figure 41. Steady State Fluorescence Yield of dark adapted (Fo), light saturated (Fm) and sodium dithionite (Dithionite) treated photosystem 2 particles as a function of pH (pH 5.5 MES). All values are an average of three (except for Fo [pH 4.5] and Fm [pH 4.0, 5.5, and 6.0] which are an average of two) individual experiments.

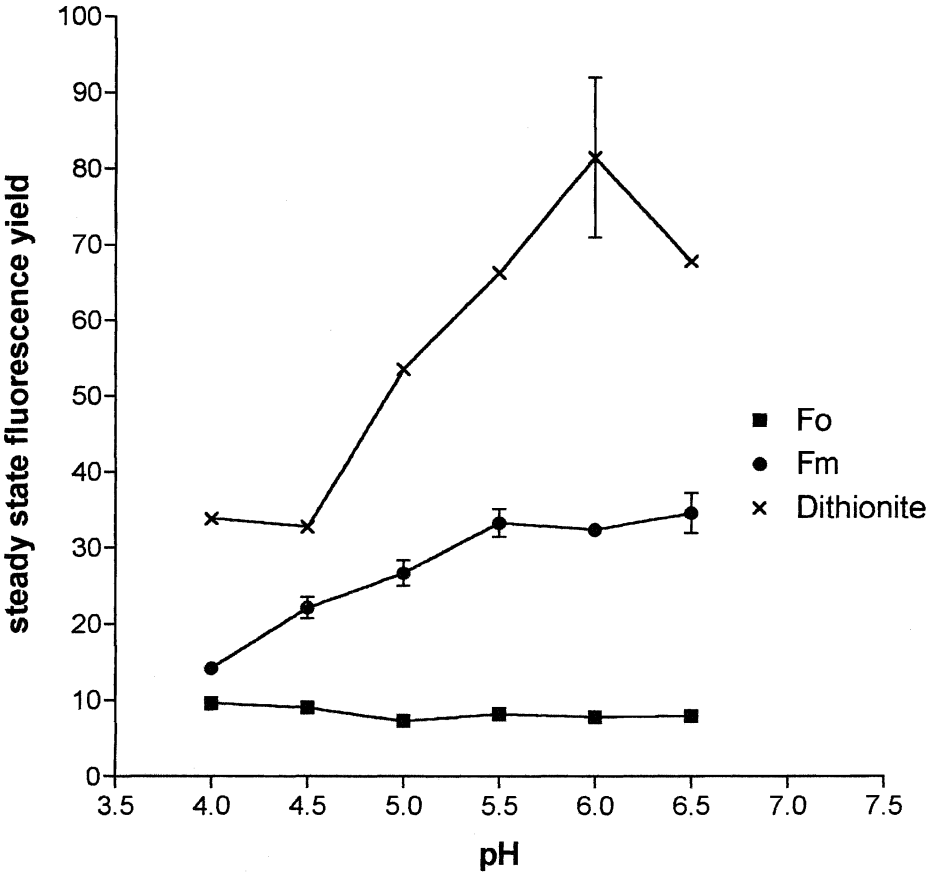
steady state fluorescence yield
100
90
80
70
60
50
40
30
20
10
0
3.5
4.0
4.5
5.0
5.5
6.0
6.5
7.0
7.5
pH
Fo
Fm
Dithionite

Figure 42. Relative yield of the four components of dark adapted photosystem 2 particles as a function of pH (pH 5.5 succinic acid). The fast component is denoted as C1, the faster of the two intermediate components is C2, the slower of the intermediate components is C3, and the slowest component is C4. All values are an average of three (except for pH 4.5 and 5.5 which are an average of two) individual experiments.

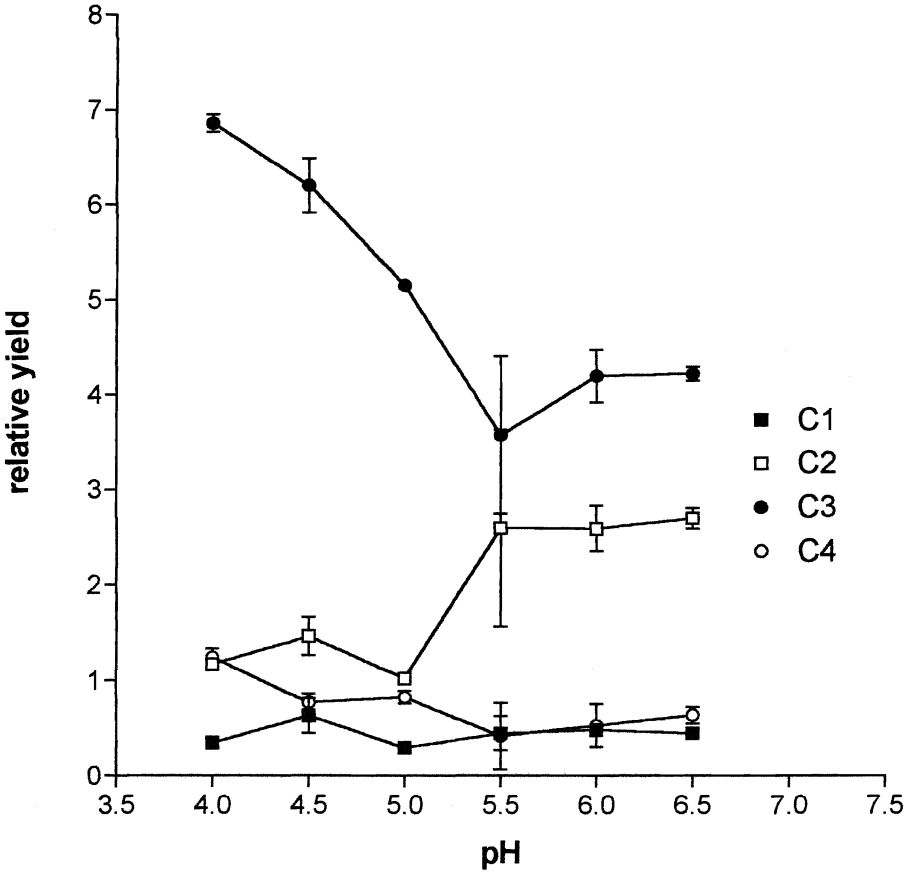
relative yield
pH
C1
C2
C3
C4
0
1
2
3
4
5
6
7
8
3.5
4.0
4.5
5.0
5.5
6.0
6.5
7.0
7.5

Figure 43. Lifetimes (in picoseconds) of the four components of dark adapted photosystem 2 particles as a function of pH (pH 5.5 succinic acid). The fast component is denoted as C1, the faster of the two intermediate components is C2, the slower of the intermediate components is C3, and the slowest component is C4. All values are an average of three (except for pH 4.5 and 5.5 which are an average of two) individual experiments.

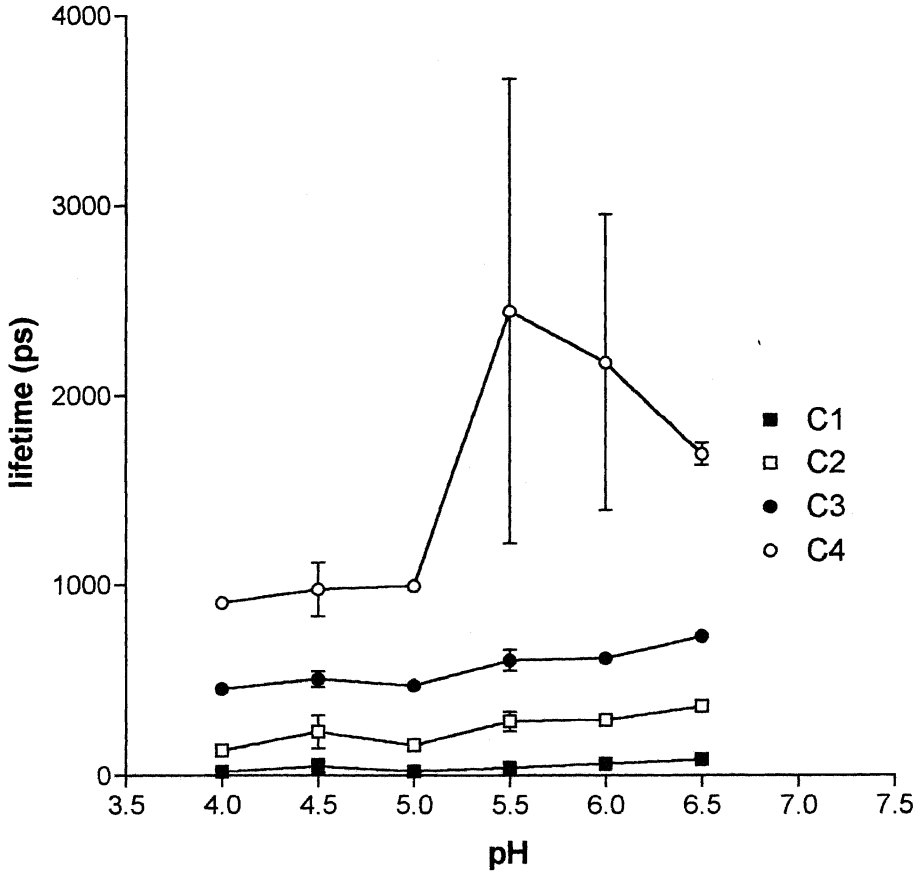
4000
3000
2000
1000
0
lifetime (ps)
3.5
4.0
4.5
5.0
5.5
6.0
6.5
7.0
7.5
pH
C1
C2
C3
C4

Figure 44. Average amplitude of the four components of dark adapted photosystem 2 particles as a function of pH (pH 5.5 succinic acid). The fast component is denoted as C1, the faster of the two intermediate components is C2, the slower of the intermediate components is C3, and the slowest component is C4. All values are an average of three (except for pH 4.5 and 5.5 which are an average of two) individual experiments.

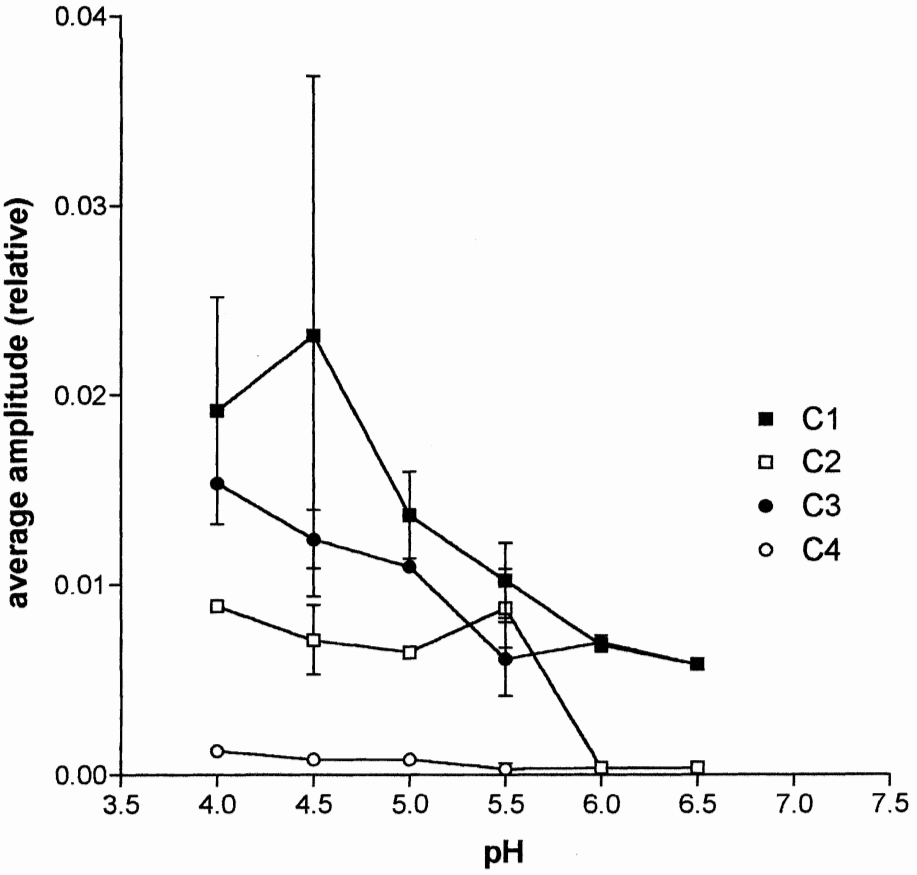
0.04
0.03
0.02
0.01
0.00
average amplitude (relative)
3.5
4.0
4.5
5.0
5.5
6.0
6.5
7.0
7.5
pH
C1
C2
C3
C4

Figure 45. Relative yield of the four components of light saturated photosystem 2 particles as a function of pH (pH 5.5 MES). The fast component is denoted as C1, the faster of the two intermediate components is C2, the slower of the intermediate components is C3, and the slowest component is C4. All values are an average of three (except for pH 4.0, 5.5, and 6.0 which are an average of two) individual experiments.

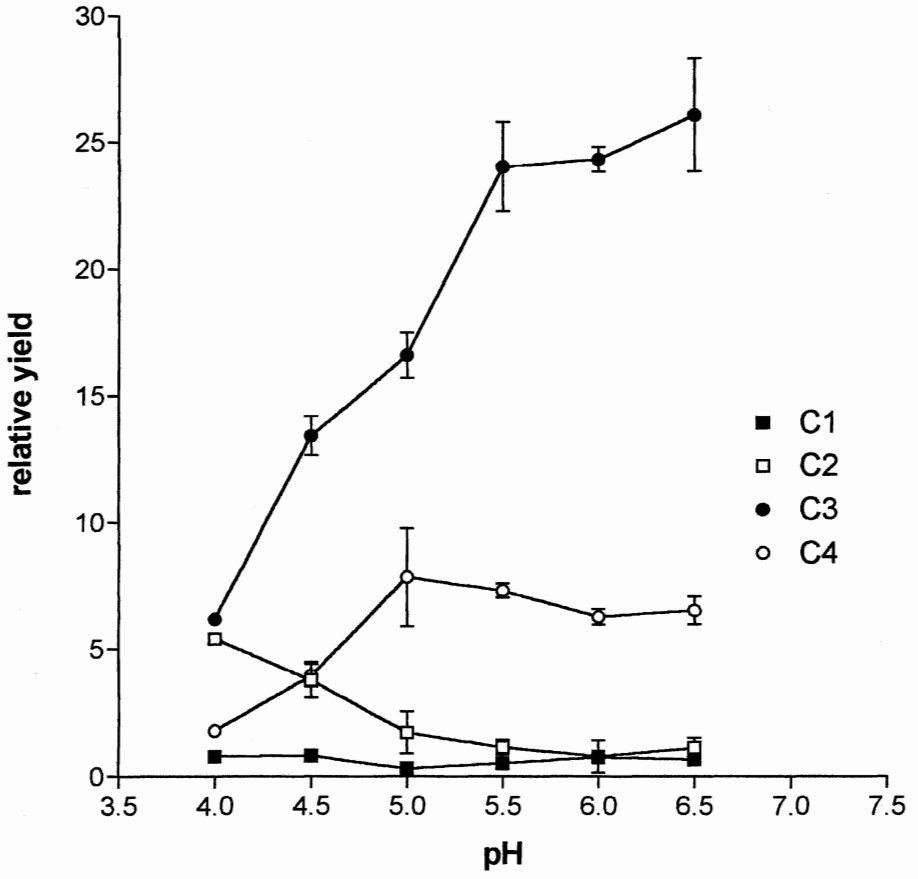
30
25
20
15
10
5
0
relative yield
3.5
4.0
4.5
5.0
5.5
6.0
6.5
7.0
7.5
pH
C1
C2
C3
C4

Figure 46. Lifetimes (in picoseconds) of the four components of light saturated photosystem 2 particles as a function of pH (pH 5.5 MES). The fast component is denoted as C1, the faster of the two intermediate components is C2, the slower of the intermediate components is C3, and the slowest component is C4. All values are an average of three (except for pH 4.0, 5.5, and 6.0 which is an average of two) individual experiments.

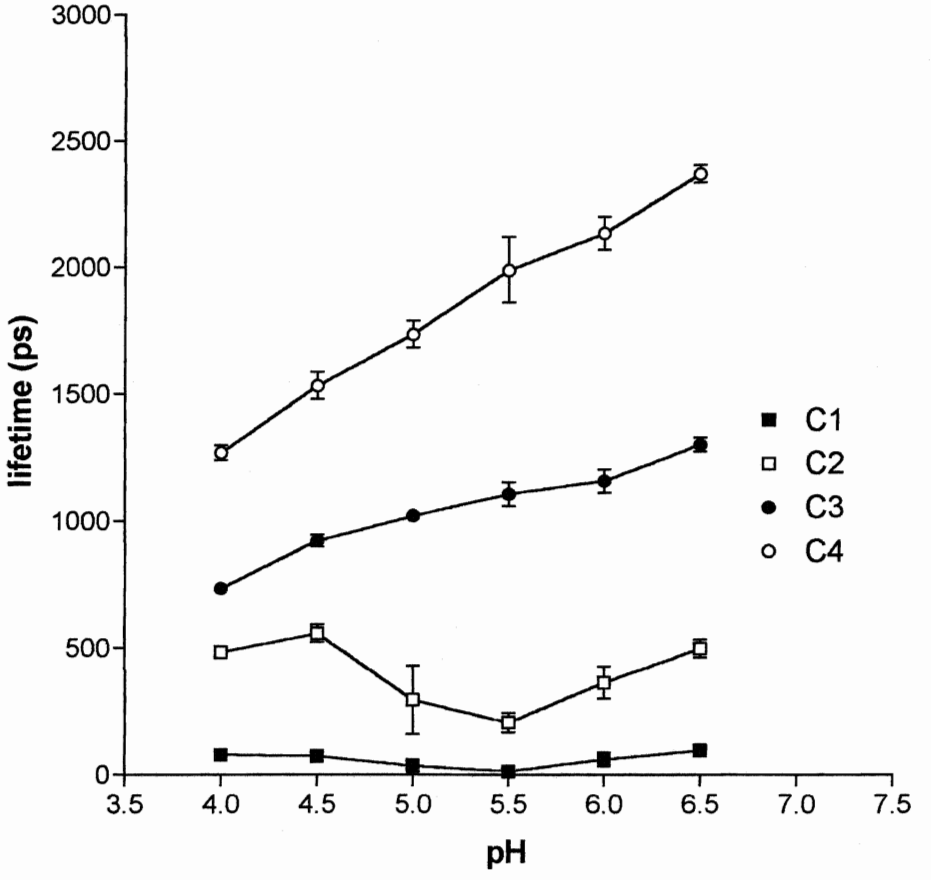
3000
2500
2000
1500
1000
500
0
lifetime (ps)
3.5
4.0
4.5
5.0
5.5
6.0
6.5
7.0
7.5
pH
C1
C2
C3
C4

Figure 47. Average amplitude of the four components of light saturated photosystem 2 particles as a function of pH (pH 5.5 MES). The fast component is denoted as C1, the faster of the two intermediate components is C2, the slower of the intermediate components is C3, and the slowest component is C4. All values are an average of three (except for pH 4.0, 5.5, and 6.0 which are an average of two) individual experiments.

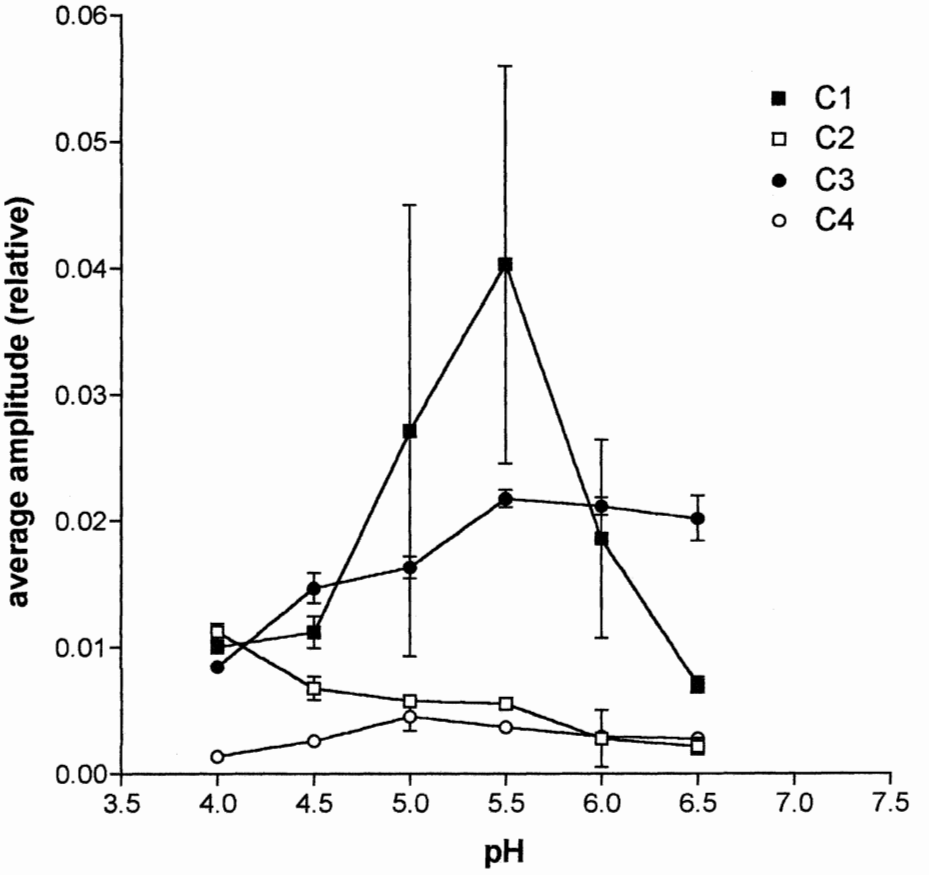
0.06
0.05
0.04
0.03
0.02
0.01
0.00
average amplitude (relative)
3.5
4.0
4.5
5.0
5.5
6.0
6.5
7.0
7.5
pH
C1
C2
C3
C4

Figure 48. Relative yield of the four components of sodium dithionite treated photosystem 2 particles as a function of pH (pH 5.5 MES). The fast component is denoted as C1, the faster of the two intermediate components is C2, the slower of the intermediate components is C3, and the slowest component is C4. All values are an average of three individual experiments.

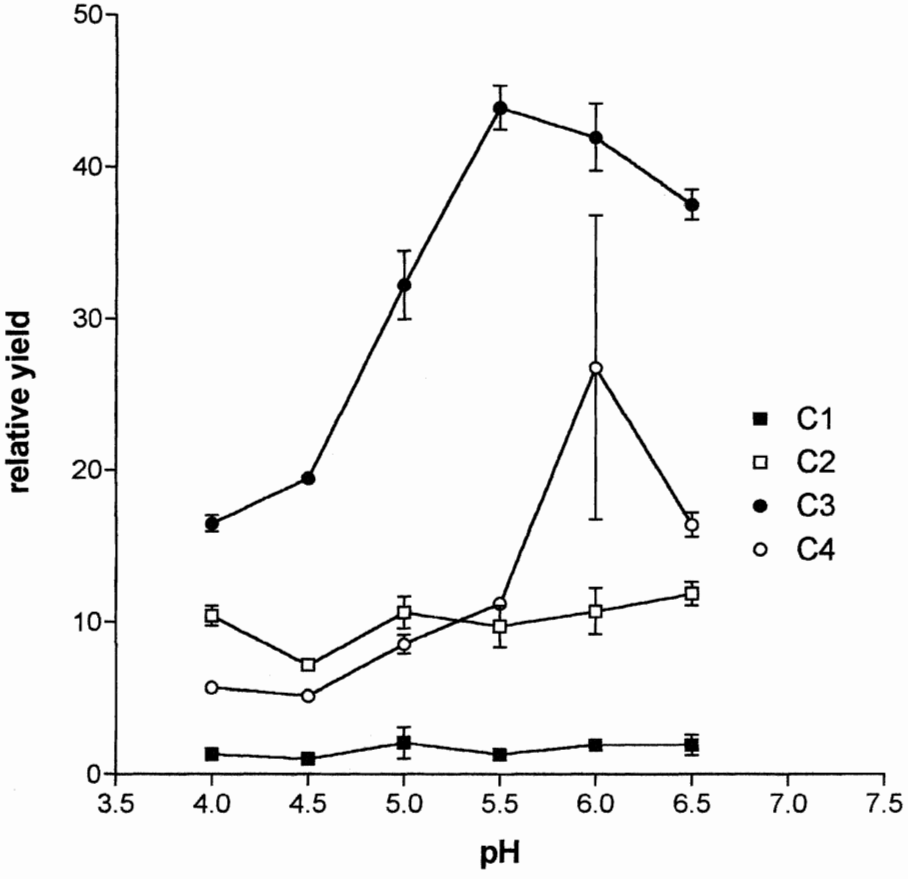
50
40
30
20
10
0
relative yield
3.5
4.0
4.5
5.0
5.5
6.0
6.5
7.0
7.5
pH
C1
C2
C3
C4

Figure 49. Lifetimes (in picoseconds) of the four components of sodium dithionite treated photosystem 2 particles as a function of pH (pH 5.5 MES). The fast component is denoted as C1, the faster of the two intermediate components is C2, the slower of the intermediate components is C3, and the slowest component is C4. All values are an average of three individual experiments.

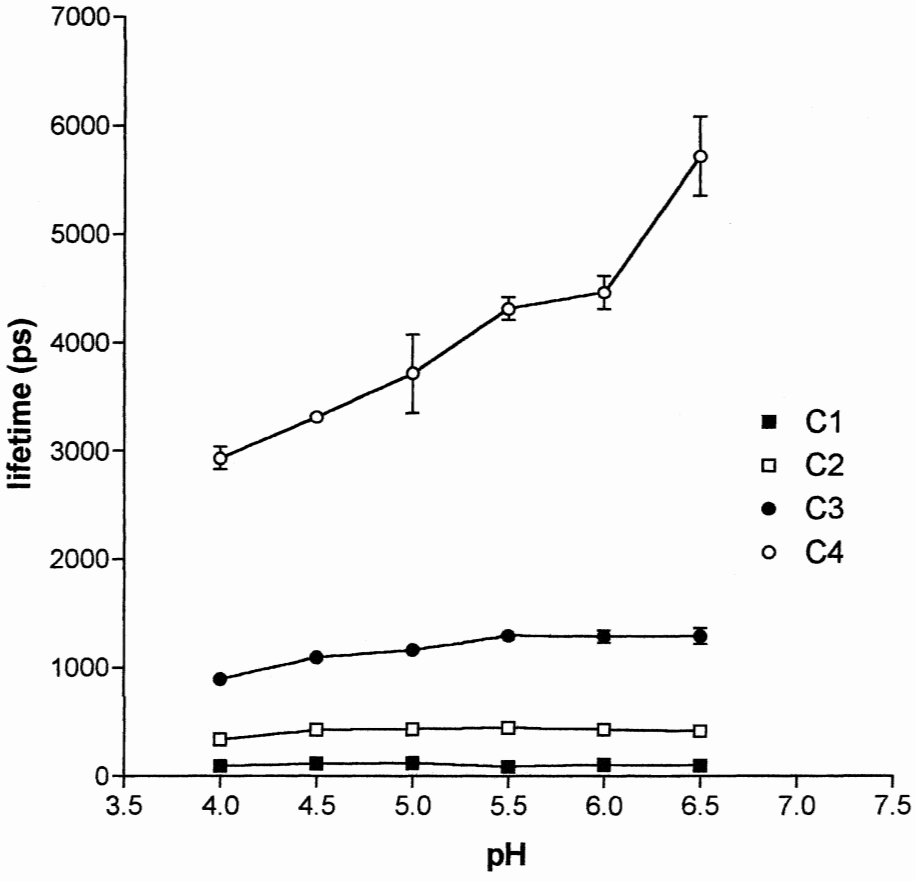
7000
6000
5000
4000
3000
2000
1000
0
lifetime (ps)
3.5
4.0
4.5
5.0
5.5
6.0
6.5
7.0
7.5
pH
C1
C2
C3
C4

Figure 50. Average amplitude of the four components of sodium dithionite treated photosystem 2 particles as a function of pH (pH 5.5 MES). The fast component is denoted as C1, the faster of the two intermediate components is C2, the slower of the intermediate components is C3, and the slowest component is C4. All values are an average of three individual experiments.

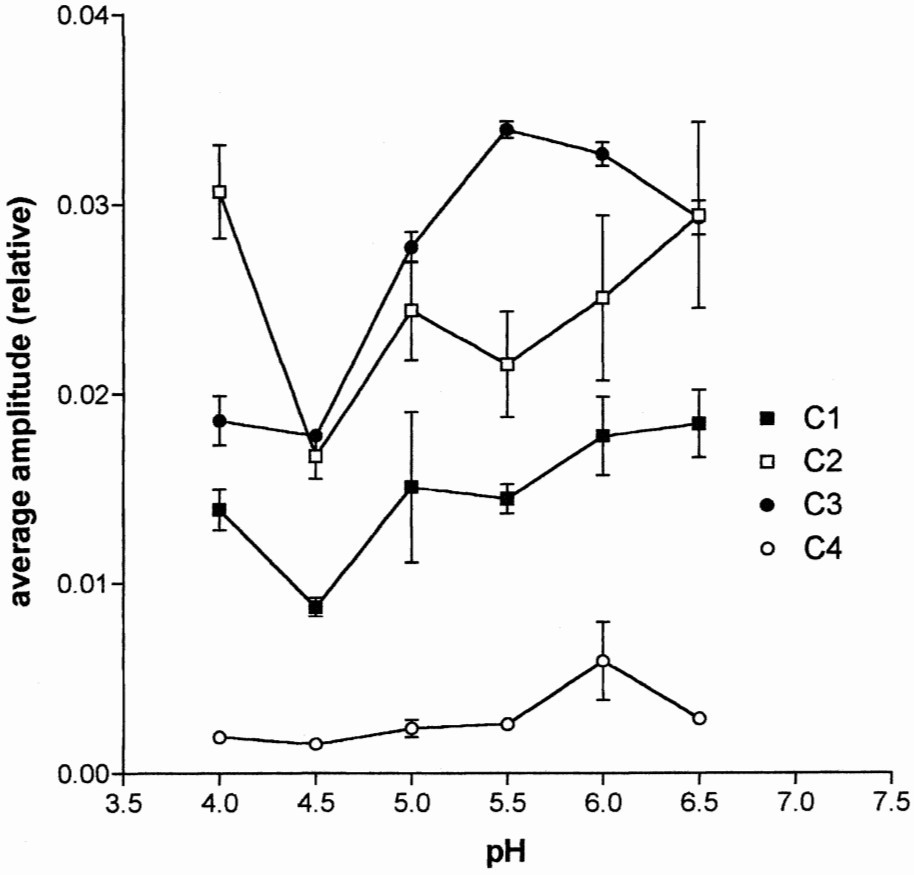
0.04
0.03
0.02
0.01
0.00
average amplitude (relative)
3.5
4.0
4.5
5.0
5.5
6.0
6.5
7.0
7.5
pH
C1
C2
C3
C4

Figure 51. Average lifetime (τ_{AVG}) of dark adapted (Fo), light saturated (Fm), and sodium dithionite treated (Dithionite) photosystem 2 particles as a function of pH (pH 5.5 MES). All values are an average of three (except for Fo [pH 4.5] and Fm [pH 4.0, 5.5, and 6.0] which are an average of two) indidvidual experiments.

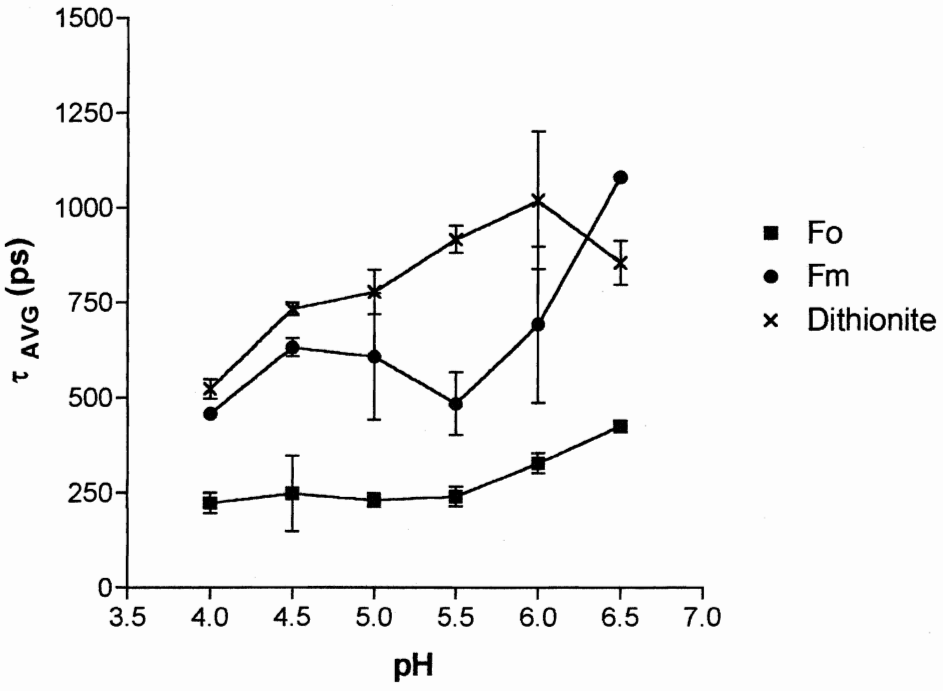
1500
1250
1000
750
500
250
0
τ AVG (ps)
3.5
4.0
4.5
5.0
5.5
6.0
6.5
7.0
pH
Fo
Fm
Dithionite